

Segment specificity of muscular and neuronal control in insect walking

Inaugural-Dissertation

zur

Erlangung des Doktorgrades

der Mathematisch-Naturwissenschaftlichen Fakultät

der Universität zu Köln

vorgelegt von

Elzbieta Irma Hammel

geb. Godlewska

aus Warschau

Köln

2017

Berichtersteller: Prof. Dr. Ansgar Büschges
Prof. Dr. Peter Kloppenburg

Tag der mündlichen Prüfung: 01. Dezember 2016

Während der Anfertigung der vorliegenden Dissertation wurde ich zunächst durch ein Stipendium der **Graduate School for Biological Sciences at the University of Cologne** und anschließend durch ein Promotionsstipendium der **Konrad-Adenauer-Stiftung** ideell gefördert und finanziell unterstützt.

ABSTRACT

Locomotion depends on an interplay of neuronal activity, muscle contraction, and sensory feedback. In the limbed animal, the individual legs of the different thoracic segments, as well as the individual leg segments of each leg, and their antagonistic muscles, have to be coordinated with each other.

For the stick insect, it is well known that the legs of the pro-, meso- and metathoracic segments have different functions in the straight walking and turning animal (Cruse 1976, Grabowska & Godlewska et al. 2012, Gruhn et al. 2009b). Despite of this, most studies on stick insect walking focused on the mesothoracic legs and their motoneuronal output (Bässler et al. 1996, Borgmann et al. 2007, Guschlbauer et al. 2007, Fischer et al. 2001, Bucher et al. 2003, Gruhn et al. 2016).

With my thesis, I wanted to contribute to increase the knowledge for other legs of the stick insect *Carausius morosus*. Therefore, I investigated thorax- and leg-segment specific differences on the muscular and the neuronal level.

In the first part of my thesis, I used mATPase histochemistry to investigate the muscle fiber composition in the six major leg muscles, *protractor* and *retractor coxae*, *levator* and *depressor trochanteris*, and *extensor* and *flexor tibiae* for the pro-, meso-, and metathorax.

I demonstrated that most of these muscles contain three different fiber types: a slow, a fast, and an intermediate contracting one. While the proportions of the fiber types differed between the individual muscles, they were mostly consistent for the three analyzed thoracic segments. The only exceptions concerned the *depressor trochanteris* and *retractor coxae*, which both had increasing percentages of slow contracting fibers towards the metathoracic segment, suggesting a greater importance of these muscles for posture and tonic force production.

In the second part of my thesis, I investigated the motor output of the deafferented meso- and metathoracic leg nerves nl2 (innervates the *protractor coxae*), nl5 (*retractor coxae*), C1 (*levator trochanteris*), C2 (*depressor trochanteris*), nl3 (*extensor tibiae*) and of branches of the nervus cruris (*flexor tibiae*) during front leg turning in a reduced preparation with only two front legs left. I showed, that the neuronal activities of the mesothoracic and metathoracic *protractor* and *retractor coxae* are specific for the turning

direction, and similar in both thoracic segments. The neuronal activation of the *levator* and *depressor trochanteris*, on the other hand, was independent of the turning direction, and showed small thorax-segment specific differences, with a stronger *depressor trochanteris* activity in the meta- than in the mesothorax. The motoneuron pools of the most distal leg joint were very variable in their motor output. The leg nerves of the *extensor* and *flexor tibiae* tended to show direction specific activity in the mesothorax, with a stronger *extensor tibiae* activity outside, and *flexor tibiae* activity inside in half of the experiments. Such a tendency was not seen in the metathoracic motoneuron pools.

In the third part of my thesis, I analyzed the involvement of local central pattern generators in the thorax-segment, and leg-segment specificity of the turning related motor output. For this purpose, I activated the local CPGs using the muscarinic agonist pilocarpine in a split-bath preparation. I was able to show that the pharmacologically evoked rhythm in the respective antagonistic motoneuron pools was changed towards the activation pattern observed in control turning conditions immediately after the initiation of front leg turning. This suggests that the observed changes in motor output are mediated through influences on the local central pattern generating networks.

ZUSAMMENFASSUNG

Fortbewegung resultiert aus einem Zusammenspiel von neuronaler Aktivität, Muskelkontraktion und sensorischer Rückkopplung. In Insekten, die mehrere Gliedmaßen besitzen, müssen während der Fortbewegung nicht nur die individuellen thorakalen Segmente aufeinander abgestimmt werden, sondern ebenfalls die einzelnen Beingelenke und die sie kontrollierenden jeweiligen antagonistischen Muskeln.

Für das Laufen der Stabheuschrecke ist schon lange bekannt, dass die einzelnen Beine unterschiedliche Funktionen haben (Cruse 1976, Grabowska & Godlewska et al. 2012, Gruhn et al. 2009b). Ungeachtet dessen, wurden in der Stabheuschrecke die meisten Studien an den Mittelbeinen und derer motoneuronalen Aktivität durchgeführt (Bässler et al. 1996, Borgmann et al. 2007, Guschlbauer et al. 2007, Fischer et al. 2001, Bucher et al. 2003, Gruhn et al. 2016).

Mit der vorliegenden Doktorarbeit wollte ich dazu beitragen, die für *Carausius morosus* vorhandenen Wissenslücken für die anderen Beinpaare zu füllen. Hierfür führte ich Untersuchungen auf muskulärer und neuronaler Ebene durch.

Im ersten Teil meiner Dissertation verwendete ich die Methode der mATPase Histochemie, um die Muskelfaser-Zusammensetzung der sechs wichtigsten Beinmuskeln zu untersuchen. Bei den untersuchten Muskeln handelte es sich um den *Protractor* und *Retractor coxae*, den *Levator* und *Depressor trochanteris*, und den *Extensor* und *Flexor tibiae*. Ich konnte zeigen, dass die meisten dieser Beinmuskeln aus langsamen, schnellen, und intermediären Muskelfasern bestanden. Während sich die Verhältnisse der Muskelfasertypen zueinander in den einzelnen Muskeln unterschieden, waren diese Verhältnisse für die einzelnen thorakalen Segmente konstant. Die einzigen Ausnahmen bildeten der *Retractor coxae* und der *Depressor trochanteris*. Diese beiden Muskeln wiesen einen in Richtung Metathorax ansteigenden Anteil an langsam kontrahierenden Muskelfasern auf, was darauf hindeutet, dass diese Muskeln für die Körperhaltung und die tonische Krafterzeugung entscheidend sind.

Im zweiten Teil meiner Arbeit, untersuchte ich die motorische Aktivität der lokalen meso- und metathorakalen Beinnerven n12 (innerviert den *Protractor coxae*), n15 (*Retractor coxae*), C1 (*Levator trochanteris*), C2 (*Depressor trochanteris*), n13 (*Extensor tibiae*), und

der Nervenäste des nervus cruris (*Flexor tibiae*) in einem reduzierten Präparat, das mit seinen zwei verbliebenen Vorderbeinen Innen- und Außenkurven lief. Hier konnte ich zeigen, dass die Aktivitäten im *Protractor* und *Retractor coxae*-Nerv abhängig von der Kurvenrichtung unterschiedlich stark waren, und dies auf ähnliche Weise in Meso- wie im Metathorax. Die Aktivität der Beinnerven des *Levator* und *Depressor trochanteris* war hingegen unabhängig von der Kurvenrichtung, zeigte allerdings leichte Thoraxsegment-spezifische Unterschiede auf, da der *Depressor trochanteris* im Metathorax eine stärkere Aktivität aufwies als im Mesothorax. Die Motoneurone des Femur-Tibia-Gelenks wiesen im kurvenlaufenden Zwei-Bein-Präparat hinsichtlich ihrer Aktivität starke Variabilitäten auf. Allerdings konnte in der Hälfte der Experimente im mesothorakalen *Extensor tibiae* eine stärkere Aktivität in Außenkurven, und im *Flexor tibiae* eine stärkere Aktivität in Innenkurven beobachtet werden. Eine solche Tendenz wurde für die metathorakalen Motoneurone des Femur-Tibia-Gelenks nicht beobachtet.

Im dritten Teil meiner Dissertation untersuchte ich die Beteiligung von lokalen zentralen Mustergeneratoren an den Thorax- und Bein-Segment spezifischen Unterschieden der motorischen Aktivität im kurvenlaufenden Präparat. Hierfür aktivierte ich die lokalen zentralen Mustergeneratoren mit dem muskarinergen Agonisten Pilocarpin in einer Split-Bath-Präparation. Dadurch konnte ich zeigen, dass sich der pharmakologisch aktivierte Rhythmus der jeweiligen Motoneuronenpaare bei Beginn der Vorderbeinbewegung soweit veränderte, als dass stets ein Aktivitätsmuster entstand, das dem ähnelte, welches in kurvenlaufenden Präparaten ohne Pilocarpin-Applikation beobachtet wurde. Dies lässt darauf schließen, dass die zuvor beobachteten Veränderungen der Motoraktivität auf Veränderungen der Aktivität der lokalen zentralen Mustergeneratoren zurückzuführen ist.

CONTENTS

ABSTRACT	i
ZUSAMMENFASSUNG	ii
1 INTRODUCTION	1
2 MATERIALS & METHODS	4
2.0 Experimental Animals	4
2.1 Histochemical Experiments	4
2.1.1 Preparation & Experimental Design	4
2.1.2 Staining Reaction	5
2.1.3 Data Analysis	7
2.1.4 Muscle Fiber Identification	7
2.1.5 Statistical Analysis & Figure Preparation	8
2.2 Electrophysiological Experiments	9
2.2.1 Preparation & Experimental Design	9
2.2.2 Split-Bath Preparation	10
2.2.3 EMG Recordings & Extracellular Recordings	10
2.2.4 Data Recording & Evaluation	11
2.2.5 Data Analysis	11
2.2.6 Circular Statistics	12
3 CHARACTERIZATION OF MUSCLE FIBER TYPES	13
3.1 <i>Protractor and Retractor Coxae</i>	15
3.1.1 Mesothorax	16
3.1.2 Metathorax	16
3.2 <i>Levator and Depressor Trochanteris</i>	19
3.2.1 Prothorax	19
3.2.2 Mesothorax	20
3.3.3 Metathorax	20

3.3	<i>Extensor and Flexor Tibiae</i>	23
3.3.1	Prothorax	24
3.3.2	Mesothorax	25
3.3.3	Metathorax	25
4	MOTOR ACTIVITY DURING CURVE WALKING	32
4.1	<i>Protractor and Retractor Coxae</i>	36
4.1.1	Mesothorax	36
4.1.2	Metathorax	40
4.2	<i>Levator and Depressor Trochanteris</i>	43
4.2.1	Mesothorax	43
4.2.2	Metathorax	47
4.3	<i>Extensor and Flexor Tibiae</i>	50
4.3.1	Mesothorax	50
4.3.2	Metathorax	55
5	INVOLVEMENT OF CENTRAL PATTERN GENERATORS IN THORAX- & LEG-SEGMENT SPECIFICITY OF THE TURNING RELATED MOTOR OUTPUT	59
5.1	<i>Protractor and Retractor Coxae</i>	62
5.1.1	Mesothorax	62
5.1.2	Metathorax	65
5.1.3	Metathorax & Abdominal Ganglia Chain	68
5.1.4	Meso- & Metathorax	71
5.2	<i>Levator and Depressor Trochanteris</i>	75
5.2.1	Mesothorax	75
5.2.2	Metathorax	79
6	DISCUSSION	82
6.1	Characterization of Muscle Fiber Types	82
6.2	Motor Activity during Curve Walking	89
6.3	Involvement of Central Pattern Generators in Thorax- & Leg-Segment Specificity of the Turning Related Motor Output	96
7	CONCLUSION	104

BIBLIOGRAPHY	107
LIST OF FIGURES	122
LIST OF TABLES	124
APPENDIX	125
TEILPUBLIKATIONEN	138
DANKSAGUNG	139
ERKLÄRUNG	140

CHAPTER 1

Introduction

Locomotion, whether in the form of walking, swimming, or flying, is one of the most important behaviors an animal can perform. This behavior relies on an interplay of neuronal activity, muscular contraction, and sensory feedback. In insects, the coordination of all leg movements depends on the coordination of the different muscles for one leg segment, on the coordination of the different leg segments to each other, and on the coordination of the different legs of all thoracic segments.

In contrast to insects with specialized limbs such as the praying mantis, from its outward appearance, the stick insect legs are all uniformly built on both, the muscular and the neuronal level. For this reason, they could share the same functional properties. Cruse reported already in 1976, that this is actually not the case, and showed that the three leg pairs of the stick insect have different functions in free walking: while the front legs have mainly feeler function, the middle legs have supporting functions, and the hind legs have supporting and propulsive functions (Cruse 1976). Later behavioral studies supported this finding (Dürr 2005, Grabowska & Godlewska et al. 2012, Theunissen 2014/2015).

As these different functions have to be based on the neuronal and / or the muscular level in segment specificities, the question arises, what kind of thorax-segment and leg-segment specificities these might be. And are these differences based on specificities on the muscular or on the neuronal level, or even on both levels?

Previous studies in which the kinematics of all legs were analyzed in straight walking and turning stick insects, either on a Styrofoam ball (Dürr & Ebeling 2005) or on a slippery surface (Gruhn et al. 2009b), gave a hint, that segment specific differences exist for the individual leg pairs on the neuronal level, as strong differences concerning the anterior and posterior extreme positions were reported for the legs of the different thoracic segments, independent of the walking direction.

A study by Borgmann et al. (2007) demonstrated thorax-segment specificities on the neuronal level. They showed that the motoneuron (MN) pools of the subcoxal joint are differently modified by descending signals in the mesothorax than in the metathorax in a reduced preparation with one front leg walking on a treadmill.

Another study (Büschges et al. 1995) showed that leg-segment specificities exist on the neuronal level. The authors concluded this from experiments in which the application of the muscarinic agonist on an isolated thoracic nerve cord revealed that the activities of the MN pools of each leg joint alternated rhythmically to each other, while only in rare cases a stereotypic cycle-to-cycle coupling between the MN pools of the different leg joints was found. From this the authors suggested that each leg joint has its own central pattern generator (CPG).

Thus, not only thorax-segment, but also leg-segment specific neuronal activation was previously reported for the stick insect.

A modeling study by Ekeberg et al. (2004), suggested the differences among the thoracic segments, as it was able to show that a simulation designed for the coordinated activation of the middle leg was also able to induce coordinated front leg, but not hind leg stepping. For the latter, the stimulation suggested that the influence of the femoral chordotonal organ (fCO; a sense organ, sensing the joint-angle of the femur-tibia joint) has a reversed effect compared to the fCOs in the front- and middle leg.

Despite all these findings, most studies in the stick insect focused on the middle thoracic segment in their analysis. This includes the investigation of neuronal activity during walking (Fischer et al. 2001, Gabriel et al. 2003, Ludwar et al. 2005a/b, Gabriel & Büschges 2007), the effect of sensory signals (Hess & Büschges 1997/1999, Akay et al. 2001/ 2004/2007, Bucher et al. 2003), behavioral adaptation (Gruhn et al. 2016), and also the analysis of muscular composition (Bässler et al. 1996) and biomechanical properties (Guschlbauer et al. 2007). Only in rare cases the properties of one or even both other leg pairs or segments were investigated as well (Borgmann et al. 2007/2009, Hellekes et al. 2012).

Since behavioral (Cruse 1976, Dürr 2005, Grabowska & Godlewska et al. 2012, Theunissen 2014/2015), kinematic (Dürr & Ebeling 2005, Gruhn et al. 2009b), and studies on neuronal level (Büschges et al. 1995, Borgmann et al. 2007) revealed that clear differences exist for the different leg joints and leg pairs, it is of major importance to analyze more than only one thorax-segment or leg-segment to be able to draw an overall drawing of muscular and neuronal control of locomotion in the stick insect. Thus, in the following, I will present new results for thorax- and leg-segment specificity on the muscular and the neuronal level.

First, I used histochemical experiments (mATPase staining) to investigate the muscular composition of the six major leg muscles of the pro-, meso- and metathorax to look for differences that may correlate with the function of the legs (see chapter 3).

Secondly, I used extracellular nerve recordings of the six major leg muscles in the meso- and metathorax to investigate the motor output in these segments during turning movements of the front legs in order to investigate if the neuronal control of the leg segments differs between the segments in this relatively simple regime of behavioral flexibility (see chapter 4).

Thirdly, I activated the central pattern generators (CPGs) of the meso- and/or metathorax to investigate the involvement of local CPGs in thorax-segment and leg-segments specificity of the turning related motor output (see chapter 5).

In each chapter, a specific introduction is presented, and all results will be discussed in chapter 6.

CHAPTER 2

Materials & Methods

2.0 Experimental Animals

All experiments were conducted on adult female stick insects of the species *Carausius morosus* (Sinéty, 1901) at room temperature under reduced light conditions. Animals were obtained from a colony maintained at the University of Cologne, Germany. The colony was kept under constant conditions at temperatures between 20°C and 25°C, high humidity (60-75%), and an artificial light-dark cycle (12 h/12 h). All animals were fed with blackberry leaves (*Rubus fruticosus*) *ad libitum*.

2.1 Histochemical Experiments

2.1.1 Preparation & Experimental Design

Animals were pinned down dorsal side up, decapitated, and the intestine was carefully removed. The thoraces, the coxae, and the femora of all segments were obtained and pinned out on Sylgard® blocks. Before the samples were carefully frozen in liquid nitrogen (~ -80 °C), they were embedded in Tissue Tek® to improve their sectioning. Samples embedded can be kept over prolonged periods of time at ~ -80°C.

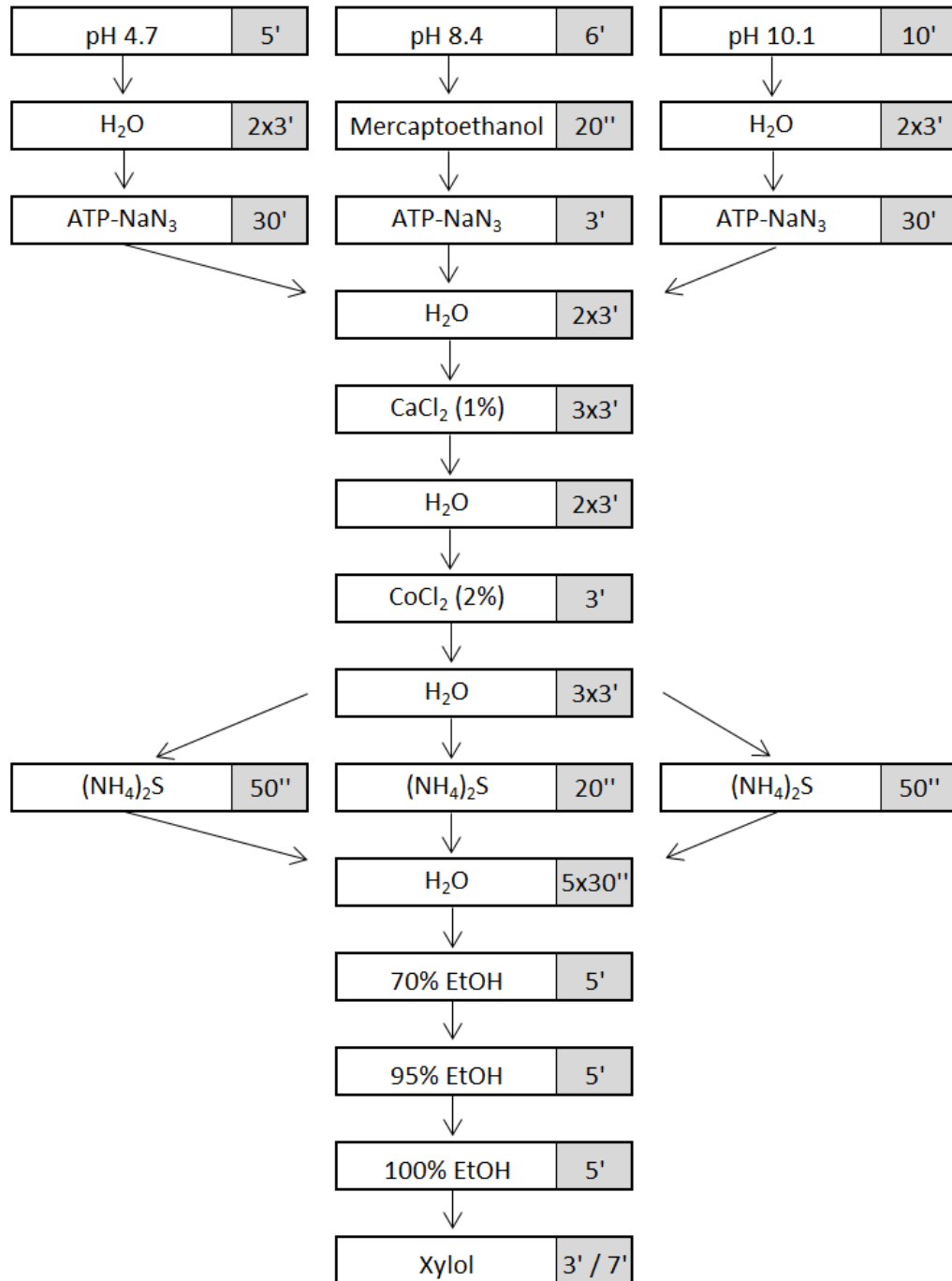
One hour before use, frozen specimens were thawed at ~ -22 °C. After that, specimens were cut with a cryostat into 25 μ m thin sections. The meso- and metathorax were cut transversally along the body axis from posterior to anterior, and the femora and coxae of all segments were cut transversally from distal to proximal. Consecutive sections were mounted on three alternating gelatinized cover slips, and dried over night at room temperature or for one hour or over night at room temperature, followed by one hour at 40 °C in a heating oven. After this procedure, sections were processed for staining.

2.1.2 *Staining Reaction*

The determination of myofibrillar ATPase (mATPase) activity was conducted according to the work of Padykula and Herman (1955b) and Gruhn and Rathmayer (2002). This staining reaction is a sequence of several consecutive redox reactions. First, mATPase converts ATP to ADP plus P_i . The obtained P_i reacts with $CaCl_2$ to $CaPO_4^-$. $CaPO_4^-$ is converted to $CoPO_4$ and precipitates to CoS when incubated in $(NH_4)_2S$ at the same ratio as the converted ATP. The stained sections can be analyzed visually, and the staining intensity correlates with the contraction properties of the muscle fibers (Barany 1967).

At the beginning of the staining procedure (Table 2.1.1; Fig. 2.1.1), the three cover slips with consecutive sections on were incubated at different pH conditions (cover slip I: pH 4.7, 5 min.; cover slip II: pH 10.1, 10 min.; cover slip III: pH 8.4, 6 min), since the different isomyosines show different pH stabilities (Padykula and Herman 1955b; Guth and Samaha 1969; Günzel et al. 1993). The starting pH values were taken from Bässler et al. (1996). After pre-incubation under different conditions, sections were either washed twice for 3 min each in distilled water (the acidic- and alkaline pre-incubated sections) or were treated with mercaptoethanol for 20 sec (sections pre-incubated at pH 8.4) to enhance the mATPase activity (see Padykula & Herman 1955a, Syrový 1989) before incubation in a reaction solution that contained ATP and NaN_3 for 3 min (sections pre-incubated at pH 8.4) or 30 min (acidic- and alkaline pre-incubated sections). After ATP incubation, all sections were washed (2x 3 min or 2x 1 min) and treated with $CaCl_2$ (1% in water; 1x 3 min), washed again (2x 3 min or 2x 1 min), and treated with $CoCl_2$ (2% in water; 1x 3 min). After that, all sections were washed again (3x 3 min or 3x 1 min) and incubated for several seconds in $(NH_4)_2S$ (20 sec or 50 sec). This procedure results in CoS precipitation within the sections. Following the staining, all sections were dehydrated in ascending alcohol concentrations (70 %, 95 %, 100 % EtOH), cleared in xylol, mounted and covered on slides in Entellan®.

Table 2.1.1: Staining protocol with incubation times. White boxes show the solution, gray boxes show the incubation time in minutes (') or seconds (") (table also used in the submitted MS Godlewska-Hammel et al. 2016).



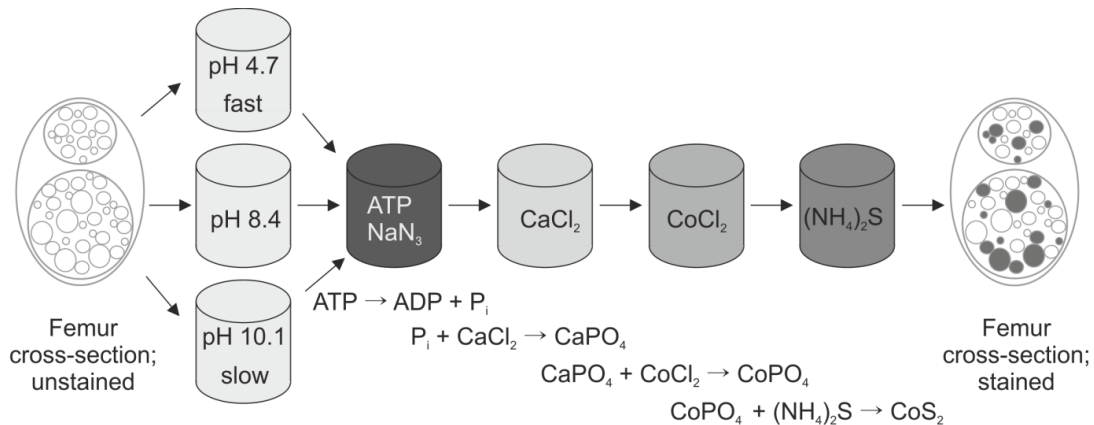


Fig. 2.1.1: Schematic of the staining reaction for determination of myofibrillar ATPase activity in serial cross-sections through the investigated stick insect muscle (figure also used in the submitted MS Godlewska-Hammel et al. 2016).

2.1.3 Data Analysis

To make sure that the length of the femora and thoraces and the possible variation in muscle fiber composition was taken into account, the femora were subdivided into three parts (1-3 = most distal sections / 4-6 = medial sections/ 7-10 = most proximal sections), and the thoraces into two parts (1-5 = posterior sections; 6-10 = anterior sections) for analysis, whereas the analyzed sections of the coxa were preferentially taken from the middle.

Stained sections of good quality were analyzed with a microscope (Olympus BX61; imaging system: Olympus cell^F) under bright field, and photographed at a total magnification of 100 (objective: 10x; ocular lens: 10x). For further analysis, corresponding alkali and acidic sections were compared to each other with regard to their staining intensities.

For muscle fiber typing, a MATLAB (R2011b) script (kindly provided by Dr. Till Bockemühl) was used. The script allows individual muscle fibers of each muscle to be marked in individual sections, and provides their gray-scale values. All fibers were classified into lightly colored (0-0.74) or darkly colored (0.75-1) according to their gray-scale value, whereby the brightest muscle fiber was classified as a gray value of 0, and the darkest muscle fiber was classified with a gray scale value of 1. This procedure was repeated for corresponding alkali and acidic pre-incubated sections.

2.1.4 Muscle Fiber Identification

Muscle fibers that were classified as faintly colored after acidic pre-incubation and darkly colored after alkaline pre-incubation are slowly contracting muscle fibers, since the slow

isoform of mATPase remains active after alkaline pre-incubation (see Brooke & Kaiser 1970, Bässler et al. 1996; Gruhn and Rathmayer 2002). An inverted staining was typical for fast contracting muscle fibers. Fibers stained darkly or faintly under both conditions were classified as intermediate fibers (ll: light-light / dd: dark-dark intermediate).

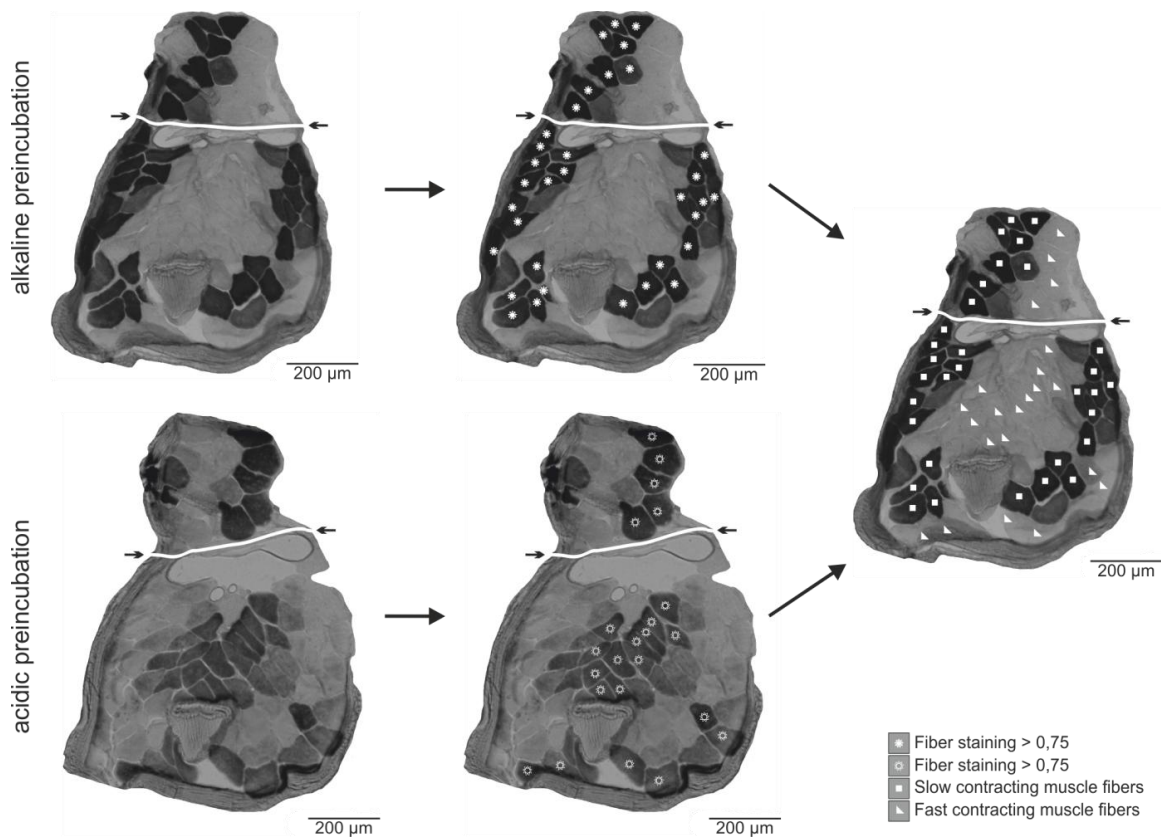


Fig. 2.1.2: Example for the analysis steps for the muscle fiber identification. Serial sections were treated either under alkaline pre-incubation (upper row) or under acidic pre-incubation (lower row). Fibers with a gray-scale value of more than 0.75 of the maximum were marked (here with a star) under both conditions. Corresponding fibers of both conditions were compared and classified as “slow contracting muscle fibers” (here squares) if they were stained darkly (gray-scale > 0.75) under alkaline pre-incubation and faintly (gray-scale < 0.75) under acidic pre-incubation. Fibers with a vice versa staining pattern were classified as “fast contracting muscle fibers” (here triangles). Intermediate contracting muscle fibers had under both conditions a gray-scale value of either less than 0.75 (ll intermediate) or more than 0.75 (dd intermediate) (not presented in this figure) (figure also used in the submitted MS Godlewska-Hammel et al. 2016).

2.1.5 Statistical Analysis & Figure Preparation

To define the reliability of muscle fiber composition, a statistical analysis was done with paired difference t-test using Prism 7 (GraphPad Software, Incorporation, La Jolla, CA, USA) which is a non-parametric test that compares two matched groups that are derived from a Gaussian population (for further information see GraphPad Statistics Guide).

All cross-sectional areas, percentages of fiber types, and statistical values are presented in tables 3.1.1 - 3.1.5.

For figure preparation, digital images of the sections were only adjusted for lighting of the entire picture without changing relative gray-scales using CorelDRAW (X6, Corel Corporation, Ottawa, Canada).

2.2 Electrophysiological Experiments

2.2.1 Preparation & Experimental Design

All experiments were performed at room temperature on an air cushioned table (MICRO-g, TMC, Peabody, MA, USA) surrounded by a darkened Faraday cage. The animal was induced to autotomize the middle and hind legs, except for in experiments in which the nerve activity of the flexor tibiae was analyzed. In that case, the leg of question was cut distally to the femur-tibia joint. Subsequently, the animal was glued ventral-side-down on a 90 mm long and 3 mm wide balsa rod using dental cement (ProTempII, ESPE, Seefeld, Germany) applied to the meso- and metathorax, and was positioned above a 13.5 cm x 13.5 cm polished acrylic glass plate at a height of about 8–12 mm to ensure resting angles of the front legs of about 110°. The plate was covered with a lubricant composed of 95% glycerin and 5% water to create a slippery surface. This surface enabled the animals to perform walking movements unrestricted in direction, in contrast to commonly used treadmills that force the animal to walk in only one direction (forward or backward). In addition, animals do not have to overcome their own body inertia or that of the treadmill (Gruhn et al. 2006). To ensure free stepping movements of the tethered animal, the front legs, prothorax, and head protruded from the rod. The coxae of the middle and hind legs were positioned pointing forward to an angle of 45° with respect to the body axis, to improve access to the investigated leg nerves. In experiments in which the nerve activity of the *flexor tibiae* was analyzed, the femur of the investigated leg was fixed with pins to an extension of the rod anteriorly at an angle of about 75° with respect to the body axis. Additionally, the coxa was glued to the extension of the rod to prevent autotomy of the analyzed leg. Subsequently, the fixed middle or hind leg were opened dorsally, and the extensor tibiae, as well as the receptor apodeme, was carefully removed to allow access to the nervus cruris and, specifically, to its delicate branches innervating the flexor tibiae.

Following this, the meso- and metathorax were opened dorsally, the intestine was moved aside, and connective tissue was carefully removed to allow access to the ganglia and their leg nerves. The body cavity was filled with saline (Weidler & Diecke 1969), and both

ganglia were completely deafferented by cutting or crushing the lateral leg nerves (nl) ipsi- and contralateral to the recording site.

To elicit walking in different directions, a progressive striped pattern was displayed in an LED arena that surrounded the animal. In most cases, stepping sequences were elicited by gently touching the abdomen with a paintbrush. The paintbrush was removed as soon as the animal began stepping. Sequences recorded during stimulation were not used for further analysis.

All sequences were filmed from above with at 75 frames per second.

2.2.2 *Split Bath Preparation*

In a second set of experiments, either the meso- or the metathoracic ganglion (or both ganglia at the same time) were superfused with saline containing pilocarpine. Pilocarpine is a muscarinic acetylcholine receptor agonist and is known to activate stick insect CPGs. Applying pilocarpine to the nervous system activates these networks and results in a basic rhythmic motor pattern (Büschges et al. 1995).

The preparation procedure for these experiments was roughly the same as before. To ensure that only a single ganglion, the meso- or metathoracic, but not the prothoracic ganglion, was superfused with pilocarpine, a small stretch of cuticle anterior and posterior to the relevant ganglion was removed. At this step, care was taken to not damage the connectives. Following this, the gap was filled with vaseline.

For control experiments, all compartments were filled with saline. Hereafter, in the relevant compartment, saline was carefully removed with a tissue and the compartment was filled with 3 mM pilocarpine solution in saline. This concentration is known to elicit a stable rhythm in the various motor neuron (MN) pools (Büschges et al. 1995).

2.2.3 *EMG Recordings & Extracellular Recordings*

In all experiments, the activity of the front legs' flexor tibiae muscles was monitored via electromyograms (EMGs) (Rosenbaum et al. 2010; Gruhn et al. 2011). For this purpose, two twisted copper wires (49 μ m diameters, insulated except for the tips) were inserted through holes in the cuticle of the ventral portion of the proximal femur (about 2 mm apart) and fixed with dental cement. In most cases, muscle potentials from the *flexor tibiae* muscle were recorded together with potentials from the *extensor tibiae* muscle.

Extracellular recordings with monopolar hook electrodes (modified from Schmitz et al. 1991) were made from leg nerves nl2 (contains *protractor coxae* MNs), nl5 (contains

retractor coxae MNs), C1 (contains *levator trochanteris* MNs), C2 (contains *depressor trochanteris* MNs) and nl3 (contains *extensor tibiae* MNs) (nomenclature according to Marquardt 1940). For extracellular recordings of the nerve activity of the *flexor tibiae*, the nerve branches that lead from the nervus cruris to the *flexor tibiae* were recorded with a very delicate monopolar hook electrode inside the femur. All nerves were crushed distally to the recording sites to abolish afferent and efferent signaling. A reference electrode was placed into the abdomen of the animal.

MNs were easily identifiable, as the investigated MNs had axons with the largest diameter in their respective leg nerve and therefore showed the largest amplitudes in the extracellular recordings (all leg nerves: Goldammer et al. 2012; further information: nl2, nl5: see Graham & Wendler 1981; nl3: see Bässler & Storrer 1980; identification of MNs based on their amplitude: see Pearson et al. 1970).

2.2.4 Data Recording & Evaluation

EMG and extracellular nerve signals were amplified 100-fold by a preamplifier (model MA101, Electronics Workshop, Zoological Institute, University of Cologne), and subsequently amplified 10-fold and band-pass filtered at 100–2000 Hz with a 4-channel amplifier/signal conditioner (Model MA102, Electronics Workshop, Zoological Institute, University of Cologne). All electrophysiological signals were digitized using the MICRO 1401 II analog-digital converter (CED, Cambridge, UK) and recorded with the data acquisition and analysis software Spike2 (version 7.01, CED, Cambridge, UK) on a personal computer running Windows 7 (Microsoft, Corporation, Redmond, WA, USA). Video files were analyzed using a MATLAB (R2011b) script (kindly provided by Dr. Till Bockemühl) that embedded them into Spike2. This allowed for determination of the direction of the front legs.

2.2.5 Data Analysis

Neuronal activity and the start of flexor tibiae activity were displayed as event channels (minimum interval: 3 ms) individually for each turning direction.

Data were first analyzed with respect to front legs' step cycles, defined by the period from the onset of activity one *flexor tibiae* muscle to the next. Phase histograms were used to show the distribution of motoneuronal activity in the step cycle in each recording, whereby each of the twelve bins corresponded to 30° of the 360°-step cycle. The bin including the highest amount of spike events determined the phase with maximal neuronal activity (see

chapter 2.2.6: Circular Statistics). The same visual approach was used to determine whether more or less activity was present during inside and outside turns.

2.2.6 *Circular Statistics*

Because stepping is a recurrent cyclic behavior, circular statistics were used to analyze the neuronal activity relating it to the stepping movements of the ipsilateral front leg, whereby the start of front legs' flexor activity was defined as the beginning of stance phase. Because most MN pools showed bi- or multimodal activation, the maximal neuronal activity was displayed in polar plots (see above). For the same reason, the omnibus test was used to detect general deviations from uniformity. The mean vectors of the maxima, as well as their lengths, were computed via the MATLAB toolbox for circular statistics (Berens 2009). Values were regarded as significantly different from each other at $P < 0.05$. All statistical analyses were performed with the open source MATLAB (R2011b) circular statistics toolbox (Berens 2009). In no case significant differences between the respective motor outputs were observed.

The number of animals is represented by N , while \acute{N} represents the number of analyzed hemiganglia, as, in many cases, leg nerves of both hemiganglia were recorded at once. In the following, analyzed hemiganglia are synonymous with "experiments". The letter n gives the number of steps analyzed in phase histograms.

Figures were prepared with Microsoft Excel (2007), MATLAB (R2011b), and CorelDRAW (X6, Corel Corporation, Ottawa, Canada).

CHAPTER 3

Characterization of Muscle Fiber Types

All forms of animal locomotion depend on an interplay of neural activity and muscle contraction. For a better understanding of the neuromuscular control of locomotion, it is of major importance to have a detailed picture of the muscle anatomy, their fiber composition, and their function. Various methods exist for analyzing muscle properties of vertebrates and invertebrates, such as electrophysiological recordings (Gruhn & Rathmayer 2002, Rosenbaum et al. 2010), biomechanical studies (Guschlbauer et al. 2007), and, resulting from these, modeling studies (Tóth et al. 2013a/b). Additionally, biochemical and histochemical studies can be used to classify single muscle fibers based on their metabolic and contractile protein profiles, since it is well known that muscle biochemical profiles match physiological parameters (Jahromi & Atwood 1969, Sherman & Atwood 1972, Silverman et al. 1987, Müller et al. 1992, Pilehvarian 2015, Gruhn & Rathmayer 2002, Bässler et al. 1996). One of these histochemical methods is the measurement of myofibrillar (or myosin) adenosine triphosphatase (mATPase) activity. This enzyme hydrolyzes ATP during cross-bridge cycle in muscle contractions (Bárány 1967, Barnard et al. 1971) and, therefore, the amount of hydrolyzed ATP in muscle sections offers an insight into the muscle fiber contraction speed (Bárány 1967, Maier et al. 1984, Maier et al. 1986, Maier et al. 1987, Müller et al. 1992). In vertebrates and invertebrates, different isoforms of mATPase occur that show differences in the rates in which they hydrolyze ATP. While fast myosin isoforms convert ATP to ADP and phosphate even after acidic-

pre-incubation (e.g. 4.7), they inactivate after alkaline pre-incubation (e.g. pH 10.2). Slow isoforms, on the other hand, have a lower ATPase activity below pH 8.4, but are still active after alkaline pre-incubation. Since intermediate isoforms show mostly medium activity at pH 8.4 and are not completely inactivated after acidic or alkaline pre-incubation, they cannot be classified into either fast or slow isoform groups (Bässler et al. 1996). In various studies muscle fiber composition was analyzed for different arthropods, like locust (Müller et al. 1992), cockroach (Stokes 1987), crayfish (Gruhn & Rathmayer 2002) and crabs (Maier et al. 1984). In the stick insects *Carausius morosus* and *Cuniculina impigra*, Bässler et al. (1996) showed, using fiber typing after alkaline pre-incubation, that the composition of fast and slow contracting muscle fibers in the mesothoracic swing muscle extensor tibiae differs between the proximal, medial, and distal areas of the muscle. While the amount of fast contracting muscle fibers decreased from proximal to distal, the opposite distribution was found for slow contracting muscle fibers. However, in neither of the mentioned studies, the fiber composition of different appendages was analyzed and compared to each other. Therefore, the possible functional differences between the different appendages were not discussed at the level of fiber composition. This, despite the fact that for the stick insect alone several behavioral and morphological studies reported about the functional differences for the different appendages and leg segments (Grabowska & Godlewska et al. 2012, Theunissen et al. 2015, Dallmann et al. 2016). These differences originate either from differences in neuronal control, or the muscle fiber composition within the individual appendages.

Therefore, in this part of my study, I investigated the presence of different muscle fiber types, based on mATPase activity, in the six major leg muscles of the different segments in the stick insect *Carausius morosus*. Histochemical analysis through mATPase staining for qualitative differences in the activity of the myofibrillar ATPase was used to discriminate between muscle fibers with fast, slow, and intermediate contractile properties. The subcoxal muscles *protractor* and *retractor coxae* were analyzed in the meso- and metathorax. Additionally, the coxa-trochanteral muscles, *levator* and *depressor trochanteris*, as well as the femur-tibial muscles, *extensor* and *flexor tibiae*, were analyzed in the pro-, meso-, and metathoracic segments. First, the different muscle fiber types in each muscle were determined, then, the relative proportions of each fiber type were analyzed with respect to the total cross-sectional area of the investigated muscle.

All following figures, tables, and data were used in the recently submitted MS Godlewska-Hammel et al. 2016.

3.1 *Protractor and Retractor Coxae*

The *protractor* and *retractor coxae* (short: protractor and retractor, respectively) are the only main leg muscles situated in the thorax and not within each leg. These muscles are responsible for the forward and backward movements of the leg (Rosenbaum et al. 2010).

The size and the location of the protractor and retractor differ in all three segments, but is particularly different in the prothoracic compared to the meso- and metathoracic muscles (Marquardt 1940). In the mesothorax, which is the longest segment, the protractor is positioned ventrally, while the retractor muscle is situated dorsally above the protractor (see Fig. 3.1.1). Both muscles are anteriorly to the coxae (Igelmund 1980, Hessenbruch 2006) and project to attach to the thorax at about 200 - 700 μm anterior to the coxa. The same is true for the metathorax, although, the metathorax is shorter compared to the mesothorax.

The prothoracic segment is even shorter than the meso- and metathorax, and has, therefore, the shortest protractor and retractor muscles. In this segment, these muscles start in the ventral part of the thorax and run in very close proximity to one another directly dorsally. Since this close proximity and the bevel position made it impossible to distinguish clearly between these muscles, no evaluation of fiber composition was done for this segment.

Figure 3.1.1A shows a schematic with the location of the protractor and retractor in the mesothorax. Figure 3.1.1B shows an exemplary cross-section of the anterior (Bi) part of the dorsally situated protractor and the ventrally located retractor after acidic pre-incubation, while figure 3.1.1B shows the posterior part. Both muscles are artificially separated from each other by a white line. The values of the parameters measured are given in tables 3.1-4. The percentages of different fiber types are shown in figure 3.1.1.

Three different fiber types were present in these muscles. The fast contracting muscle fibers (short: fast fibers) made up most of the central parts of both muscles, while the slow contracting muscle fibers (short: slow fibers) formed a ribbon-like arrangement in the protractor and a bundle-like arrangement in the retractor, both towards the lateral and dorsal side of the muscles. The third fiber type, the intermediate fibers, is in both muscles mostly located around the slow fibers towards the cuticle.

3.1.1 *Mesothorax*

In the mesothorax, muscle fiber types and their distribution were analyzed in the anterior and posterior sub-sections of the muscles. The anterior part of the protractor had an average total cross-sectional area of 0.19 mm^2 (SD: 0.05), while the posterior part had approximately twice the size (mean: 0.36, SD: 0.16). The same tendency was seen for the retractor (anterior mean: 0.31 mm^2 , SD: 0.16; posterior: mean: 0.51 mm^2 , SD: 0.19).

The largest proportion of muscle fibers in the anterior and posterior protractor were the fast fibers which made up on average 53.6 % (SD: 33.7) of the anterior and 78.2 % (SD: 15.0) of the posterior mesothorax, while the slow fibers made up the smallest proportion of muscle fibers (anterior: 2.4 %, SD: 1.4; posterior: 10.4, SD: 5.1). The intermediate fibers covered between 44.1 % (SD: 34.8) in the anterior and 11.3 % (SD: 10.4) in the posterior region.

In contrast to this fiber type distribution, in the anterior and posterior retractor, the fast and intermediate fibers covered approximately the same area (fast: anterior: 37.3 %, SD: 15, posterior: 42.5 %, SD: 42.5; intermediate: anterior: 45.3 %, SD: 18.4, posterior: 46.2 %, SD: 18.8). Again, the slow fibers made up the smallest proportion of the muscle (anterior: 16.9 %, SD: 7.4; posterior: 11.3, SD: 2.7). The amount of slow and intermediate fibers differed significantly between the anterior and posterior sub-sections, while the proportion of fast fibers did not differ significantly from each other between the parts of the muscle.

In summary, in the mesothorax the majority of the protractor and retractor were made up of fast and intermediate fibers, while slow fibers made up only a small fraction of the muscle.

3.1.2 *Metathorax*

In the metathorax, muscle fiber types and their distribution were equally analyzed in the anterior and posterior sub-sections of the muscles. The anterior part of the protractor had a total cross-sectional area of 0.23 mm^2 (SD: 0.08), while the posterior part had approximately twice the size (mean: 0.4, SD: 0.09). In the retractor, on the other hand, the total cross-sectional area did not differ that much between the anterior (mean: 0.3, SD: 0.09) and posterior (mean: 0.32, SD: 0.1) part.

As before for the mesothorax, three different fiber types were present in these muscles. Again, the fast and intermediate muscle fibers covered the largest fraction of the protractor muscle, in both, the anterior (fast: mean: 56.0 %, SD: 37.9; intermediate: 43.9 %, SD: 37.7) and the posterior part (fast: mean: 35.4 %, SD: 21.5; intermediate: mean: 57.8 %,

SD: 25.1). The same is true for the anterior (fast: mean: 31.6 %, SD: 23.9; intermediate: 35.2 %, SD: 27.8) and posterior (fast: mean: 25.5 %, SD: 10.0; intermediate: 45.8 %, SD: 12.3) retractor. The slow fibers made up the smallest fraction of the anterior (mean: 0.2 %, SD: 0.4) and posterior (mean: 6.8 %, SD: 4.3) protractor, whereas they covered up to one-third in the anterior (mean: 33.2 %, SD: 11.1) and posterior (mean: 28.6 %, SD: 4.5) retractor. Taking this together, the metathoracic retractor had more slow contracting muscle fibers than the mesothoracic one, while the proportion of fast and intermediate fibers did not differ significantly from each other.

In summary, the metathoracic protractor consisted only in small portion of slow contracting muscle fibers, whereas fast and intermediate fibers together made up the largest portion of the muscle. The retractor, on the other hand, was made up of up to one-third of slow contracting muscle fibers.

Taken all together, the retractor of the meso- and metathorax contained more slow and fewer fast fibers than the protractor, while the amount of intermediate fibers in approximately the same. However, the amount of slow fibers in the metathoracic anterior retractor is prominent, as it made up to one-third of the muscle in total.

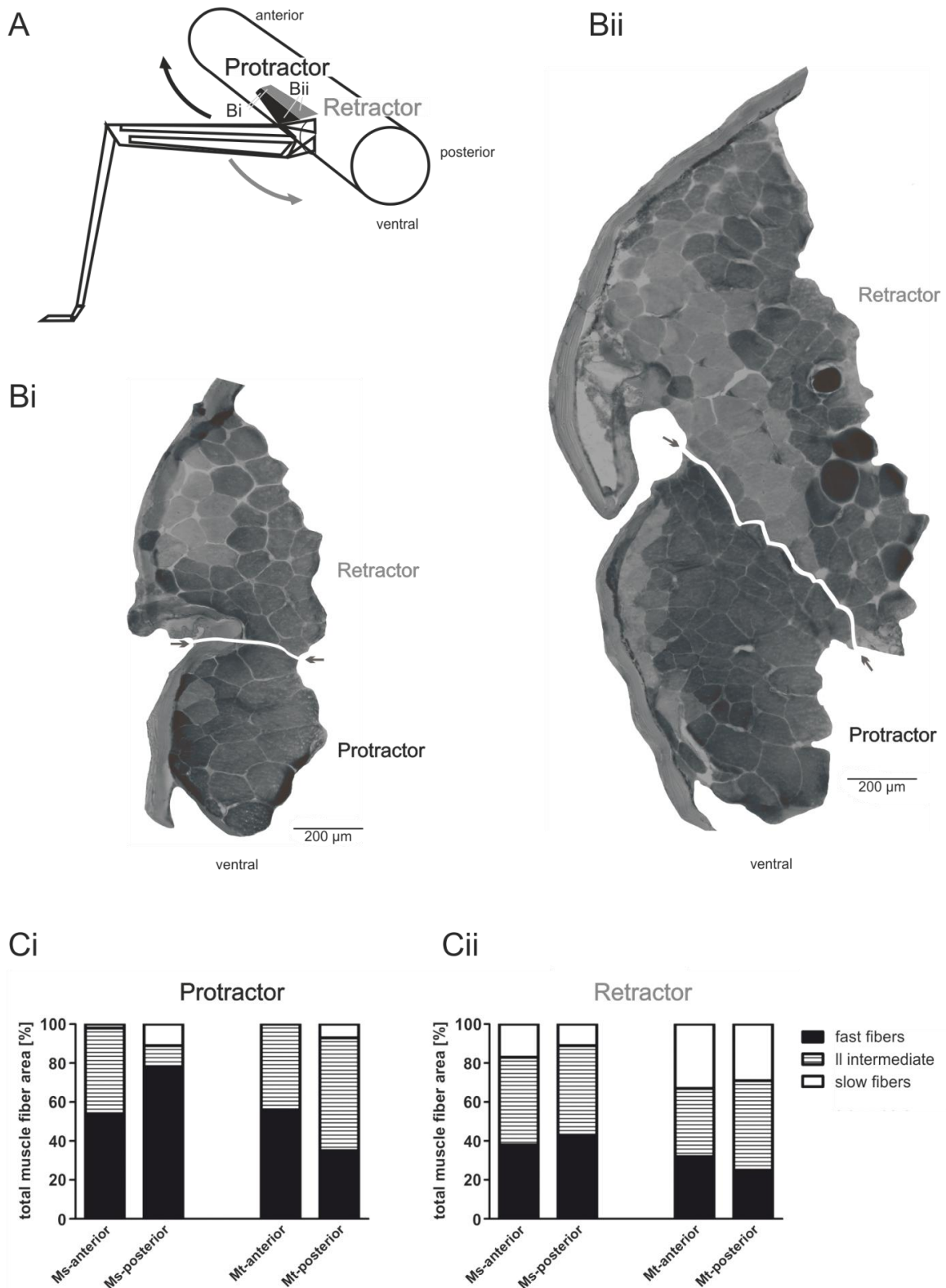


Fig. 3.1.1: Characterization of muscle fibers using mATPase staining procedure in the *protractor* and *retractor coxae*. A) Schematic drawing of a stick insect leg with its muscles protractor (black) and retractor (gray). B) Example section of the anterior (Bi) and posterior (Bii) part of the mesothoracic protractor and retractor after acidic pre-incubation. The arrows mark the artificial border between both muscles. C) Percentages of the muscle fiber types normalized to the respective maximum cross-sectional area in the meso- (Ms) and metathoracic (Mt) protractor (Ci) and retractor (Cii) (figure also used in the submitted MS Godlewska-Hammel et al. 2016).

3.2 Levator and Depressor Trochanteris

The coxae of the three thoracic segments all have roughly the same size and structure. In all segments the anatomical organization of both muscles is the same: the *levator trochanteris* (short: levator) is located dorsally, and arises in the coxa and attaches to the trochanter's dorsal edge (see Fig. 3.2). The ventrally located *depressor trochanteris* (short: depressor), on the other hand, arises partly in the coxa and partly in the thorax (Schmitz 1986, Hessenbruch 2006). One can easily distinguish between these two muscles due to their muscle fiber arrangement. Functionally, the levator is a swing phase muscle, responsible for lifting the leg, while the depressor is a stance phase muscle, responsible for lowering the leg and providing lift to the body. Since both muscles are short, they were not subdivided in the following analysis.

Figure 3.2.1A shows a schematic with the location of the levator and depressor in the mesothorax. Figure 3.2.1B shows an exemplary cross-section of the dorsally situated levator and the ventrally located depressor after acidic pre-incubation. Both muscles are artificially separated from each other by a white line. The values of the parameters measured are given in tables 3.1-4. The percentages of different fiber types are shown in figure 3.2.1.

Three different fiber types were present in both muscles. The fast contracting muscle fibers (short: fast fibers) were mostly located in the ventral part of the muscle, towards the center of the coxa, while slow and intermediate fibers were found interspersed at the dorsal side of the muscle towards the cuticle.

3.2.1 Prothorax

In the prothorax, muscle fiber types and their distribution was analyzed in the muscles. The levator showed a total cross-sectional area of 0.22 mm^2 (SD: 0.04), while the depressor had approximately twice the size (mean: 0.41 mm^2 , SD: 0.07).

The largest proportion of muscle fibers in the levator and depressor was taken up by fast fibers, which made up on average 67.6 % (SD: 15.7) and 48.3 % (SD: 15.2), respectively. The slow fibers, in contrast to this, made up the smallest proportion of muscle fibers in both muscles (levator: 5.7 %, SD: 4.4; depressor: 11.1, SD: 2.7). The intermediate fibers

covered on average 26.7 % (SD: 17.7) in the levator, and 40.6 % (SD: 17.7) in the depressor.

In summary, in the prothoracic levator and depressor, the majority of fibers are of the fast type, the intermediate ones made up the second largest group, and in both muscles the slow contracting muscle fibers covered the smallest area.

3.2.2 *Mesothorax*

In the mesothorax, the levator had a cross-sectional area of about 0.26 mm² (SD: 0.05), which was slightly larger compared to the prothoracic one. In contrast, the depressor had a slightly smaller area (mean: 0.38 mm², SD: 0.12) compared to the prothoracic depressor.

In the mesothoracic levator and depressor, again three different fiber types were present. The fast muscle fibers covered the largest fraction of the levator (mean: 72.3 %, SD: 11.1) and the depressor (mean: 55.8 %, SD: 13.2), while the intermediate fibers covered either 12.9 % (SD: 9.8) in the levator, or even 27.5 % (SD: 20.6) in the depressor. The slow fibers made up the smallest fraction in both muscles (levator: mean: 12.8 %, SD: 4.5; depressor: mean: 16.3 %, SD: 8.7). In two different experiments, a fourth fiber type (dark-dark intermediate) that was strongly stained after acidic and alkaline pre-incubation, was found as one single fiber.

In summary, the levator and the depressor were mostly made up of fast contracting muscle fibers, followed by the amount of intermediate (II) muscle fibers. The area covered by slow fibers was clearly smaller than of the beforehand mentioned fiber types. In this segment a fourth fiber type (dd intermediate) made up the smallest fraction.

3.2.3 *Metathorax*

In the metathorax, both, the levator and the depressor, had larger cross-sectional areas compared to the pro- and mesothorax (levator: mean: 0.36 mm², SD: 0.08; depressor: mean: 0.48 mm², SD: 0.09).

In the metathorax, the fiber type distribution was similar to the one in the mesothorax. Again, the fast contracting muscle fibers made up the largest proportion of the levator (mean: 72.8 %; SD: 12.3) and depressor muscles (mean: 49.0 %; SD: 9.2), while the intermediate fibers formed the second major group (levator: 15.7 %, SD: 16.4; depressor: mean: 32.7 %, SD: 11.5). The slow contracting muscle fibers made up only 11.5 % (SD: 6.7) in the levator, and 18.3 % (SD: 3.7) in the depressor muscle.

In summary, the metathoracic levator and depressor trochanteris were mostly made up of fast contracting muscle fibers, followed by the amount of intermediate muscle fibers. Slow fibers covered the smallest area in both analyzed muscles.

Taken all together, in all thoracic segments the levator mostly consisted of fast contracting muscle fibers, while the amount of slow muscle fibers was significant reduced to the fast ones in all segments. The depressor muscle, on the other hand, consisted in the prothorax mostly of fast and intermediate muscle fibers, while in the meso- and metathoracic depressor the amount of intermediate muscle fibers was reduced, although in no case significantly. Additionally, an increase in slow fiber proportion was observed from prothorax, through meso- and metathorax.

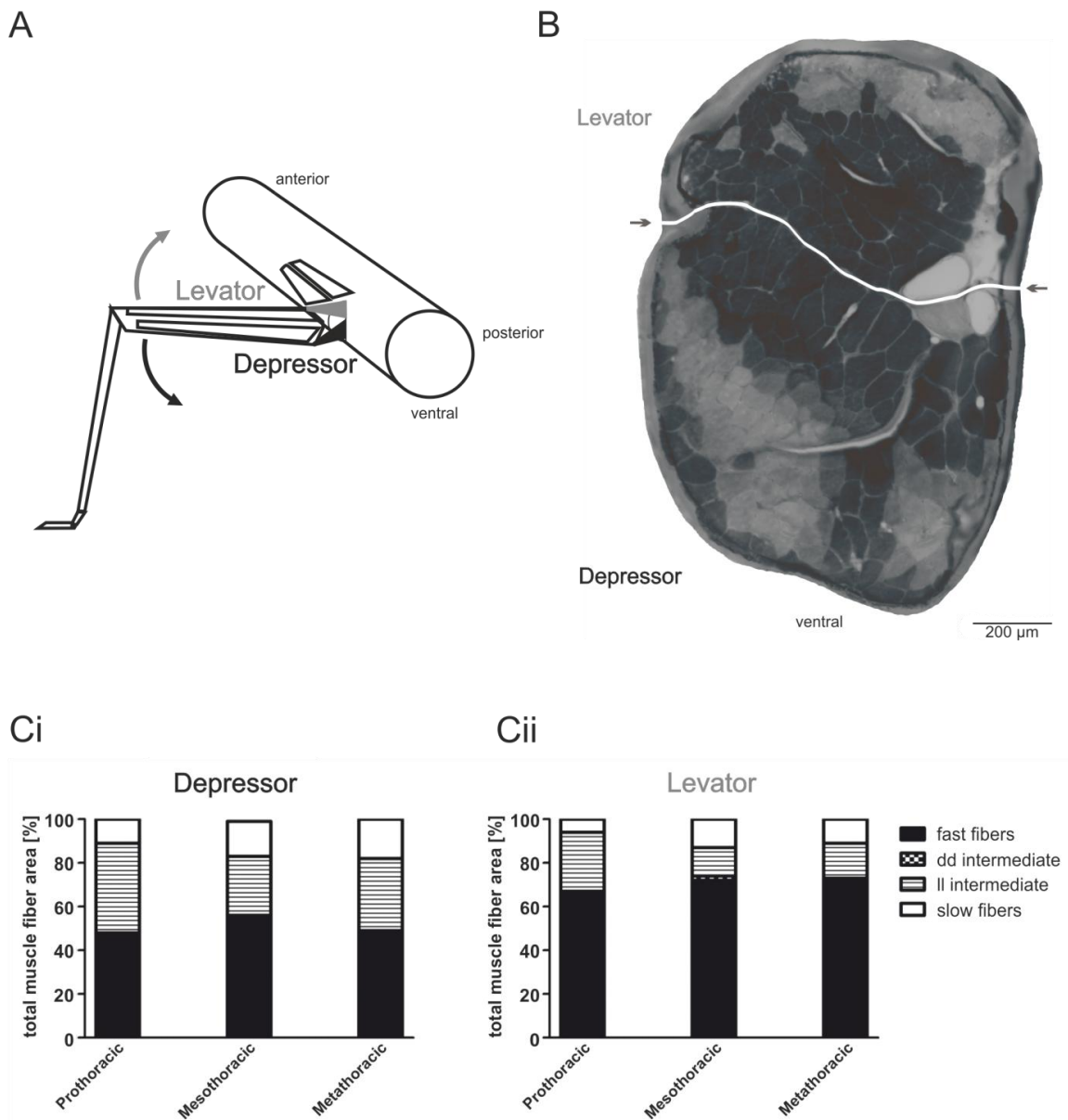


Fig. 3.2.1: Characterization of muscle fibers using mATPase staining procedure in the *levator* and *depressor trochanteris*. A) Schematic drawing of a stick insect leg with its muscles levator (gray) and depressor (black). B) Example section of the mesothoracic levator and depressor after acidic pre-incubation. The arrows mark the artificial border between both muscles. C) Percentages of the muscle fiber types normalized to the respective maximum cross-sectional area in the pro-, meso-, and metathoracic depressor (Ci) and levator (Cii) (figure also used in the submitted MS Godlewska-Hammel et al. 2016).

3.3 Extensor and Flexor Tibiae

The stick insect femora contain the ventrally located *flexor tibiae* and the dorsally located *extensor tibiae* (short: flexor and extensor, respectively) (see Fig. 3.3.1), which is of smaller size and separated from a flexor by a tendon. These femoral muscles move the tibia around the femur-tibia joint and are responsible its extension and flexion (Rosenbaum et al. 2010).

The femora itself differ in their anatomy depending on the leg in question: while the meso- and metathoracic femora are similar in structure, the prothoracic femora are longer and have a narrowing close to the coxa. Independent of the thoracic segment, the height of every femur decreases from proximal to distal, while the width increases, causing the largest cross-sectional area to be in the center of each femur. The muscle fibers of the extensor originate at the dorsal roof of the femur and attach at a tendon, while the flexor muscle fibers span between the side walls of the femur and the flexor tendon (Bässler 1983).

Figure 3.3.1A shows a schematic with the location of the flexor and extensor in the mesothorax. Figure 3.3.1B shows an exemplary cross-section of the distal (Bi) part of the dorsally situated extensor and the ventrally located flexor after acidic pre-incubation, while figure 3.3.1Bii and Biii show the medial and proximal part, respectively. Both muscles are artificially separated from each other by a white line. The values of the parameters measured are given in tables 3.1-4. The percentages of different fiber types are shown in figure 3.3.1.

Three different fiber types were present in these muscles. In both muscles, the amount of slow contracting muscle fibers (short: slow fibers) decreased from distal to proximal, and vice versa for fast contracting muscle fibers (short: fast fibers). While in the proximal part of the flexor, fast fibers formed the majority and slow fibers were only found interspersed along the midline of the flexor at the level of the tendon, in the medial part, fast fibers were located more ventrally of the tendon forming a wide band, and several slow fibers formed a stretch that spanned from the anterior to the posterior part of the cuticle. In the most distal area, the amount of fast fibers decreased. These fibers were concentrated at the center of the flexor, while that increased number of slow muscle fibers was located towards the cuticle of the femur. In the proximal and medial part of the extensor, on the other hand,

slow fibers were present in the center of the muscle, only, while fast fibers formed again the majority and were spread all around. The amount of slow fibers increased towards the most distal part. There, slow fibers formed a band from dorsal to ventral through the center of the muscle, whereas the fast fibers are mostly located towards the cuticle and the tendon.

3.3.1 *Prothorax*

The proximal part of the extensor had a total averaged cross-sectional area of 0.09 mm^2 (SD: 0.02), while the medial and distal part had a cross-sectional area of 0.07 mm^2 and were therefore slightly smaller (SD_{med} : 0.02, SD_{dis} : 0.04). Compared to this, the flexor had a larger cross-sectional area in all three sub-sections. In the proximal part it was about 0.47 mm^2 (SD: 0.06), in the medial part 0.5 mm^2 (SD: 0.11), and in the distal part about 0.34 mm^2 (SD: 0.08).

As already mentioned above, three different fiber types were present in the prothoracic femoral muscles. In the proximal extensor and flexor, the largest proportion were the intermediate fibers (extensor: mean: 52.1 %, SD: 10.2; flexor: mean: 76.1 %, SD: 10.3), followed by the fast contracting muscle fibers (extensor: mean: 44.9 %, SD: 11.8; flexor: mean: 23.1 %, SD: 10.4), while the slow contracting muscle fibers were only occasionally present in both muscles (extensor: mean: 3.0 %, SD: 1.9; flexor: mean: 0.9 %, SD: 0.8). The distribution slightly differed in the medial part of both muscles. Here, in the extensor the amount of fast fibers increased up to 59.0 % (SD: 17.6) and for the slow fibers up to 4.4 % (SD: 3.2), while the amount of intermediate fibers decreased to one-third (36.7 %, SD: 15.8). The amount of slow fibers increased in the medial part of the flexor, too, to 4.4 % (SD: 1.4), at the cost of intermediate fibers (70.5 %, SD: 12.9), while the amount of fast fibers was almost constant (24.9 %, SD: 12.2). In the distal part of the extensor and flexor, the amount of slow fibers increased (extensor: mean: 17.3 %, SD: 8.6; flexor: mean: 17.1 %, SD: 4.2), whereas the amount of fast fibers decreased (extensor: mean: 32.8 %, SD: 9.0; flexor: mean: 16.4 %, SD: 3.2) which, in case of the flexor, was nearly the same amount of fast as of slow fibers. Here, in both muscles, the intermediate fibers formed the largest proportion (extensor: mean: 49.9 %, SD: 13.2; flexor: mean: 66.5 %, SD: 3.5).

In summary, in the prothoracic extensor, slow fibers formed the significantly smallest proportion, while in the proximal and distal sub-sections the intermediate fibers formed the majority. In the prothoracic flexor, again, the amount of slow fibers was in most cases

significantly smaller than that of fast and intermediate fibers. Only in the most distal part, the amount of fast and slow fibers was nearly the same in both muscles.

3.3.2 Mesothorax

In the mesothorax, in the proximal part of the extensor showed a total cross-sectional area of 0.06 mm^2 (SD: 0.01), while the medial and distal part had a cross-sectional area of 0.08 mm^2 and 0.1 mm^2 , respectively, and were therefore slightly larger (SD_{med}: 0.01, SD_{dis}: 0.03). Compared to the extensor, the flexor had a much larger cross-sectional area in all three sub-sections. In the proximal part it was on average 0.3 mm^2 (SD: 0.05), in the medial part 0.43 mm^2 (SD: 0.05), and in the distal part the cross-sectional area was 0.29 mm^2 (SD: 0.05).

Again, three different fiber types were present in the mesothoracic extensor and flexor. While the amount of slow fibers increased from proximal to distal in the extensor (Ext_{prox}: 0.7 %, SD: 1.6, Ext_{med}: 2.4 %, SD: 3.0, Ext_{dis}: 22.8 %, SD: 10.1) and flexor (Flex_{prox}: 1.2 %, SD: 1.9, Flex_{med}: 3.3 %, SD: 1.6, Flex_{prox}: 25.8 %, SD: 11.5), the amount of fast fibers decreased in both muscles concomitantly (Ext_{prox}: 59.6 %, SD: 23.3, Ext_{med}: 49.8 %, SD: 31.5, Ext_{dis}: 33.8 %, SD: 18.2; Flex_{prox}: 32.8 %, SD: 20.2, Flex_{med}: 20.6 %, SD: 6.4, Flex_{prox}: 10.5 %, SD: 5.8). The amount of intermediate fibers, on the other hand, stayed roughly the same in all sections for each muscle (Ext_{prox}: 39.7 %, SD: 22.3, Ext_{med}: 47.0 %, SD: 32.8, Ext_{dis}: 43.1 %, SD: 22.8; Flex_{prox}: 66.0 %, SD: 18.9, Flex_{med}: 76.1 %, SD: 7.6, Flex_{prox}: 63.7 %, SD: 10.9).

In summary, in the mesothoracic extensor and flexor the amount of slow fibers increased from proximal to distal, while it was the opposite for the fast contracting muscle fibers. Besides the distal part of the extensor, in all other sub-sections of the extensor and flexor the proportion of slow fibers was significantly different from fast and intermediate fibers.

All in all, the fiber type distribution was comparable to that in the prothoracic extensor and flexor.

3.3.1 Metathorax

In the metathorax, in the proximal part of the extensor had a total cross-sectional area of 0.06 mm^2 (SD: 0.01), and the medial and distal part had a cross-sectional area of 0.07 mm^2 (SD_{med}: 0.02, SD_{dis}: 0.01). Compared to this, the flexor had a larger cross-sectional area in all three sub-sections. In the proximal part it was about 0.34 mm^2 (SD: 0.05), in the medial

part 0.39 mm^2 (SD: 0.08), and in the distal part the cross-sectional area was about 0.31 mm^2 (SD: 0.09).

Again, three different fiber types were present in the metathoracic femoral muscles. While the amount of slow fibers increased from proximal to distal in the extensor (Ext_{prox} : 6.3 %, SD: 3.0, Ext_{med} : 8.5 %, SD: 5.0, Ext_{dis} : 29.2 %, SD: 29.5) and flexor ($\text{Flex}_{\text{prox}}$: 0.6 %, SD: 1.0, Flex_{med} : 9.8 %, SD: 8.5, $\text{Flex}_{\text{prox}}$: 25.9 %, SD: 24.8), the amount of fast fibers decreased in both muscles at the same time (Ext_{prox} : 47.3 %, SD: 29.8, Ext_{med} : 38.1 %, SD: 15.4, Ext_{dis} : 29.8 %, SD: 5.1; $\text{Flex}_{\text{prox}}$: 22.9 %, SD: 12.8, Flex_{med} : 20.9 %, SD: 13.2, $\text{Flex}_{\text{prox}}$: 18.1 %, SD: 8.7). The amount of intermediate fibers, as already seen in the mesothorax, stayed roughly the same in all sections in the extensor (Ext_{prox} : 46.3 %, SD: 26.8, Ext_{med} : 53.5 %, SD: 16.4, Ext_{dis} : 41.0 %, SD: 32.3), whereas the amount intermediate fibers decreased from proximal to distal in the flexor ($\text{Flex}_{\text{prox}}$: 76.4 %, SD: 13.6, Flex_{med} : 69.2 %, SD: 18.2, $\text{Flex}_{\text{prox}}$: 55.5 %, SD: 27.1).

In summary, in the metathoracic extensor and flexor the amount of slow fibers increased from proximal to distal, while it was the other way around for the fast contracting muscle fibers. In this segment, only in the medial extensor and the proximal flexor the amount of slow and fast muscle fibers was significantly different from one another.

Taken all together, in the femoral muscles of all segments the proportion of slow fibers increased from proximal to distal, while the proportion of fast fibers decreased from proximal to distal. The intermediate fibers stayed nearly constantly the same for each muscle.

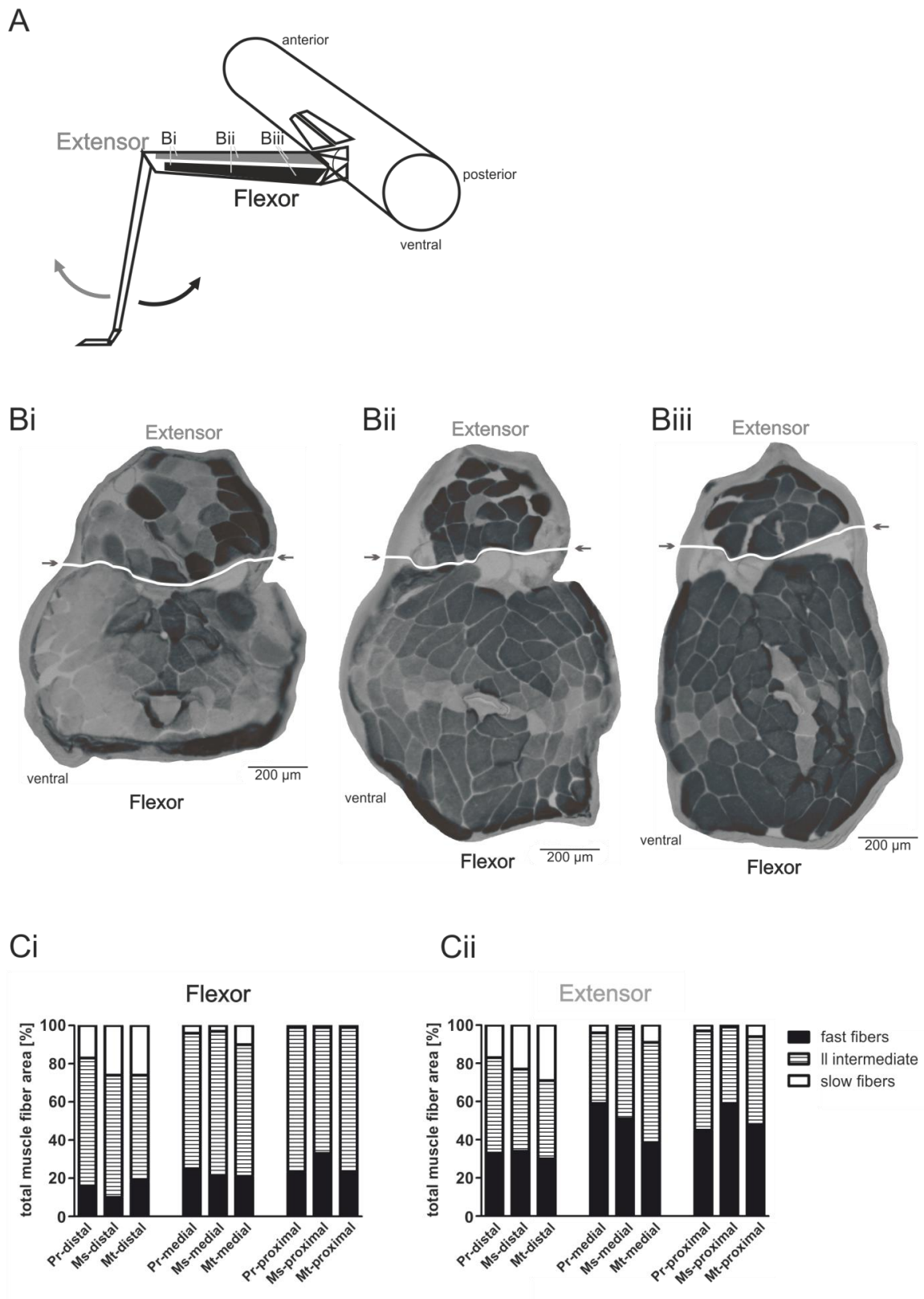


Fig. 3.3.1: Characterization of muscle fibers using mATPase staining procedure in the *extensor* and *flexor tibiae*. A) Schematic drawing of a stick insect leg with its muscles *extensor* (gray) and *flexor* (black). B) Example section of the distal (Bi), medial (Bii), and proximal (Biii) mesothoracic *extensor* and *flexor* after acidic pre-incubation. The arrows mark the artificial border between both muscles. C) Percentages of the muscle fiber types normalized to the respective maximum cross-sectional area in the pro-, meso-, and metathoracic *flexor* (Ci) and *extensor* (Cii) (figure also used in the submitted MS Godlewska-Hammel et al. 2016).

Table 3.1: Averaged muscle cross-sectional area (in mm²). Analyzed thoracic segments: prothorax (Pr), mesothorax (Ms), and metathorax (Mt), and their division into sub-sections anterior (ant) and posterior (post) for protractor and retractor, as well as into proximal (prox), medial (med), and distal (dist) for extensor and flexor (table also used in the submitted MS Godlewska-Hammel et al. 2016).

	thoracic segment	sub-section	mean	SD
Protractor	Ms	ant	0.19	0.05
	Ms	post	0.36	0.16
	Mt	ant	0.23	0.08
	Mt	post	0.4	0.09
Retractor	Ms	ant	0.31	0.16
	Ms	post	0.51	0.19
	Mt	ant	0.3	0.09
	Mt	post	0.32	0.1
Levator	Pr		0.22	0.04
	Ms		0.26	0.05
	Mt		0.36	0.08
Depressor	Pr		0.41	0.07
	Ms		0.38	0.12
	Mt		0.48	0.09
Extensor	Pr	prox	0.09	0.02
	Pr	med	0.07	0.02
	Pr	dis	0.07	0.04
	Ms	prox	0.06	0.01
	Ms	med	0.08	0.01
	Ms	dis	0.1	0.03
	Mt	prox	0.06	0.01
	Mt	med	0.07	0.02
	Mt	dis	0.07	0.01
Flexor	Pr	prox	0.47	0.06
	Pr	med	0.5	0.11
	Pr	dis	0.34	0.08
	Ms	prox	0.3	0.05
	Ms	med	0.43	0.05
	Ms	dis	0.29	0.05
	Mt	prox	0.34	0.05
	Mt	med	0.39	0.08
	Mt	dis	0.31	0.09

Table 3.2: Averaged percentage of muscle fiber types in the individual muscles after mATPase classification (in %). Classification into the groups slow contracting muscle fibers (slow), fast contracting muscle fibers (fast) and intermediate contracting muscle fibers (int). Analyzed thoracic segments: prothorax (Pr), mesothorax (Ms), and metathorax (Mt), and their division into sub-sections anterior (ant) and posterior (post) for protractor and retractor, as well as into proximal (prox), medial (med), and distal (dist) for extensor and flexor (table also used in the submitted MS Godlewska-Hammel et al. 2016).

	thoracic segment	sub-section	slow		fast		int	
			mean	SD	mean	SD	mean	SD
Protractor	Ms	ant	2.4	1.4	53.6	33.7	44.1	34.8
	Ms	post	10.4	5.1	78.2	15.0	11.3	10.4
	Mt	ant	0.2	0.4	56.0	37.9	43.9	37.7
	Mt	post	6.8	4.3	35.4	21.5	57.8	25.1
Retractor	Ms	ant	16.9	7.4	37.3	15.0	45.3	18.4
	Ms	post	11.3	2.7	42.5	18.3	46.2	18.8
	Mt	ant	33.2	11.1	31.6	23.9	35.2	27.8
	Mt	post	28.6	4.5	25.5	10.0	45.8	12.3
Levator	Pr		5.7	4.4	67.6	15.7	26.7	17.7
	Ms		12.8	4.5	72.3	11.1	12.9	9.8
	Mt		11.5	6.7	72.8	12.3	15.7	16.4
Depressor	Pr		11.1	2.7	48.3	15.2	40.6	17.7
	Ms		16.3	8.7	55.8	13.2	27.5	20.6
	Mt		18.3	3.7	49.0	9.2	32.7	11.5
Extensor	Pr	prox	3.0	1.9	44.9	11.8	52.1	10.2
	Pr	med	4.4	3.2	59.0	17.6	36.7	15.8
	Pr	dis	17.3	8.6	32.8	9.0	49.9	13.2
	Ms	prox	0.7	1.6	59.6	23.3	39.7	22.3
	Ms	med	2.4	3.0	49.8	31.5	47.0	32.8
	Ms	dis	22.8	10.1	33.8	18.2	43.1	22.8
	Mt	prox	6.3	3.0	47.3	29.8	46.3	26.8
	Mt	med	8.5	5.0	38.1	15.4	53.5	16.4
	Mt	dis	29.2	29.5	29.8	5.1	41.0	32.3
Flexor	Pr	prox	0.9	0.8	23.1	10.4	76.1	10.3
	Pr	med	4.4	1.4	24.9	12.2	70.5	12.9
	Pr	dis	17.1	4.2	16.4	3.2	66.5	3.5
	Ms	prox	1.2	1.9	32.8	20.2	66.0	18.9
	Ms	med	3.3	1.6	20.6	6.4	76.1	7.6
	Ms	dis	25.8	11.5	10.5	5.8	63.7	10.9
	Mt	prox	0.6	1.0	22.9	12.8	76.4	13.6
	Mt	med	9.8	8.5	20.9	13.2	69.2	18.2
	Mt	dis	25.9	24.8	18.1	8.7	55.5	27.1

Table 3.3: Statistical results for intersegmental comparison of the different muscle fiber types using the paired t-test, after classification into the groups slow contracting muscle fibers (slow), fast contracting muscle fibers (fast) and intermediate contracting muscle fibers (int). Taking into account that ns \triangleq not significant, * \triangleq $p < 0.05$, ** \triangleq $p < 0.01$, *** \triangleq $p < 0.001$, **** \triangleq $p < 0.0001$). Analyzed thoracic segments: prothorax (Pr), mesothorax (Ms), and metathorax (Mt), and their division into sub-sections anterior (ant) and posterior (post) for protractor and retractor, as well as into proximal (prox), medial (med), and distal (dist) for extensor and flexor (table also used in the submitted MS Godlewska-Hammel et al. 2016).

	thoracic segment	sub-section	slow vs. fast	slow vs. int	fast vs. int	n
Protractor	Ms	ant	**	*	ns	7
	Ms	post	***	ns	**	6
	Mt	ant	**	*	ns	7
	Mt	post	**	**	ns	7
Retractor	Ms	ant	*	*	ns	7
	Ms	post	**	**	ns	6
	Mt	ant	ns	ns	ns	7
	Mt	post	ns	*	ns	6
Levator	Pr		***	ns	ns	5
	Ms		***	ns	**	5
	Mt		****	ns	**	6
Depressor	Pr		***	*	ns	6
	Ms		**	ns	ns	4
	Mt		**	ns	ns	4
Extensor	Pr	prox	***	****	ns	6
	Pr	med	**	**	ns	6
	Pr	dis	*	*	ns	6
	Ms	prox	**	**	ns	6
	Ms	med	*	*	ns	6
	Ms	dis	ns	ns	ns	6
	Mt	prox	ns	ns	ns	2
	Mt	med	*	*	ns	4
	Mt	dis	ns	ns	ns	4
Flexor	Pr	prox	**	****	**	5
	Pr	med	**	****	**	6
	Pr	dis	ns	***	**	4
	Ms	prox	*	***	ns	6
	Ms	med	***	****	***	6
	Ms	dis	*	**	***	6
	Mt	prox	*	**	*	4
	Mt	med	ns	*	ns	4
	Mt	dis	ns	ns	ns	4

Table 3.4: Statistical results for intrasegmental comparison of the different muscle fiber types between analyzed muscle regions using the paired t-test, after classification into the groups slow contracting muscle fibers (slow), fast contracting muscle fibers (fast) and intermediate contracting muscle fibers (int). Taking into account that ns \triangleq not significant, * \triangleq $p < 0.05$, ** \triangleq $p < 0.01$, *** \triangleq $p < 0.001$, **** \triangleq $p < 0.0001$. Analyzed thoracic segments: prothorax (Pr), mesothorax (Ms), and metathorax (Mt), and their division into sub-sections anterior (ant) and posterior (post) for protractor and retractor, as well as into proximal (prox), medial (med), and distal (dist) for extensor and flexor (table also used in the submitted MS Godlewska-Hammel et al. 2016).

	thoracic segment	compared sub-section	compared thoracic segments	slow vs. slow	int vs. int	fast vs. fast	n
Protractor	Ms	ant vs. post		**	*	ns	6
	Mt	ant vs. post		**	ns	ns	7
		ant	Ms vs. Mt	**	ns	ns	
		post	Ms vs. Mt	ns	**	**	
Retractor	Ms	ant vs. post		ns	ns	ns	6
	Mt	ant vs. post		ns	ns	ns	6
		ant	Ms vs. Mt	**	ns	ns	
		post	Ms vs. Mt	**	ns	ns	
Levator			Pr vs. Ms	*	ns	ns	5
			Pr vs. Mt	ns	ns	ns	5
			Ms vs. Mt	ns	ns	ns	6
Depressor			Pr vs. Ms	ns	ns	ns	6
			Pr vs. Mt	*	ns	ns	4
			Ms vs. Mt	ns	ns	ns	4
Extensor	Pr	dist vs. med		**	ns	**	6
	Pr	dist vs. prox		**	ns	ns	6
	Pr	med vs. prox		ns	ns	ns	6
	Ms	dist vs. med		**	ns	ns	6
	Ms	dist vs. prox		***	ns	ns	6
	Ms	med vs. prox		ns	ns	ns	6
	Mt	dist vs. med		ns	ns	ns	4
	Mt	dist vs. prox		ns	ns	ns	2
	Mt	med vs. prox		ns	ns	ns	2
Flexor	Pr	dist vs. med		***	ns	ns	4
	Pr	dist vs. prox		****	ns	ns	4
	Pr	med vs. prox		***	ns	ns	5
	Ms	dist vs. med		***	*	*	6
	Ms	dist vs. prox		***	ns	*	6
	Ms	med vs. prox		ns	ns	ns	6
	Mt	dist vs. med		ns	ns	ns	4
	Mt	dist vs. prox		ns	ns	ns	4
	Mt	med vs. prox		ns	ns	ns	4

CHAPTER 4

Motor Activity during Curve Walking

All forms of locomotion emerge from a complex interaction of neuronal activity, muscle contraction, sensory feedback and the environment (Orlovsky et al. 1999). Depending on the type and the speed of locomotion, muscle groups are activated differently and generate various forms of locomotion. Antagonistic muscles of the two body sides are in alternation active to generate movements like swimming (lamprey: Cohen & Wallén 1980; turtle: Davenport et al. 1984) or slow walking (cat: Miller et al. 1975), whereas flying depends on a synchronous activation of the homologue muscles on the two body sides (locust: Wilson 1961; Tobalske 2007). In the stick insect, much is known about the generation of straight walking and the local neuronal activity underlying basic locomotor patterns in the single leg (Büschges 2005, Ludwar et al. 2005a, Borgmann et al. 2007). For the straight walking stick insect with only one front leg left walking on a treadmill, Ludwar et al. (2005a) showed that the mesothoracic protractor MN activity was modulated in nine of ten animals depending on the front leg step cycle. More specifically, mesothoracic protractor activity was reduced during front leg stance, and the retractor activity was alternating with the protractor one. Borgmann et al. (2007) showed in the same experimental setting, that retractor activity reached its maximum between 30° and 60° of front leg step cycle, and sharply decreased at phase angles above 180°. At this angle, on the other hand, protractor MN activity increased and reached its maximum between 270° and 300°. The MN activity of the next distal joint, the coxa-trochanteral joint, was also correlated with front leg

stepping (Ludwar et al. 2005a). Here, the authors showed that in four of five animals tested for modulation, levator activity was always greatest shortly after front leg stance phase, while the activity pattern of the antagonist was not so clear. While in two animals depressor activity was lowest during front leg stance phase, in four animals it was the other way around. In a fifth animal, no modulation was observed. For the most distal joint, Ludwar et al. (2005a) found that in four tested animals the activity of fast *extensor tibiae* MNs (FETi) were correlated with front leg stepping, whereas the slow *extensor tibiae* MNs (SETi) showed such a modulation in three animals. In three experiments, electromyography (EMG) recordings of the flexor revealed that its activity was modulated in phase with front leg stepping and alternating to the antagonistic extensor activity. Hence, in all six major leg MN pools of the mesothorax a general increase of activity was observed when the front leg performed straight stepping movements on a treadmill. In addition, all MN pools showed a specific pattern of modulation (Ludwar et al. 2005a).

As knowing so much about the local neuronal activity during straight walking, the question arises, in how far these local neuronal activities are changed during adaptive movements.

However, the knowledge on local segmental activity during adaptive locomotion – like turning movements – is scarce (stick insect: Gruhn et al. 2006, Hellekes et al. 2012; cockroach: Martin et al. 2015). In curve walking insects, the outside and inside legs behave with different kinematics (Jindrich & Full 1999, Dürr & Ebeling 2005, Gruhn et al. 2009b). In stick insects, the inside front- and middle leg pull the animal into the targeted direction, while the respective outside legs push the animal into that direction. Both hind legs, on the other hand, push the animal into the opposite direction of the curve (Jander 1982, Dürr & Ebeling 2005, Gruhn et al. 2009b). Experiments with reduced preparations with only one or two legs showed that each leg for itself – lacking the influence of its neighboring legs – can express typical inside or outside turning kinematics (Gruhn et al. 2009b). Furthermore, Rosenbaum et al. (2010) demonstrated, when comparing the muscle activity in the six major leg muscles of the stick insect during forward and backward movements, that the muscle activity differed between these movement types only in the most proximal leg joint, the subcoxal joint. Therefore, besides the above mentioned leg specificities, a joint specific motor activity is present during inside and outside turns. At the same time, the local sensory processing is modified in a context specific way: while an activation of the femoral chordotonalorgan in the inside middle leg resulted in a reflex reversal, it did not occur in an outside middle leg (Hellekes et al. 2012). All in all, though, relatively little insight exists, what kind of changes occur, neither in the descending signals nor in the local

activity in thoracic ganglia, that cause the body side specific motor output (Gruhn et al. 2009b, Rosenbaum et al. 2010). It is well known that turning is induced by descending neuronal signals targeting the same neuronal networks that are also responsible for producing the basic locomotor pattern (lamprey: McClellan 1984; cockroach: Guo & Ritzmann 2013, Harley & Ritzmann 2010, Mu & Ritzmann 2008a; fruitfly: Strauss & Heisenberg 1993; zebrafish: Huang et al. 2013). Studies on lamprey revealed that during lateral turns the activity of motoneurons of one body side is increased by descending inputs from the brain stem, whereas the activity on the contralateral side is decreased (Fagerstedt et al. 2001, Fagerstedt & Ullén 2001, Grillner et al. 2008). In the turning lamprey, no uncoupling of both body sides is achieved. In terrestrial animals, on the other hand, such a decoupling would be necessary to generate turning. To gain more insight into the neuronal control of flexible motoneuronal activity it is of major importance to reveal what kind of modifications occur in local neuronal activity.

First insights into this complex topic were gained by Gruhn et al. (2016) who found that the motoneuronal activity of the subcoxal joint in a reduced stick insect preparation with only two front legs left is direction dependent. While the mesothoracic retractor activity is decreased and the protractor activity is increased and even modulated during inside turns, the activity is strikingly different during outside turns, where retractor activity is much stronger than protractor activity, and the retractor activity is not modulated in any case. This finding raises the question how the motoneuron (MN) pools of the other major leg joints are excited during turning movements, since it had also been shown that during forward and backward walking the only affected muscles are that of the subcoxal joint (Rosenbaum et al. 2010). On the other hand, Hellekes et al. (2012) showed that the extensor MNs are affected differently when the femoral chordotonal organ was stimulated during inside and outside turns. Since Borgmann et al. (2007) showed in a single leg preparation that straight stepping of the front leg induces alternating activity in the mesothoracic protractor and retractor MN pools, and only a general increase in the respective MN pools of the metathorax, it is interesting to see whether the MN pools of the meso- and metathorax behave similarly, or whether a thorax-segment specific influence is present during turning.

In this part of my PhD thesis, I therefore investigated the motor activity in the three major leg joints of the turning stick insect.

I analyzed the neuronal mechanisms underlying curve walking in the stick insect *Carausius morosus*, and, specifically, the effects of the descending input from the curve walking front legs on the meso- and metathoracic leg nerves and whether this input differs between inside- and outside-turning front legs. For this, I used a reduced preparation with all legs removed except the two forelegs and recorded extracellularly from the deafferented meso- and metathoracic leg nerves n12 (innervates *protractor coxae*), n15 (*retractor coxae*), C1 (*levator trochanteris*), C2 (*depressor trochanteris*), n13 (*extensor tibiae*) and from branches of nervus cruris that innervate the *flexor tibiae*. During these recordings, curve walking in tethered animals on a slippery surface was induced by a moving LED stripe pattern while recording video from above.

4.1 *Protractor and Retractor Coxae*

The meso- and metathoracic leg nerves nl2 and nl5 innervate the *protractor* and *retractor coxae* muscles, respectively. When these muscles contract, the leg is moved forward or backward. The nl2 ramifies into four branches, A-D, where branch A innervates pleurosternal muscles, B the tergopleural ventilatory muscles, C the *protractor coxae*, and D the tergotrochantinal muscle (Graham & Wendler 1981, Goldammer et al. 2012). Since the hook electrodes were mainly positioned shortly distal from the beginning of branch A (which had been cut off), extracellular recordings often showed rhythmic ventilatory activity (as reported in Graham & Wendler 1981). Further discrimination between individual motoneurons (MNs) was not possible because branch C alone contains the axons of 12-17 MNs, 4-5 dorsal unpaired median (DUM) cells, and the common inhibitor 1 (CI1), in branch C alone (Goldammer et al. 2012).

The nl5 is the first branch of the nervus cruris and ramifies into three branches, A, B, and p. While branches A and B innervate the *tergal retractor coxae*, branch p innervates the *sternal remotor* and the *adductor coxae* (Graham & Wendler 1981, Goldammer et al. 2012; naming after Goldammer et al. 2012). Again, a discrimination into individual MNs was not possible because branch A contains the axons of 7 MNs, 4 DUM cells, and CI1, and branch B the axons of 16-17 MNs, 4 DUM cells, and the CI1 (Goldammer et al. 2012). Individual MNs of both nerves show spontaneous activity between stepping sequences (Büschges & Schmitz 1991, Graham & Wendler 1981).

4.1.1 *Mesothorax*

Gruhn et al. (2016) showed in a reduced preparation, that protractor activity was increased compared to retractor activity during inside steps, and that the activities of these protractor MNs was tightly correlated and largely in phase with the steps of the ipsilateral front leg. The same was previously reported for straight walking animals (Borgmann et al. 2007).

Figure 4.1.1 shows similar results as in Gruhn's publication. While the mesothoracic leg nerve nl2 was strongly active during inside steps of the front leg, retractor activity was decreased ($N \ \& \ \dot{N} = 4$) (Fig. 4.1.1A&B). Protractor activity was strongest at about 270° of the front leg's step cycle (range: 240°-300°) (Fig. 4.1.1C, right polar plot). Retractor activity was strongest at about 52° (range: 30°-90°) (Fig. 4.1.1C, left polar plot). Contrary

to this, retractor activity exceeded protractor activity during outside steps of the ipsilateral front leg (Fig. 4.1.2A). For the retractor activity, the maximal activity was reached at 277° (range: 240° - 300°) (Fig. 4.1.2C, left polar plot). In all four experiments, the phase of maximal protractor activity differed and did not show a clear tendency (range: 150° - 300°), though the overall maximal activity was at 195° (4.1.2C, right polar plot).

In summary, mesothoracic subcoxal MN activity differed between outside and inside curve stepping of the front leg. During inside steps, protractor activity was increased while retractor activity was decreased. The activity in the two MN pools alternated. During outside steps, retractor activity was increased, whereas protractor activity was decreased. In this situation, MN pools did not alternate.

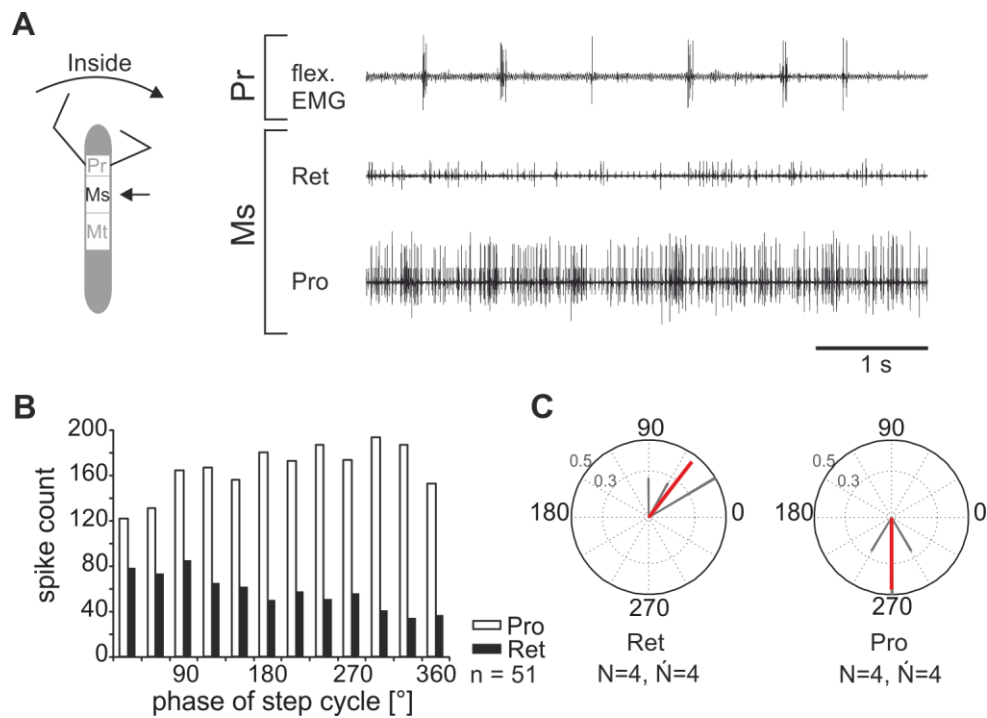


Fig. 4.1.1: Motor output of *protractor* and *retractor coxae* MN pools in the deafferented mesothoracic ganglion during front leg inside stepping; A) Schematic of stick insect and the analyzed ganglion (left), and flexor EMG recording of the front leg (top trace), together with extracellular recordings of the ipsilateral mesothoracic retractor (second trace) and protractor (third trace) nerve during an inside stepping sequence; B) Phase histogram of retractor and protractor nerve activity from the experiment presented in (A) during inside stepping with respect to the step cycle of the ipsilateral front leg; C) Polar plots with the spike event maxima (grey vectors) and their means (red bars) with respect to the step cycle of the ipsilateral front leg for the mesothoracic retractor (left) and protractor (right); N gives the number of analyzed animals; \acute{N} gives the number of analyzed hemiganglia; n gives the number of analyzed steps

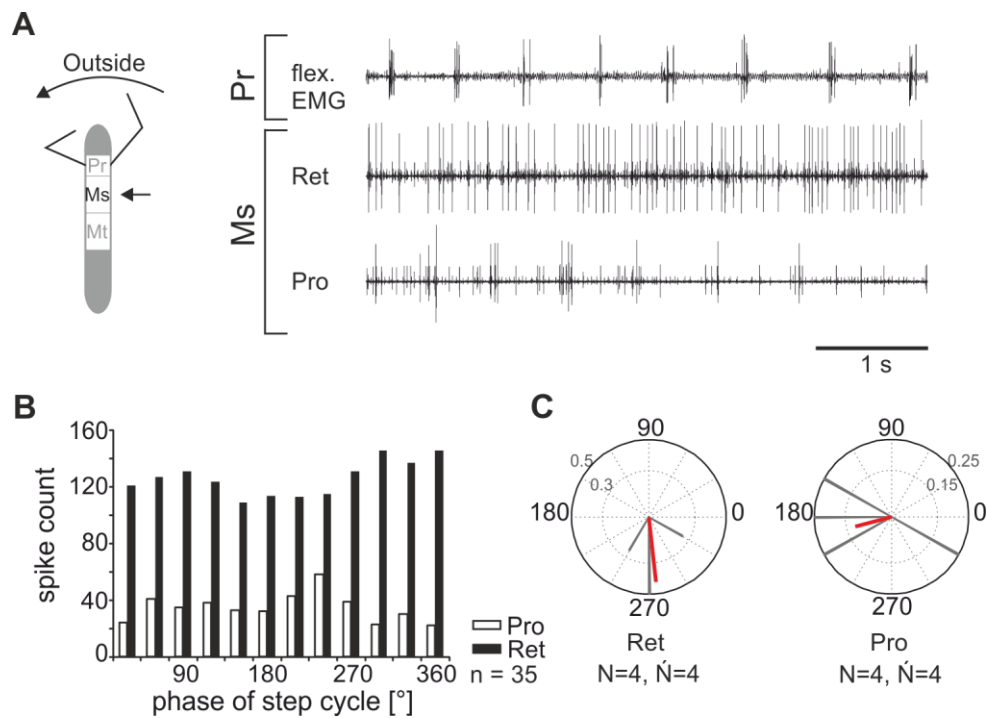


Fig. 4.1.2: Motor output of *protractor* and *retractor coxae* MN pools in the deafferented mesothoracic ganglion during front leg outside stepping; A) Schematic of stick insect and the analyzed ganglion (left), and flexor EMG recording of the front leg (top trace), together with extracellular recordings of the ipsilateral mesothoracic retractor (second trace) and protractor (third trace) nerve during an outside stepping sequence; B) Phase histogram of retractor and protractor nerve activity from the experiment presented in (A) during outside stepping with respect to the step cycle of the ipsilateral front leg; C) Polar plots with the spike event maxima (grey vectors) and their means (red bars) with respect to the step cycle of the ipsilateral front leg for the mesothoracic retractor (left) and protractor (right); N gives the number of analyzed animals; \acute{N} gives the number of analyzed hemiganglia; n gives the number of analyzed steps

4.1.2 *Metathorax*

Since Borgmann et al. (2007) found thorax-segment specificities in neuronal activity in the straight walking animal, I wanted to investigate, whether this is also true during front leg turning. Therefore, I performed the same experiments as in the mesothorax in the metathoracic ganglion.

As shown in figure 4.1.3, the results from the metathorax are very similar to those from the mesothoracic protractor and retractor. While the metathoracic leg nerve n12 was highly active during inside steps of the front leg, retractor activity was decreased ($N = 4$, $\acute{N} = 8$) (Fig. 4.1.3A&B). Protractor activity was strongest at about 294° of the front leg's step cycle (range: 60° - 300° ; $N = 6$, $\acute{N} = 12$) (Fig. 4.1.3C, right polar plot), whereas retractor activity was strongest at about 64° (range: 30° - 210°) (Fig. 4.1.3C, left polar plot). In five experiments, protractor activity was stronger compared to retractor activity, but in three further experiments, both MN pools showed comparable activity levels. In two of these experiments a clear alternation between protractor and retractor activity was found.

During outside steps, retractor activity increased (Fig. 4.1.4A&B), as in the mesothoracic nerve recordings. The maximal retractor activity was present at 291° (range: 240° - 30°) (Fig. 4.1.4C, left polar plot). Protractor activity was strongly decreased compared to retractor activity, and to protractor activity during inside steps. In all six experiments (and twelve analyzed hemiganglia), the phase of maximal protractor activity differed and did not show a clear tendency (range: 30° - 330°), though the overall maximal activity was at 175° (4.1.4C, right polar plot).

In summary, the metathoracic protractor and retractor were activated in a similar manner as the mesothoracic protractor and retractor MN pools. This means that while the protractor was highly active during inside steps, its activity decreased during outside steps. The opposite was found for the retractor activity.

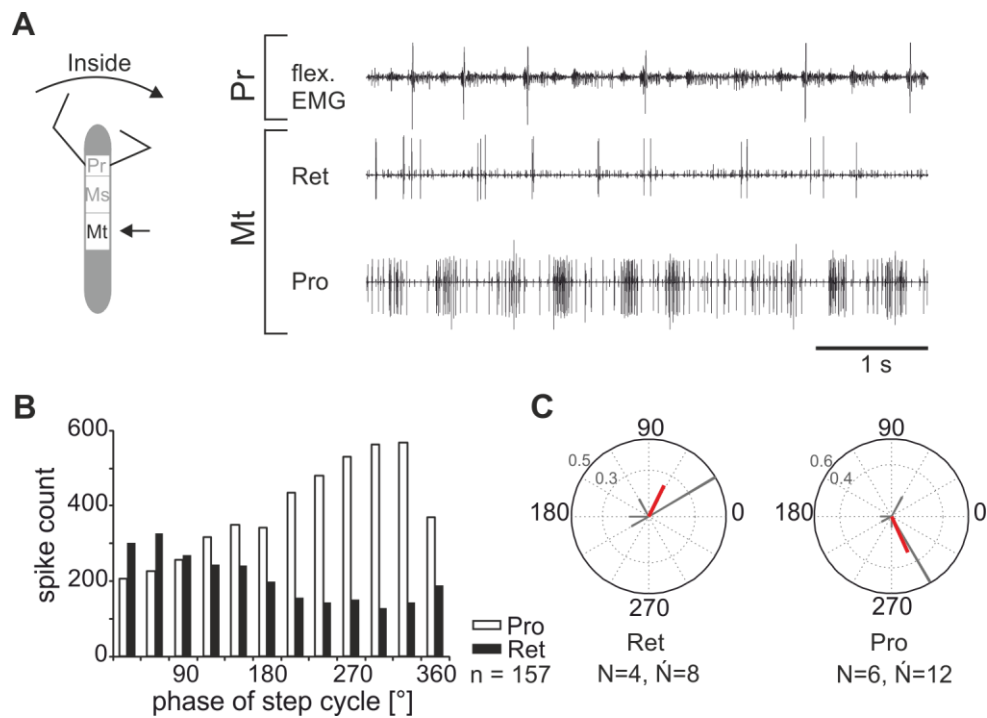


Fig. 4.1.3: Motor output of *protractor* and *retractor coxae* MN pools in the deafferented metathoracic ganglion during front leg inside stepping; A) Schematic of stick insect and the analyzed ganglion (left), and flexor EMG recording of the front leg (top trace), together with extracellular recordings of the ipsilateral metathoracic retractor (second trace) and protractor (third trace) nerve during an inside stepping sequence; B) Phase histogram of retractor and protractor nerve activity from the experiment presented in (A) during inside stepping with respect to the step cycle of the ipsilateral front leg; C) Polar plots with the spike event maxima (grey vectors) and their mean (red bars) with respect to the step cycle of the ipsilateral front leg for the metathoracic retractor (left) and protractor (right); N gives the number of analyzed animals; \dot{N} gives the number of analyzed hemiganglia; n gives the number of analyzed steps

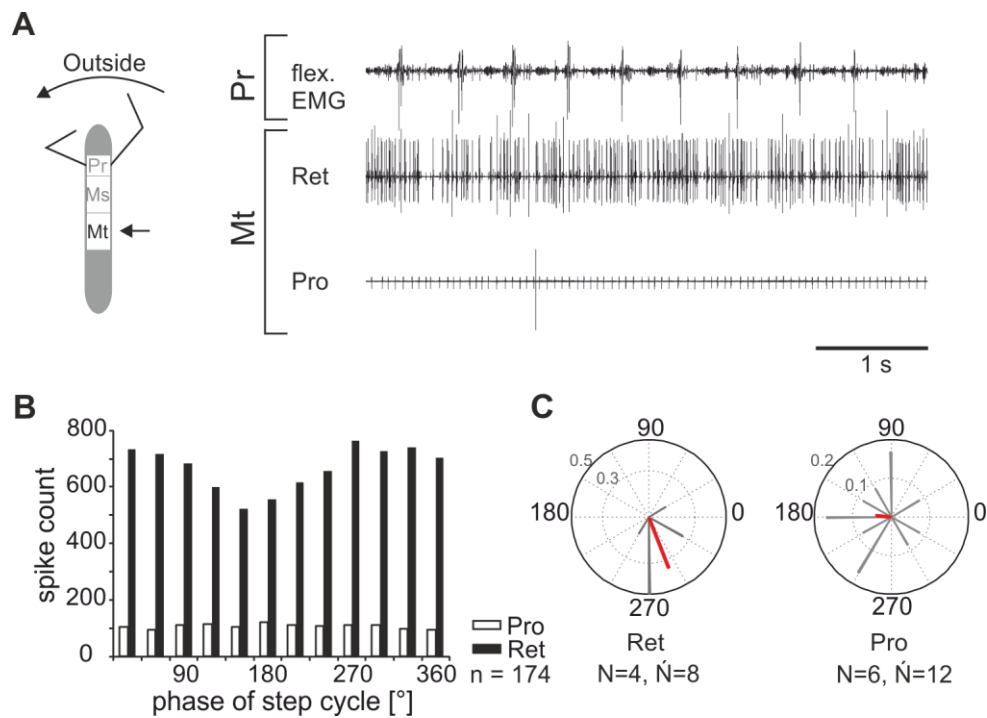


Fig. 4.1.4: Motor output of *protractor* and *retractor coxae* MN pools in the deafferented metathoracic ganglion during front leg outside stepping; A) Schematic of stick insect and the analyzed ganglion (left), and flexor EMG recording of the front leg (top trace), together with extracellular recordings of the ipsilateral metathoracic retractor (second trace) and protractor (third trace) nerve during an outside stepping sequence; B) Phase histogram of retractor and protractor nerve activity from the experiment presented in (A) during inside stepping with respect to the step cycle of the ipsilateral front leg; C) Polar plots with the spike event maxima (grey vectors) and their mean (red bars) with respect to the step cycle of the ipsilateral front leg for the metathoracic retractor (left) and protractor (right); N gives the number of analyzed animals; \bar{N} gives the number of analyzed hemiganglia; n gives the number of analyzed steps

4.2 Levator and Depressor Trochanteris

The meso- and metathoracic leg nerves C1 and C2 innervate the muscles *levator* and *depressor trochanteris*, respectively. When these muscles contract, the trochanterofemur of the leg is moved up or down.

Single MNs of C2 can be distinguished easily from each other, since this nerve contains three large axons (Schmitz 1986) and many small axons that are rarely measurable in extracellular recordings. The large MNs can be identified due to the different amplitudes of their spikes. The fast *depressor trochanteris* (FDTr) produces spikes with the largest amplitude, while the common inhibitor (CI) that is also found in other leg nerves (nl2, nl3, nl5, and C1), produces the spikes with the smallest amplitudes of these three axons. The spikes of the slow *depressor trochanteris* (SDTr) are medium sized compared to the other two, and the MN is spontaneously active (Schmitz 1986).

While single MN of the depressor can be distinguished easily from each other, the larger number of levator MNs (9-11 MNs & CI & 3 DUM cells; see Goldammer et al. 2012) makes a similar characterization more difficult in C1 recordings. Only a differentiation between large and small units was possible, while a classification according to Hess & Büschges (1997) into the three groups A, B, and C was impossible due to the fact that the extracellularly recorded amplitude sizes were not different enough for MN categorization in this nerve.

4.2.1 Mesothorax

As soon as the animal started walking with the front legs, levator activity increased drastically and continued throughout the entire walking sequence (Fig. 4.2.1A & B, Fig. 4.2.2A & B) ($N = 4$, $\dot{N} = 6$). During inside stepping, the spike activity maxima were widely distributed and did not show a preferred phase (Fig. 4.2.1C & 4.2.2C), however, the overall maximal activity was at 0° . During outside stepping, the spike event maxima ranged from 240° to 30° , and had an overall maximum at 25° .

In two hemiganglia (of the same animal, therefore $N = 1$, $\dot{N} = 2$), no difference was seen with respect to the activity pattern between inside and outside steps. In three analyzed hemiganglia, the levator activity was slightly stronger in inside steps compared to outside steps ($N = 2$, $\dot{N} = 3$), and in one further experiment the opposite activation pattern was

seen. In contrast to this, the SDTr neuron of the antagonistic depressor fired spontaneous action potentials in the resting animal ($N = 3$, $\check{N} = 4$). In all cases, the activity ceased as soon as front leg stepping began (Fig. 4.2.1A-C & 4.2.2A-C). During inside and outside front leg stepping sequences, only the CI of the depressor MN pool showed continuous activity. This stopped as soon as the animal terminated stepping. FDTr activity was not present in any of the experiments (four analyzed hemiganglia in three animals, therefore $N=3$, $N=4$).

In summary, with the begin of a front leg stepping sequence, mesothoracic levator activity increased strongly, while this leg nerve showed no activity in the resting animal. In the depressor only the common inhibitor showed tonic activity, whereas other MNs were silent as soon as front leg stepping began.

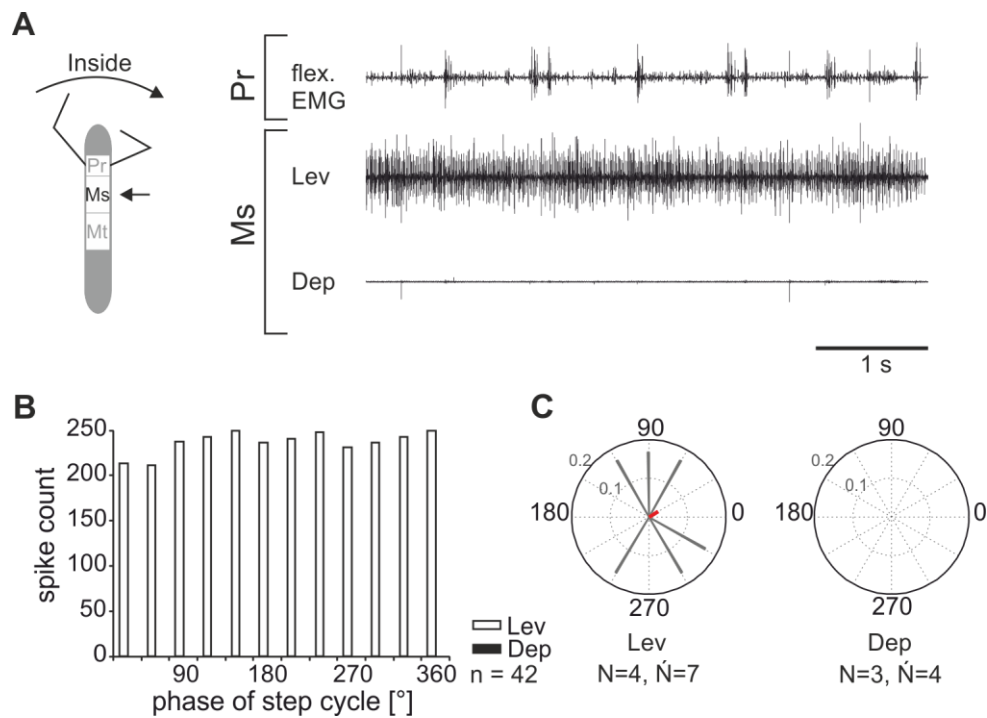


Fig. 4.2.1: Motor output of *levator* and *depressor trochanteris* MN pools in the deafferented mesothoracic ganglion during front leg inside stepping; A) Schematic of stick insect and the analyzed ganglion (left), and flexor EMG recording of the front leg (top trace), together with extracellular recordings of the ipsilateral mesothoracic levator (second trace) and depressor (third trace) nerve during an inside stepping sequence; B) Phase histogram of levator and depressor nerve activity from the experiment presented in (A) during inside stepping with respect to the step cycle of the ipsilateral front leg; C) Polar plots with the spike event maxima (grey vectors) and their mean (red bar) with respect to the step cycle of the ipsilateral front leg for the mesothoracic levator (left) and depressor (right); N gives the number of analyzed animals; \dot{N} gives the number of analyzed hemiganglia; n gives the number of analyzed steps

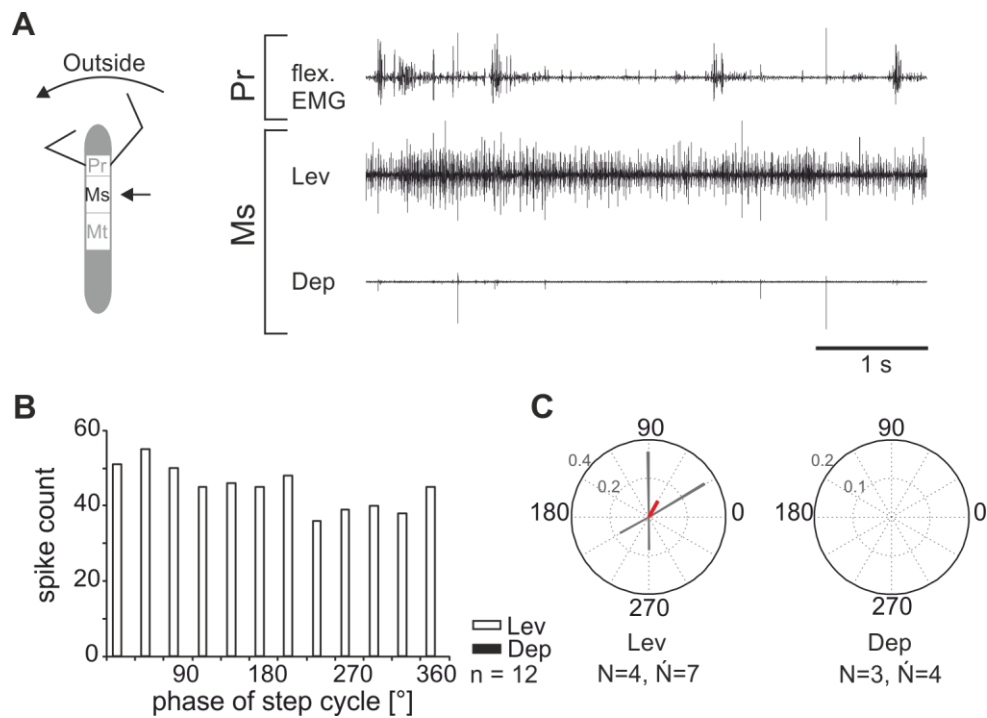


Fig. 4.2.2: Motor output of *levator* and *depressor trochanteris* MN pools in the deafferented mesothoracic ganglion during front leg outside stepping; A) Schematic of stick insect and the analyzed ganglion (left), and flexor EMG recording of the front leg (top trace), together with extracellular recordings of ipsilateral mesothoracic levator (second trace) and depressor (third trace) nerve during an outside stepping sequence; B) Phase histogram of levator and depressor nerve activity from the experiment presented in (A) during outside stepping with respect to the step cycle of the ipsilateral front leg; C) Polar plots with the spike event maxima (grey vectors) and their mean (red bar) with respect to the step cycle of the ipsilateral front leg for the mesothoracic levator (left) and depressor (right); N gives the number of analyzed animals; \dot{N} gives the number of analyzed hemiganglia; n gives the number of analyzed steps

4.2.2 *Metathorax*

As thorax-segment specificity was previously reported for the subcoxal joint (Borgmann et al. 2007), I wanted to find out whether this is also the case for the next distal joint, the coxa-trochanteral joint. Therefore, I performed the same experiments in the metathorax as before for the mesothorax.

Figure 4.2.3 shows approximately the same results as in the mesothoracic series of experiments. Again, levator activity drastically increased during stepping sequences of the front legs and terminated as soon as front leg stepping ended ($N = 6$, $\acute{N} = 6$), independent of walking direction (Fig. 4.2.3A & 4.2.4A). During inside steps, levator activity was strongest at 323° of the front leg's step cycle (range: 120° - 330°) ($N = 6$, $\acute{N} = 6$). During outside steps the maximal levator activity ranged from 210° to 300° and had an overall maximum at 249° of the front leg's step cycle ($N = 6$, $\acute{N} = 6$).

In contrast to the mesothoracic C2 recording, in the metathoracic C2 recording the SDTr MN was active during front leg stepping, although rarely (Fig. 4.2.3B-C & 4.2.4A-C). During inside turns of the front leg, the SDTr was active during movements of the front legs, but only in half of the analyzed hemiganglia ($N = 3$, $\acute{N} = 3$) (overall maximal activity at 255°), though it was active in most of the experiments during outside turns ($N = 5$, $\acute{N} = 5$) (overall maximal activity at around 324°). This activity was usually stronger than during inside turns. The activity during inside steps was only stronger than that during outside steps in one hemiganglion. Here, one has to note that this MN activity was only six spike events total in 34 step cycles.

In summary, the metathoracic C1 (levator) was activated as soon as the front leg stepping sequence began. With the begin of front leg stepping, the activity of the metathoracic decreased either totally or to a great extend.

All in all, the metathoracic levator was activated in a similar manner to the mesothoracic MN pool. This means that levator activity increased as soon as the animal started stepping movements, independent of the direction. In contrast to this, the metathoracic C2 (depressor) showed slight changes in its activation pattern compared to the mesothoracic MN pool. While in the mesothoracic depressor, spontaneous activity of SDTr was terminated instantly at the beginning of a stepping sequence independent of the turning direction, in the metathoracic depressor, some SDTr activation remained.

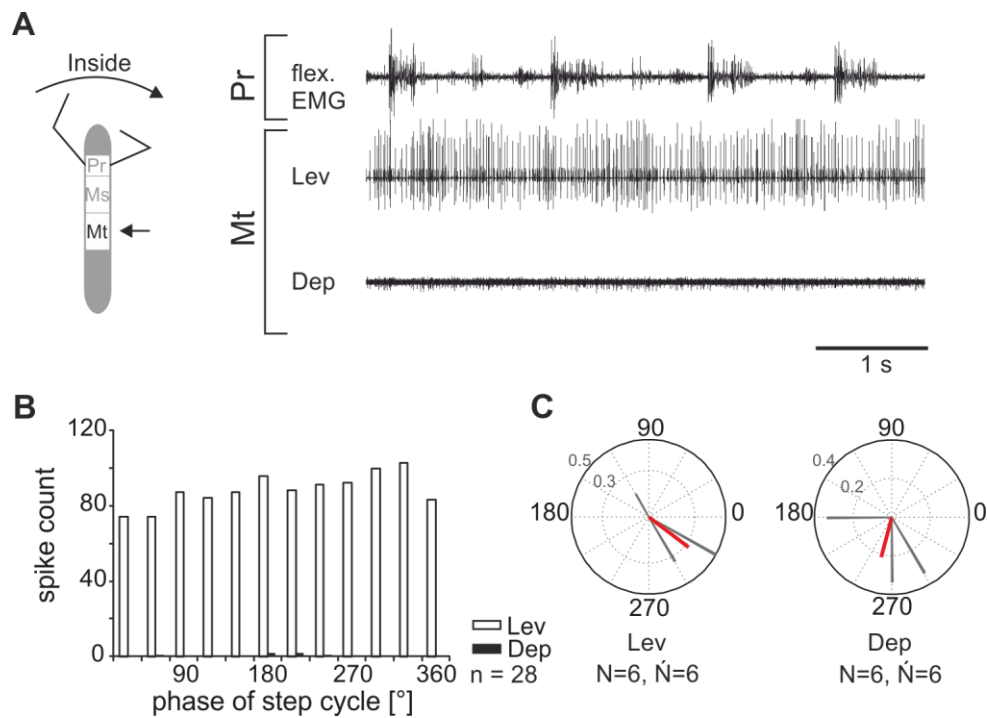


Fig. 4.2.3: Motor output of *levator* and *depressor trochanteris* MN pools in the deafferented metathoracic ganglion during front leg inside stepping; A) Schematic of stick insect and the analyzed ganglion (left), and flexor EMG recording of the front leg (top trace), together with extracellular recordings of the ipsilateral metathoracic levator (second trace) and depressor (third trace) nerve during an inside stepping sequence; B) Phase histogram of levator and depressor nerve activity from the experiment presented in (A) during inside stepping with respect to the step cycle of the ipsilateral front leg; C) Polar plots with the spike event maxima (grey vectors) and their means (red bars) with respect to the step cycle of the ipsilateral front leg for the metathoracic levator (left) and depressor (right); N gives the number of analyzed animals; \dot{N} gives the number of analyzed hemiganglia; n gives the number of analyzed steps

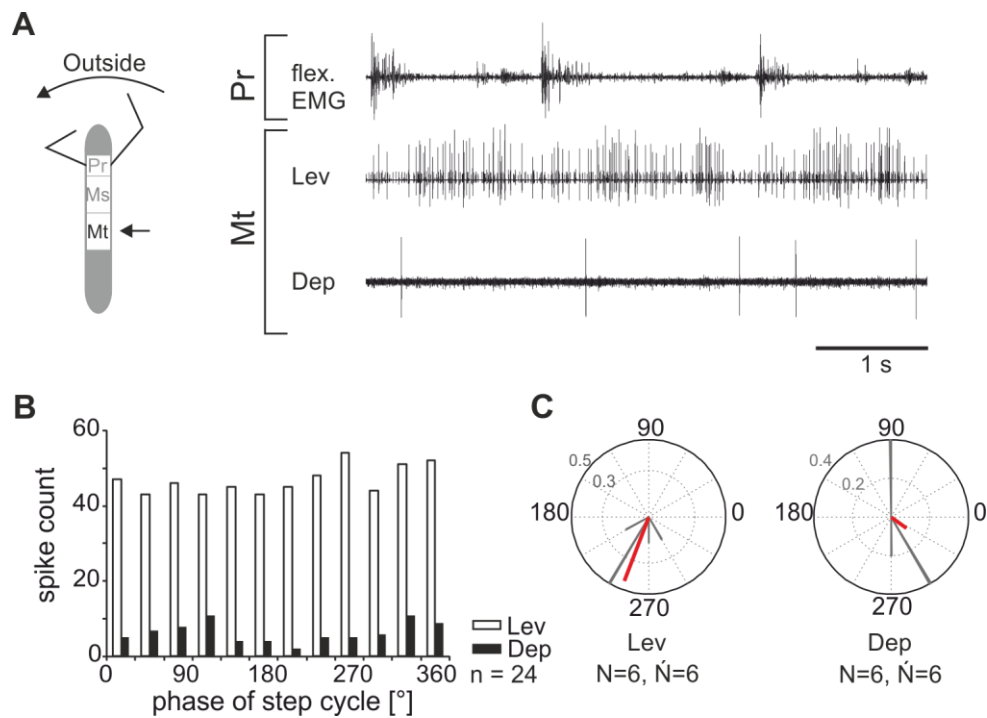


Fig. 4.2.4: Motor output of *levator* and *depressor trochanteris* MN pools in the deafferented metathoracic ganglion during front leg outside stepping; A) Schematic of stick insect and the analyzed ganglion (left), and flexor EMG recording of the front leg (top trace), together with extracellular recordings of the ipsilateral metathoracic levator (second trace) and depressor (third trace) nerve during an outside stepping sequence; B) Phase histogram of levator and depressor nerve activity from the experiment presented in (A) during outside stepping with respect to the step cycle of the ipsilateral front leg; C) Polar plots with the spike event maxima (grey vectors) and their means (red bars) with respect to the step cycle of the ipsilateral front leg for the metathoracic levator (left) and depressor (right); N gives the number of analyzed animals; \dot{N} gives the number of analyzed hemiganglia; n gives the number of analyzed steps

4.3 Extensor and Flexor Tibiae

The meso- and metathoracic leg nerves n13 and the main leg nerve nervus cruris innervate the *extensor* and *flexor tibiae* muscles, respectively. When these muscles contract, the tibia is extended or flexed around the femur-tibia joint.

The mesothoracic n13 contains the axons of about 8 MNs, 3 DUM cells, and the CI1. It innervates the *accessory depressor trochanteris*, *accessory levator trochanteris* and the *extensor tibiae* (Goldammer et al. 2012). The extensor itself is innervated by 3 MNs, only: the slow *extensor tibiae* (SETi), the fast *extensor tibiae* (FETi), and the CI1 (Bässler 1977; Bässler & Storrer, 1980). These three MNs are easily identifiable in extracellular recordings due to their amplitude. FETi produces spikes with the largest amplitudes, CI1 produces spikes with the smallest amplitudes, and SETi spikes have amplitudes of medium size (Goddon 1972; Bässler & Storrer 1980, Bässler & Wegner 1983). In addition, SETi is spontaneously active (Bässler 1976).

The flexor, on the other hand, is innervated by small branches of the main leg nerve, the nervus cruris. These branches contain axons of 8-25 MNs, 1-2 DUM cells, and the CI2 and CI3 (Goldammer et al. 2012). Therefore, individual MNs cannot be distinguished from each other in the branches of the nervus cruris.

4.3.1 Mesothorax

In all experiments (N=5, $\bar{N} = 8$) SETi and FETi activities were easily distinguishable. SETi activity was always spontaneously present, whereas FETi activity started with the begin of a stepping sequence. In addition, the amplitude of SETi spikes was smaller than the amplitude of FETi spikes.

In this series of experiments, no characteristic activity pattern depending on the direction of front leg steps was found, neither for SETi nor for FETi. Figure 4.3.1A shows extracellular recordings of the mesothoracic n13 and the respective front leg flexor EMG for two different experiments (left and right column). In the upper two rows (i & iii), the neuronal activity during inside turning is shown, while in the lower two rows (ii & iv), the neuronal activity during outside turning is presented.

In the left experiment (one analyzed hemiganglion of one animal) during inside (i) versus outside turns (ii), the extensor activity was clearly stronger during outside turning movements. This effect is also presented in the left phase histogram (Fig. 4.3.1 B).

In the right experiment (another analyzed hemiganglion of one animal) (Fig. 4.3.1 A iii/iv & right phase histogram in B), on the other hand, the neuronal activity of the extensor was the same, independent of the turning direction. The maximal neuronal activity did not show a clear tendency, neither during inside nor during outside turns (inside: 0 - 180°, overall max: 121.5°; outside: 60 - 300°; overall max: 260.1°) (see Fig. 4.3.1 C).

In half of all analyzed hemiganglia ($N = 4$, $\acute{N} = 4$) the extensor activity was greater during outside than during inside turns (see Fig. 4.3.1, left experiment), while in the other half of the analyzed hemiganglia the neuronal activity was similar for both conditions ($N = 3$, $\acute{N} = 4$) (Fig. 4.3.1 D) (see Fig. 4.3.1, right experiment).

A similar distribution was seen for the mesothoracic flexor MNs activity (Fig. 4.3.2). In these extracellular recordings, no individual MNs were distinguishable in any experiment ($N = 10$, $\acute{N} = 11$). Figure 4.3.2A shows extracellular recordings of the nervus cruris branches and the respective front leg flexor EMG for two different analyzed hemiganglia (left and right column). In the upper two rows, the neuronal activity during inside (i & iii) turning is shown, while in the lower two rows the neuronal activity during outside turning (ii & iv) is presented. When comparing the neuronal activity of the left experiment during inside versus outside turns (Fig. 4.3.2 Ai/ii), one can see, that the flexor activity was clearly stronger during inside turning. This effect is also presented in the left phase histogram (Fig. 4.3.2 B). In the right experiment (Fig. 4.3.2 A iii/iv & right phase histogram in B), on the other hand, the neuronal activity of the flexor was similar during inside and outside turns. The neuronal activity did not have a clear maximum within the front leg step cycle, neither during inside nor during outside steps (inside: range: 30 - 330°, overall max: 307.8°; outside: range: 0 - 270°; overall max: 309.9°) (see Fig. 4.3.1 C).

In more than half of all analyzed hemiganglia ($N = 6$, $\acute{N} = 6$) the flexor activity was higher during inside than during outside turns like in the first presented experiment (see Fig. 4.3.2 left column), while in five experiments ($N = 4$, $\acute{N} = 5$) the neuronal activation was roughly the same for both conditions like in the second experiment (see Fig. 4.3.2, right column), as shown in Fig. 4.3.2 D.

In summary, no clearly defined activity pattern was observed for the mesothoracic extensor and flexor MNs during inside or outside turns of the ipsilateral front leg. However, in the extensor the activity during inside front leg steps was never stronger than the activity during outside front leg steps. Correspondingly, the antagonist flexor MN activity was never stronger during outside steps than during inside steps.

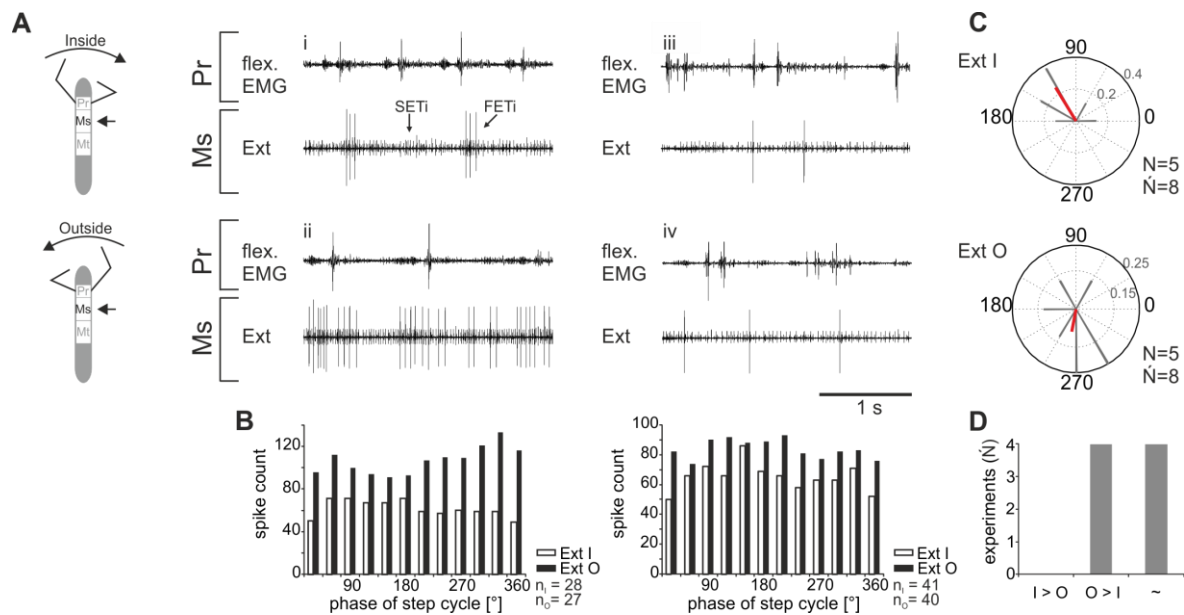


Fig. 4.3.1: Motor output of *extensor tibiae* MNs in the deafferented mesothoracic ganglion during front leg inside and outside stepping; A) Schematic of stick insect and the analyzed ganglion (left), and flexor EMG recording of the front leg (top trace & third trace), together with extracellular recordings of the ipsilateral mesothoracic extensor nerve during inside (second trace) and outside (fourth trace) stepping sequences; B) Phase histogram of extensor nerve activity from the experiments presented in (A) during inside and outside stepping with respect to the step cycle of the ipsilateral front leg; Each phase histogram belongs to the experiment of the nerve recordings above, respectively. C) Polar plots with the spike event maxima (grey vectors) and their means (red bars) with respect to the step cycle of the ipsilateral front leg for the mesothoracic extensor during inside (top phase plot) and outside (bottom phase plot) stepping movements; D) Overview of the number of experiments (\hat{N}) in which a extensor activity was higher during inside than during outside stepping ($I > O$), vice versa ($O > I$), or when activities were approximately equal (\sim); N gives the number of analyzed animals; \hat{N} gives the number of analyzed hemiganglia; n gives the number of analyzed steps

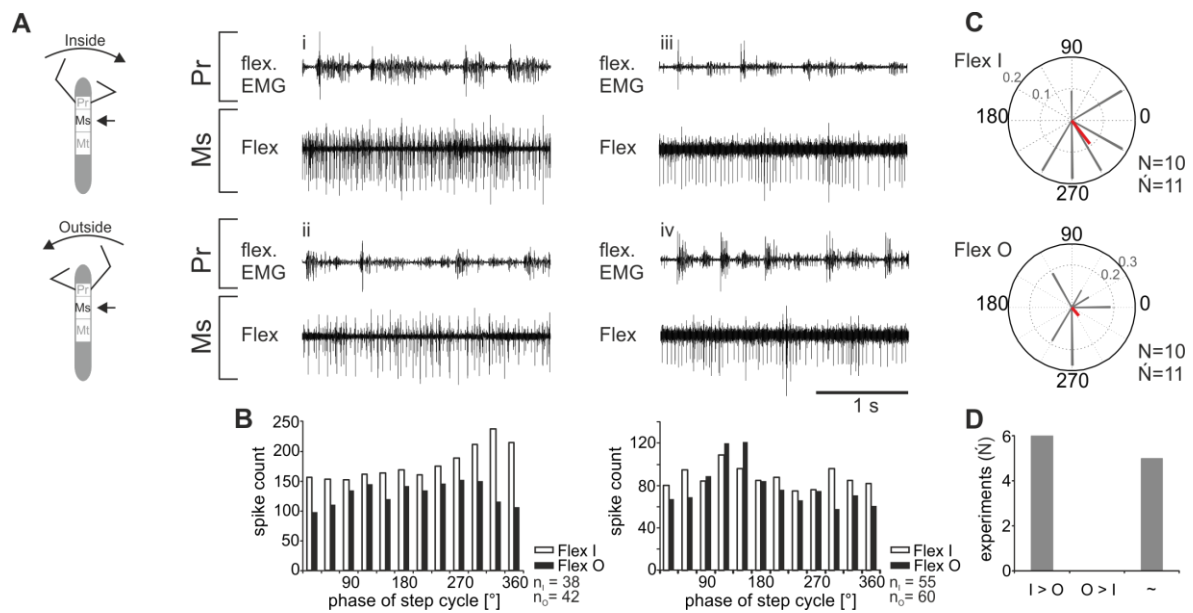


Fig. 4.3.2: Motor output of *flexor tibiae* MNs in the mesothoracic femur (deafferented mesothoracic ganglion) during front leg inside and outside stepping; A) Schematic of stick insect and the analyzed ganglion (left), and flexor EMG recording of the front leg (top trace & third trace), together with extracellular recordings of the ipsilateral mesothoracic flexor nerve during an inside (second trace) and outside (fourth trace) stepping sequence; B) Phase histogram of flexor nerve activity from the experiments presented in (A) during inside and outside stepping with respect to the step cycle of the ipsilateral front leg; Each phase histogram belongs to the experiment of the nerve recordings above, respectively. C) Polar plots with the spike event maxima (grey vectors) and their means (red bars) with respect to the step cycle of the ipsilateral front leg for the mesothoracic flexor during inside (top phase plot) and outside (bottom phase plot) stepping; D) Overview of the number of experiments (\hat{N}) in which flexor activity was higher during inside than during outside stepping ($I > O$), vice versa ($O > I$), or when activities were approximately equal (\sim); N gives the number of analyzed animals; \hat{N} gives the number of analyzed hemiganglia; n gives the number of analyzed steps

4.3.2 *Metathorax*

Next, I analyzed whether the previously detected tendency of mesothoracic extensor MNs to fire stronger during outside than inside turns, and the opposite tendency for the flexor MNs, will be similar in the next posterior segment. Therefore, I performed the same experiments as before in the metathoracic ganglion.

Figure 7 shows approximately the same results as in the mesothoracic series of experiments. Once again, in all analyzed hemiganglia ($N=5$, $\acute{N} = 9$) SETi and FETi activity was easily distinguishable. SETi activity was always spontaneously active, whereas FETi activity started with the begin of a stepping sequence. In addition, the amplitudes of SETi and FETi spikes could always be distinguished based on the smaller SETi amplitudes.

Again, no characteristic activity pattern depending on the direction of movement in the front leg was found, neither for SETi nor for FETi. Figure 4.3.3A shows extracellular recordings of the metathoracic n13 and the respective front leg flexor EMG for two different analyzed hemiganglia (left and right column). In the upper two rows, the neuronal activity during front leg inside turning is shown (i & iii), while in the lower two rows the neuronal activity during front leg outside turning (ii & iv) is presented.

When comparing the neuronal activity of the left analyzed hemiganglia during inside (i) versus outside (ii) turns, one can see that the extensor activity was clearly stronger during front leg outside turning. This effect is also presented in the left phase histogram (Fig. 4.3.3 B).

In the right experiment (Fig. 4.3.3 A&B), on the other hand, the neuronal activity of the extensor was higher during inside turns (iii) compared to outside (iv) turns.

The neuronal activity did not have a clear maximum within the front leg step cycle, neither during inside, nor during outside steps (inside: 30 - 240°, overall max: 108.4°; outside: 30 - 300°; overall max: 95.9°) (see Fig. 4.3.3 C).

In most experiments (in 5 out of 9 analyzed hemiganglia, $N = 3$, $\acute{N} = 5$), the neuronal activation was roughly the same for both conditions, while in two experiments, each, either the extensor activity was higher during outside than during inside turns ($N = 2$, $\acute{N} = 2$), or vice versa ($N = 2$, $\acute{N} = 2$) (Fig. 4.3.3 D).

Similarly, metathoracic flexor MN activity did not show clear patterns depending on the ipsilateral front leg stepping direction (Fig. 4.3.4). In none of the extracellular recordings, individual MNs could be distinguished ($N = 6$, $\acute{N} = 8$).

Figure 4.3.4A shows extracellular recordings of the nervus cruris branches and the respective front leg flexor EMG for two different analyzed hemiganglia (left and right column). In the upper two rows, the neuronal activity during front leg inside turning is shown (i & iii), while in the lower two rows the neuronal activity during front leg outside turning is presented (ii & iv).

When comparing the neuronal activity of the left analyzed hemiganglion during front leg inside (i) versus outside (ii) turns, one can see that the flexor activity was clearly stronger during outside turning. This effect is also presented in the left phase histogram (Fig. 4.3.2 B).

In the right experiment (Fig. 4.3.4 A&B), on the other hand, the neuronal activity of the flexor was similar during front leg inside (iii) and outside (iv) turns.

The neuronal activity did not have a clear maximum within the front leg step cycle, neither during inside, nor during outside steps (inside: 90 - 360°, overall max: 326.1°; outside: 0 - 270°; overall max: 129.9°) (see Fig. 4.3.4 C).

In most experiments (in 3 out of 8 analyzed hemiganglia, $N = 3$, $\dot{N} = 3$) the flexor MNs activity was either roughly the same for both conditions, or higher during outside turns than during inside turns (in 3 out of 8 analyzed hemiganglia, $N = 2$, $\dot{N} = 3$). While in two analyzed hemiganglia, the flexor activity was higher during inside than during outside turns ($N = 2$, $\dot{N} = 2$) (Fig. 4.3.4 D).

In summary, no specific activity pattern was observed for the metathoracic extensor and flexor MNs during inside or outside turns of the ipsilateral front leg, similarly to the mesothoracic extensor and flexor activity. Interestingly, compared to the mesothorax, in both, the extensor and flexor nerve recordings, activity could be stronger during inside vs. outside steps of the front leg and vice versa. The implications will be discussed.

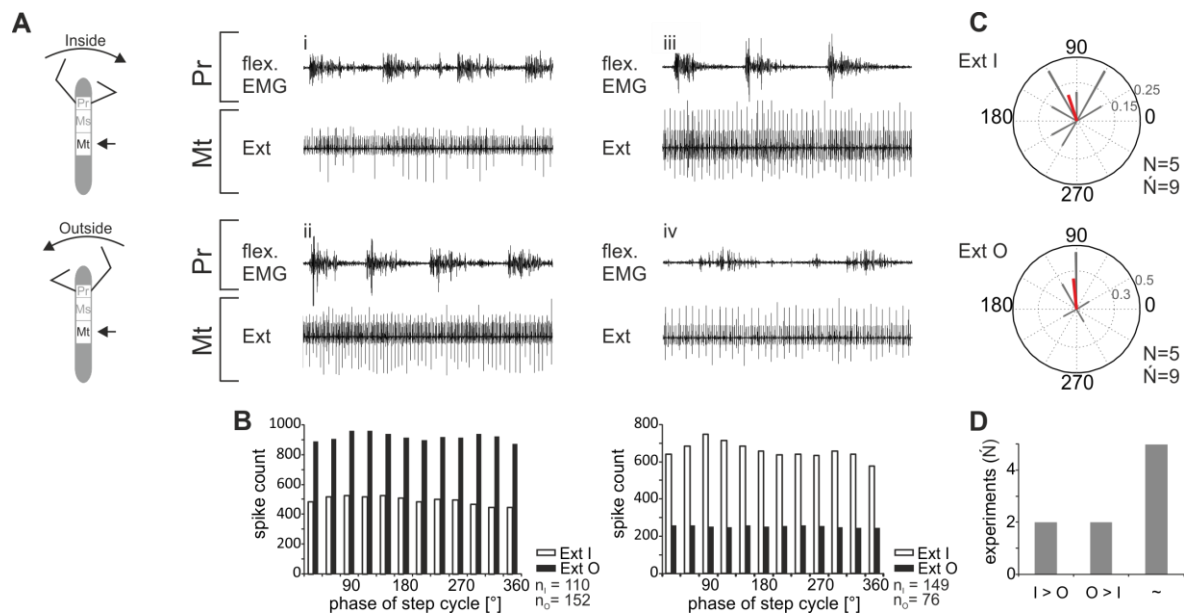


Fig. 4.3.3: Motor output of *extensor tibiae* MNs in the deafferented mesothoracic ganglion during front leg inside and outside stepping; A) Schematic of stick insect and the analyzed ganglion (left), and flexor EMG recording of the front leg (top trace & third trace), together with extracellular recordings of the ipsilateral mesothoracic extensor nerve during an inside (second trace) and outside (fourth trace) stepping sequence; B) Phase histogram of extensor nerve activity from the experiments presented in (A) during inside and outside stepping with respect to the step cycle of the ipsilateral front leg; Each phase histogram belongs to the experiment of the nerve recordings above, respectively. C) Polar plots with the spike event maxima (grey vectors) and their means (red bars) with respect to the step cycle of the ipsilateral front leg for the mesothoracic extensor during inside (top phase plot) and outside (bottom phase plot) stepping; D) Overview of the number of experiments (\bar{N}) in which extensor activity was stronger during inside stepping than during outside stepping ($I > O$), vice versa ($O > I$), or when activities were approximately equal (\sim); N gives the number of analyzed animals; \bar{N} gives the number of analyzed hemiganglia; n gives the number of analyzed steps

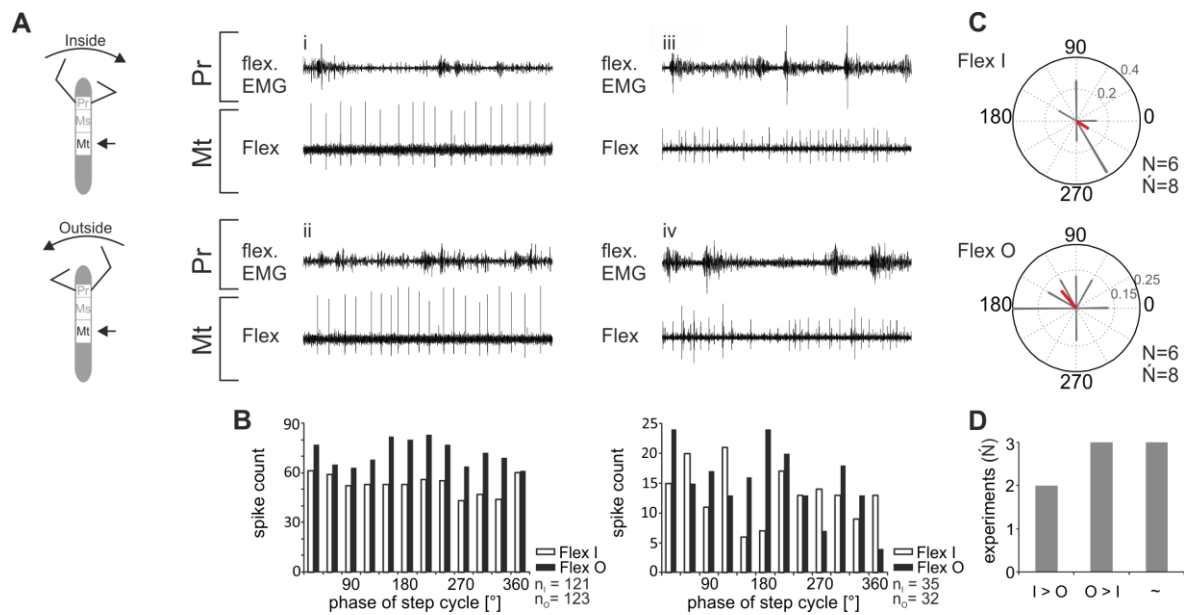


Fig. 4.3.4: Motor output of *flexor tibiae* MNs in the metathoracic femur (deafferented metathoracic ganglion) during front leg inside and outside stepping; A) Schematic of stick insect and the analyzed ganglion (left), and flexor EMG recording of the front leg (top trace & third trace), together with extracellular recordings of the ipsilateral metathoracic flexor nerve during an inside (second trace) and outside (fourth trace) stepping sequence; B) Phase histogram of flexor nerve activity from experiments presented in (A) during inside and outside stepping with respect to the step cycle of the ipsilateral front leg; Each phase histogram belongs to the experiment of the nerve recordings above, respectively. C) Polar plots with the spike event maxima (grey vectors) and their means (red bars) with respect to the step cycle of the ipsilateral front leg for the metathoracic flexor during inside (top phase plot) and outside (bottom phase plot) stepping; D) Overview of the number of experiments (\bar{N}) in which flexor activity was stronger during inside stepping than during outside stepping ($I > O$), vice versa ($O > I$), or when activities were approximately equal (\sim); N gives the number of analyzed animals; \bar{N} gives the number of analyzed hemiganglia; n gives the number of analyzed steps

CHAPTER 5

Involvement of Central Pattern Generators in Thorax- & Leg-Segment Specificity of the Turning Related Motor Output

All coordinated and rhythmical contractions of antagonistic muscle groups depend on neuronal networks within the central nervous system, called central pattern generators (CPGs). These networks can generate motor rhythms in the absence of sensory feedback and descending input from higher brain centers (Delcomyn 1980, Bässler 1986, Chrachri & Clarac 1990, Ryckebusch & Laurent 1993, Büschges et al. 1995, Johnston & Levine 1996 / 2002), however, the descending input from higher brain centers – e.g. the central body complex in insects (Strausfeld 1999) – can activate and modify this CPG activity (vertebrates review: Grillner & Wallén 1985; lamprey: Fagerstedt & Ullén 2001a, Orlovsky et al. 1999; drosophila: Strauss & Heisenberg 1993, salamander: Cabelguen et al. 2003). It is still relatively poorly understood how these descending signals influence local CPGs that control locomotion in walking animals (Field & Stein 1997a, Ridgel et al. 2007, Dyson et al. 2014).

In order to better understand the involvement of local CPGs in locomotion, it might be a good idea to first establish a preparation with an activated CPG only (producing “fictive motor patterns”), and in a next step, induce different descending inputs – e.g. inside and

outside turns of front legs – to the established preparation. This could help to differentiate between intrinsic CPG driven activity, and CPG activity that is under modulatory descending influence. The stick insect is an excellent experimental animal to answer the above question for several reasons. Most importantly, much is already known about the local CPG activity in the stick insect. Büschges et al. (1995) showed by applying the muscarinic agonist pilocarpine onto the deafferented thoracic nerve cord that each leg joint is driven by its own CPG. While all antagonistic MN pools showed a strong coupling to each other, only in rare cases a stereotypic cycle-to-cycle coupling between the MN pools of the different leg joints was found. These so called SRPs (spontaneous recurrent patterns) resembled motor output during step-phase transitions in walking, and, therefore, were referred to as “fictive step phase transitions”. On the intersegmental level, Büschges et al. (1995) showed that in the isolated ventral nerve cord, consisting of the deafferented pro-, meso-, and metathoracic ganglia and the abdominal cord, application of pilocarpine resulted in rhythmic activity of the subcoxal MN pools of all thoracic ganglia (in 9 out of 11 experiments). This rhythmicity could be different in the individual ganglia, but in many cases the protractor MNs of the different segments bursted at similar frequencies. However, the authors reported that, despite periods of in-phase activity, in general no stereotyped or fixed coupling, and more interestingly, no alternating activity between the segments was present. This does represent a motor pattern that had never been observed in the intact animal. Therefore, Ludwar et al. (2005a) investigated in the isolated two-ganglia-chain system, whether pharmacological activation of one segment (e.g. the activation of the mesothoracic ganglion) would entrain the MN activity in the adjacent ganglion (e.g. the metathoracic ganglion). In their study, they demonstrated that in the isolated preparation the pharmacologically activated CPGs were not able to entrain MN activities in the adjacent ganglia. However, Borgmann et al. (2007) found out that front leg stepping could activate the ipsilateral mesothoracic CPG: in the pharmacologically activated, rhythmic mesothoracic subcoxal MN pools front leg stepping led to a decreased burst duration and cycle period, on the one hand, and, more important, to a neuronal activity that was entrained to the front leg stepping. The metathoracic CPG was entrained in four of five experiments to the front leg stepping cycle, and it took three to five front leg steps for the metathoracic rhythm to become entrained. Recently, Gruhn et al. (2016) investigated the involvement of mesothoracic CPGs in the turning related motor output by applying pilocarpine to the isolated mesothoracic ganglion in a split-bath preparation and comparing the results for motoneuronal activity in the protractor and retractor to former not

pharmacologically activated preparations. There he found out, that body-side specific influences in the mesothoracic ganglion, resulting from inside and outside turning front legs of the stick insect *Carausius morosus*, are generated by local changes in CPG activity.

Taken together, these studies demonstrate that in the stick insect, each joint is driven by its own CPG (Büschges et al. 1995), that pharmacologically activated CPGs do not have an influence on adjacent inactive ganglia (Ludwar et al. 2005a), that front leg stepping can entrain meso- and metathoracic CPG activity (Borgmann et al. 2009), and most importantly, that motor activity of the mesothoracic subcoxal joint is modified depending on the behavioral context, and this results from local changes in CPG activity (Gruhn et al. 2016).

Knowing this, the question arises, whether the previously observed side-specific and / or segment-specific changes in subcoxal and coxa-trochanteral MN activity described in chapter 4, were due to modifications in local central pattern generator (CPG) activity.

To investigate this, I used the following experimental setting up: in a reduced preparation with all but the two front legs cut off, the animals tethered above a slippery surface were optically stimulated to produce turning movements. Their walking sequences were monitored by video and by EMG recordings of the *flexor tibiae* muscles in both front legs. To study the influence of optomotor induced turning on motor activities of all three major leg joints, extracellular recordings were made from the leg nerves nl2 (innervates *protractor coxae*), nl5 (*retractor coxae*), C1 (*levator trochanteris*), and C2 (*depressor trochanteris*) of the deafferented meso- and metathorax.

To clarify the influence of the descending signals on the local CPGs, the muscarinic agonist pilocarpine was used in a split bath preparation to activate these local CPGs of the isolated meso- or metathorax. In all experiments, before applying pilocarpine, a control sequence was recorded, and after that, turning was elicited after a stable pilocarpine rhythm was obtained.

5.1 Protractor and Retractor Coxae

In the isolated deafferented thoracic nerve cord of the stick insect, Büschges et al. (1995) induced a stable rhythm between the antagonistic subcoxal MN pools that innervate the *protractor* and *retractor coxae* by applying pilocarpine. The clearly defined bursts of the two MN pools were in antiphase to each other and showed only rarely overlapping activity. From these findings, the authors suggested that the subcoxal MN pools were output neurons of the same central pattern generating network.

5.1.1 Mesothorax

Recently, Gruhn et al. (2016) showed in a split-bath preparation, in which the mesothoracic ganglion was superfused with pilocarpine, that, after a stable pilocarpine-rhythm was obtained, protractor activity was increased compared to retractor activity during inside steps of the front legs. These MN pools were phase-coupled to the front leg stepping, with protractor activity peaking around 270°, and retractor activity peaking at around 90° of the front leg step cycle. A reversed activation was present during outside steps.

The results of Gruhn et al. could be confirmed in that the mesothoracic leg nerve nl2 was strongly active during inside steps of the front leg, while retractor activity was weak (Fig. 5.1.1.1A-C). Protractor activity was strongest at about 270° of the front leg's step cycle (range: 180°-300°) (Fig. 5.1.1.1D, right polar plot), and retractor activity was strongest at about 30° (range: 240°-60°) (Fig. 5.1.1.1D, left polar plot) in my experiments. In contrast to this, retractor activity exceeded protractor activity during outside steps of the ipsilateral front leg (Fig. 5.1.1.2A-C). During outside steps, the maximal retractor activity ranged from 270° to 90° and had an overall maximum of 20.1° of the front leg step cycle (N = 3, \bar{N} = 5). The maximal protractor activity, on the other hand, ranged from 210° to 330°, and had an overall maximum of 262.6° of the front leg step cycle (N = 3, \bar{N} = 5).

In summary, mesothoracic coxal MN activity differed between outside and inside turns of the front leg. During inside steps, protractor activity was increased, while retractor activity was decreased. In contrast to this, during outside steps, retractor activity was increased, whereas protractor activity was decreased. As the previously pilocarpine-induced rhythm was strongly interrupted with the begin of front leg stepping, my data indicate an

involvement of the subcoxal CPG in the changes of mesothoracic motor activity during front leg turning.

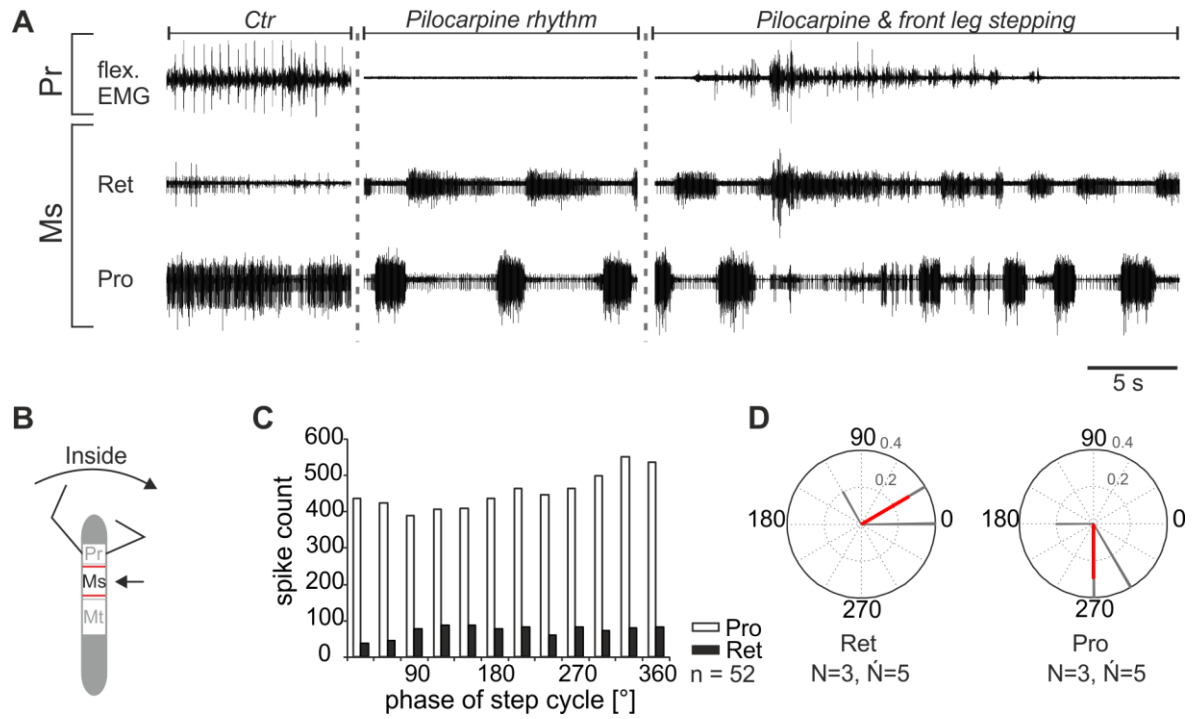


Fig. 5.1.1.1: Motor output of *protractor* (Pro) and *retractor* (Ret) *coxae* MN pools in the pilocarpine activated deafferented mesothoracic ganglion during front leg inside stepping; A) Flexor EMG recording of the front leg (top trace), together with extracellular recordings of the ipsilateral mesothoracic retractor (second trace) and protractor (third trace) nerve during inside stepping, first in control condition, and, subsequently, with pilocarpine superfusion in the quiescent animal, and during inside stepping under pilocarpine superfusion; B) Schematic of stick insect and the analyzed ganglion in the split-bath configuration; C) Phase histogram of retractor and protractor nerve activity from the experiment presented in (A) during inside stepping with respect to the step cycle of the ipsilateral front leg under pilocarpine superfusion; D) Polar plots with the spike event maxima (grey vectors) and their means (red bars) with respect to the step cycle of the ipsilateral front leg for the mesothoracic retractor (left) and protractor (right) during pilocarpine superfusion; N gives the number of analyzed animals; \bar{N} gives the number of analyzed hemiganglia; n gives the number of analyzed steps

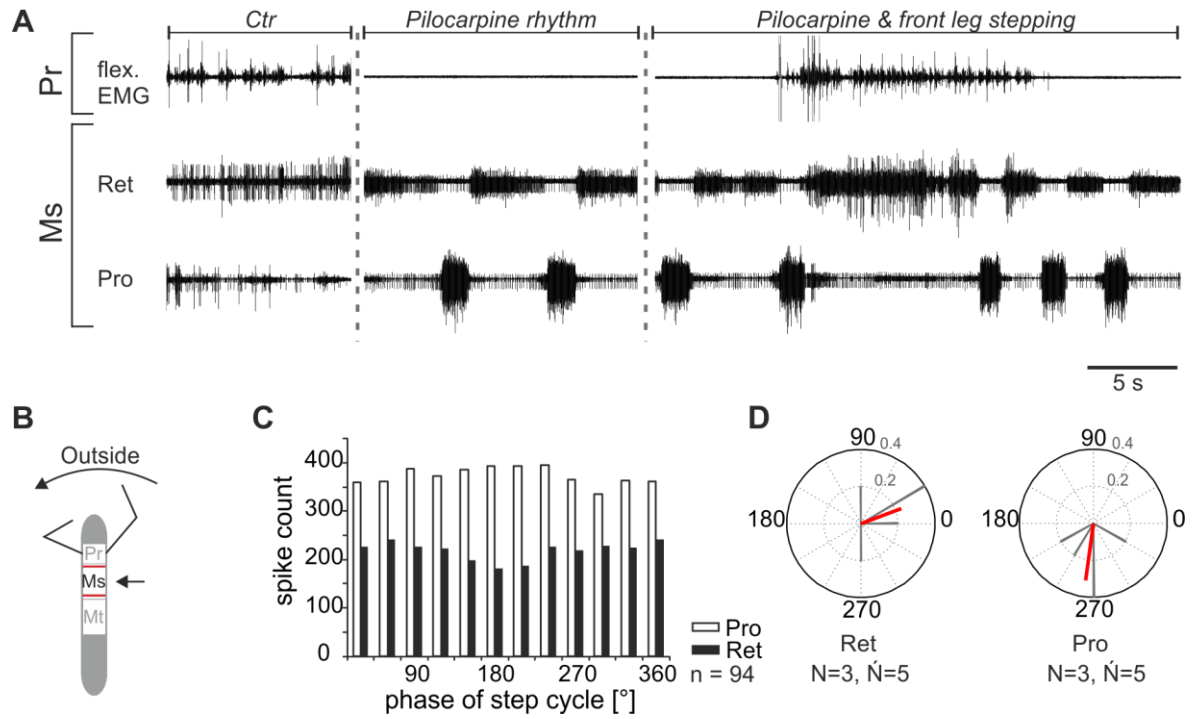


Fig. 5.1.1.2: Motor output of *protractor* (Pro) and *retractor* (Ret) *coxae* MN pools in the pilocarpine activated deafferented mesothoracic ganglion during front leg outside stepping; A) Flexor EMG recording of the front leg (top trace), together with extracellular recordings of the ipsilateral mesothoracic retractor (second trace) and protractor (third trace) nerve during outside stepping, first in control condition, and, subsequently, with pilocarpine superfusion in the quiescent animal, and during outside stepping under pilocarpine superfusion; B) Schematic of stick insect and the analyzed ganglion in the split-bath configuration; C) Phase histogram of retractor and protractor nerve activity from the experiment presented in (A) during outside stepping with respect to the step cycle of the ipsilateral front leg under pilocarpine superfusion; D) Polar plots with the spike event maxima (grey vectors) and their means (red bars) with respect to the step cycle of the ipsilateral front leg for the mesothoracic retractor (left) and protractor (right) during pilocarpine superfusion; N gives the number of analyzed animals; \dot{N} gives the number of analyzed hemiganglia; n gives the number of analyzed steps

5.1.2 *Metathorax*

As already shown by Borgmann et al. (2009), segment specificities exist for the pharmacologically activated system, as, contrary to the mesothorax, for the activated metathoracic protractor and retractor MNs it always took three to five front leg steps to become entrained.

To investigate thorax-segment specificity under modulatory descending influence, I performed experiments in the same way as in the mesothorax: the protractor and retractor nerves nl2 and nl5 were recorded from during pilocarpine superfusion and simultaneous front leg stepping. The results are summarized in figure 5.1.2.1 and in figure 5.1.2.2.

While the metathoracic leg nerve nl2 was relatively active during inside steps of the front leg, retractor activity was decreased compared to its activity during outside turns ($N = 2$, $\dot{N}_{Ret} = 3$, $\dot{N}_{Pro} = 4$) (Fig. 5.1.2.1A-C). Protractor activity had a maximal activity at 330° (range: 120° - 330°) (Fig. 5.1.2.1D, right polar plot) of the front leg step cycle, while retractor activity was in average strongest at 65.1° (range: 0° - 150°) (5.1.2.1D, left polar plot). Alternating activity between protractor and retractor MNs was found in two analyzed hemiganglia of two different animals (therefore: $N = 2$, $\dot{N} = 2$).

During outside steps, retractor activity increased in two experiments ($N = 2$, $\dot{N} = 2$) (Fig. 5.1.2.2A-C), as in the mesothoracic nerve recordings. The maximal activity peaked at 90° (range: 60° - 270°) of the front leg step cycle. In two experiments ($N = 2$, $\dot{N} = 2$), protractor activity was decreased during outside steps compared to protractor activity during inside steps, and had a widely distribution of spike event maxima with respect to the front leg stepping cycle, ranging from 120° to 300° (Fig. 5.1.2.2D, right polar plot), though the averaged maximal activity was at 195° of the front leg stepping cycle.

In summary, in the pharmacologically activated metathorax, the metathoracic protractor and retractor showed a similar activation upon front leg inside and outside stepping as the mesothoracic protractor and retractor. During inside turns, protractor activity increased, while retractor activity decreased. The opposite was seen during outside turns. Most importantly, the pilocarpine activated CPG rhythm was interrupted, independent of the turning direction. This indicates a change of local CPG activity due to front leg steps.

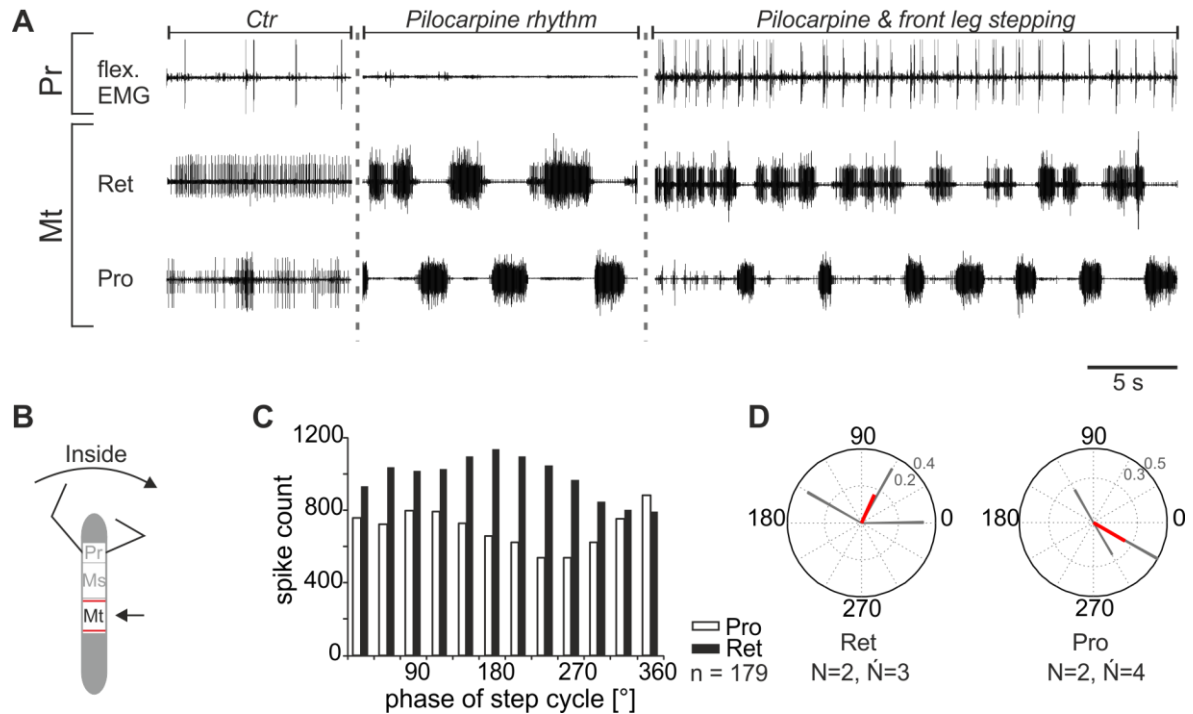


Fig. 5.1.2.1: Motor output of *protractor* (Pro) and *retractor* (Ret) *coxae* MN pools in the pilocarpine activated deafferented metathoracic ganglion during front leg inside stepping; A) Flexor EMG recording of the front leg (top trace), together with extracellular recordings of the ipsilateral metathoracic retractor (second trace) and protractor (third trace) nerve during inside stepping, first in control condition, and, subsequently, with pilocarpine superfusion in the quiescent animal, and during inside stepping under pilocarpine superfusion; B) Schematic of stick insect and the analyzed ganglion in the split-bath configuration; C) Phase histogram of retractor and protractor nerve activity from the experiment presented in (A) during inside stepping with respect to the step cycle of the ipsilateral front leg under pilocarpine superfusion; D) Polar plots with the spike event maxima (grey vectors) and their means (red bars) with respect to the step cycle of the ipsilateral front leg for the metathoracic retractor (left) and protractor (right) during pilocarpine superfusion; N gives the number of analyzed animals; \dot{N} gives the number of analyzed hemiganglia; n gives the number of analyzed steps

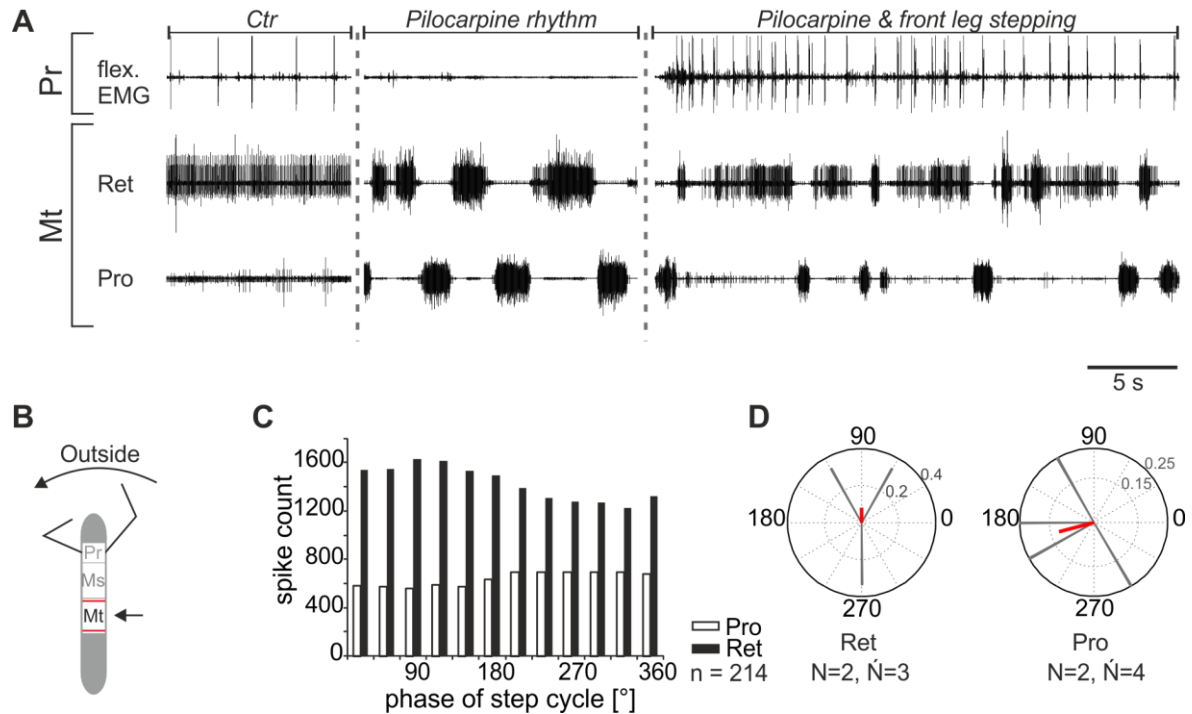


Fig. 5.1.2.2: Motor output of *protractor* (Pro) and *retractor* (Ret) *coxae* MN pools in the pilocarpine activated deafferented metathoracic ganglion during front leg outside stepping; A) Flexor EMG recording of the front leg (top trace), together with extracellular recordings of the ipsilateral metathoracic retractor (second trace) and protractor (third trace) nerve during outside stepping, first in control condition, and, subsequently, with pilocarpine superfusion in the quiescent animal, and during outside stepping under pilocarpine superfusion; B) Schematic of stick insect and the analyzed ganglion in the split-bath configuration; C) Phase histogram of retractor and protractor nerve activity from the experiment presented in (A) during outside stepping with respect to the step cycle of the ipsilateral front leg under pilocarpine superfusion; D) Polar plots with the spike event maxima (grey vectors) and their means (red bars) with respect to the step cycle of the ipsilateral front leg for the metathoracic retractor (left) and protractor (right) during pilocarpine superfusion; N gives the number of analyzed animals; \dot{N} gives the number of analyzed hemiganglia; n gives the number of analyzed steps

5.1.3 *Metathorax & Abdominal Ganglia Chain*

Büschges et al. (1995) reported that pilocarpine application onto a ventral nerve cord consisting of the deafferented pro-, meso-, and metathoracic ganglia and the intact abdominal cord elicited a different motor output in the thoracic segments compared to that when pilocarpine was applied on the thoracic ganglia chain alone. Specifically, the burst duration of the protractor MN pools was only weakly correlated with the cycle period in the preparation without the abdominal ganglia chain. Therefore, I wanted to investigate whether the pharmacological activation of the metathoracic and abdominal MN pools would result in a different metathoracic motor output than in my previous experiments, in which I activated pharmacologically only the metathoracic ganglion. For this, I applied pilocarpine on the metathorax and the abdomen, and recorded extracellularly from the leg nerves n12 and n15 in the metathorax during turning movements of the front legs. The results obtained in this preparation were very similar to those obtained without abdominal ganglia attached. This is shown in figure 5.1.3.1 and figure 5.1.3.2.

The metathoracic leg nerve n12 showed increased activity of medium-sized spikes during inside steps of the front leg, while retractor bursts were not as dense as during outside turns (Fig. 5.1.3.1A-C). Protractor activity peaked at 309° of the front leg's step cycle (range: 150°-330°; N = 3, \dot{N} = 5) (Fig. 5.1.3.1D, right polar plot), whereas retractor activity was in average strongest at 45° (range: 0°-120°; N = 3, \dot{N} = 5) (Fig. 5.1.3.1D, left polar plot).

During outside steps, retractor activity increased in two experiments (Fig. 5.1.3.2A-C), as demonstrated for the metathoracic nerve recordings in the previous experiments, where only the metathoracic ganglion was superfused with pilocarpine. Protractor activity, on the other hand, was strongly decreased compared to retractor activity, and in three experiments also compared to protractor activity during inside steps. The averaged maximal retractor activity was at 345° (range: 300°-90°), and the averaged maximal protractor activity was at 243.4°, ranging from 180°-330°.

In summary, the response of the pilocarpine activated metathoracic protractor and retractor MN pools with attached abdominal ganglia chain to front leg inside and outside stepping was similar to that of the preparation without abdominal ganglia. During inside turns protractor activity was stronger than during outside turns, whereas the opposite activity was seen for the retractor MNs.

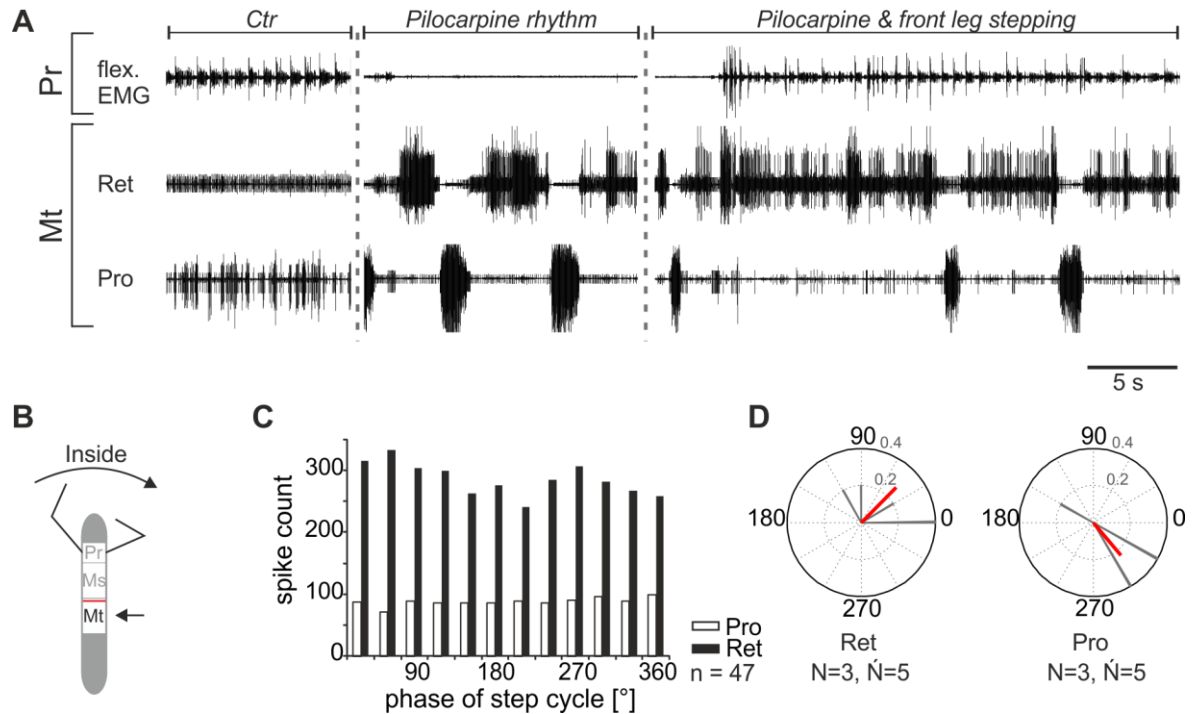


Fig. 5.1.3.1: Motor output of *protractor* (Pro) and *retractor* (Ret) *coxae* MN pools in the pilocarpine activated deafferented metathoracic ganglion during front leg inside stepping; A) Flexor EMG recording of the front leg (top trace), together with extracellular recordings of the ipsilateral metathoracic retractor (second trace) and protractor (third trace) nerve during inside stepping, first in control condition, and, subsequently, with pilocarpine superfusion in the quiescent animal, and during inside stepping under pilocarpine superfusion; B) Schematic of stick insect and the analyzed ganglion in the split-bath configuration, note that the abdominal ganglia chain is also superfused with pilocarpine; C) Phase histogram of retractor and protractor nerve activity from the experiment presented in (A) during inside stepping with respect to the step cycle of the ipsilateral front leg under pilocarpine superfusion; D) Polar plots with the spike event maxima (grey vectors) and their means (red bars) with respect to the step cycle of the ipsilateral front leg for the metathoracic retractor (left) and protractor (right) during pilocarpine superfusion; N gives the number of analyzed animals; \dot{N} gives the number of analyzed hemiganglia; n gives the number of analyzed steps

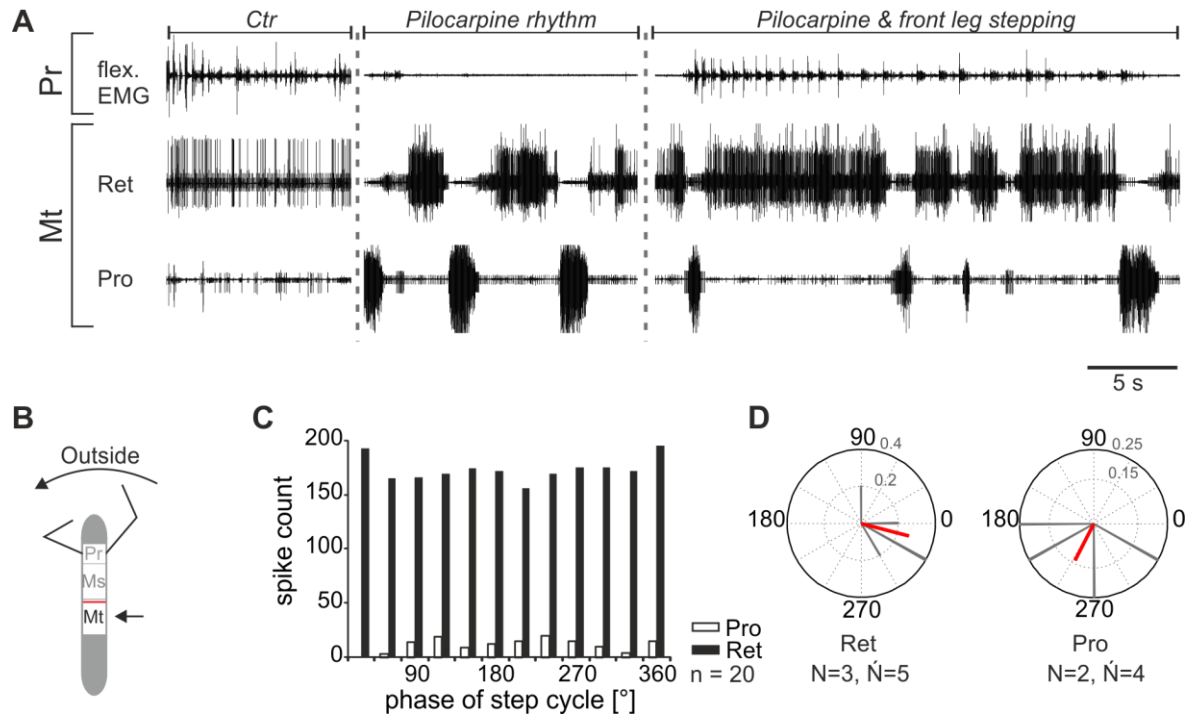


Fig. 5.1.3.2: Motor output of *protractor* (Pro) and *retractor* (Ret) *coxae* MN pools in the pilocarpine activated deafferented metathoracic ganglion during front leg outside stepping; A) Flexor EMG recording of the front leg (top trace), together with extracellular recordings of the ipsilateral metathoracic retractor (second trace) and protractor (third trace) nerve during outside stepping, first in control condition, and, subsequently, with pilocarpine superfusion in the quiescent animal, and during outside stepping under pilocarpine superfusion; B) Schematic of stick insect and the analyzed ganglion in the split-bath configuration, note that the abdominal ganglia chain is also superfused with pilocarpine; C) Phase histogram of retractor and protractor nerve activity from the experiment presented in (A) during outside stepping with respect to the step cycle of the ipsilateral front leg under pilocarpine superfusion; D) Polar plots with the spike event maxima (grey vectors) and their means (red bars) with respect to the step cycle of the ipsilateral front leg for the metathoracic retractor (left) and protractor (right) during pilocarpine superfusion; N gives the number of analyzed animals; \bar{N} gives the number of analyzed hemiganglia; n gives the number of analyzed steps

5.1.4 *Meso- & Metathorax*

The study by Büschges et al. (1995) is the only one, in which a simultaneous pharmacological activation of two or even three thoracic CPGs was reported for the stick insect. There, the authors demonstrated that in the isolated thoracic ganglia chain, the simultaneous activation of pro-, meso- and metathoracic CPGs resulted in long periods of in-phase activity in the protractor MN pools of all three thoracic segments. Beforehand, I reported for the individually activated meso- and metathoracic MN pools, that front leg stepping had a similar effect on both thoracic MN pools, for both turning directions (during inside turns: increased protractor activity, and decreased retractor activity; during outside turns the opposite activity was seen).

Now, I wanted to investigate, whether the motor output of the meso- and metathoracic subcoxal MN pools would be similar to that in the isolated activated thoracic MN pools, or whether the simultaneous activation of the CPGs of both thoracic segments would result in a different motor output.

Therefore, I applied pilocarpine on the meso- and metathoracic ganglia, and recorded extracellularly from the leg nerves nl2 and nl5 in both segments during turning of the front legs. In eight (out of 25) experiments, the exposure to pilocarpine was too short to evaluate the data. In another nine experiments, metathoracic activity ceased before a stable rhythm was obtained. In two additional experiments, animals could not be induced to perform walking. In two experiments, a stable rhythm was observed in the meso- but not in the metathorax, even after applying more pilocarpine to the body cavity. In one experiment, a stable rhythm was present in the meso- and metathorax, but only for a short time. In one other experiment, a stable rhythm was obtained in the meso- and metathorax, but the cycle duration was extraordinarily long (with approximately 30 s, three times as long as in other recordings). Finally, two experiments (out of 25) showed a stable rhythm in the meso- and metathorax: one of that animals only performed outside turning, and the other inside and outside turning after pilocarpine application. The results are summarized in figure 5.1.4.1 and figure 5.1.4.2.

During inside steps of the front leg, the meso- and metathoracic nl2 nerves were strongly active, while retractor activity was relatively low ($N = 1$, $\hat{N} = 1$) (Fig. 5.1.4.1A-C). Both, meso- and metathoracic protractor activity was strongest at about 300° of the front leg's step cycle (Fig. 5.1.4.1Di & Dii, right polar plot), whereas mesothoracic retractor activity was strongest at about 90° , and metathoracic retractor activity had its maximum at 60° of

the front leg step cycle (Fig. 5.1.4.1Di & Dii, left polar plot). Clear alternation between protractor and retractor activity was seen in both segments (Fig. 5.1.4.1B&C).

The two successful experiments in which the animal did outside turns are summarized in figure 5.1.4.2. During outside steps, retractor activity increased, while protractor activity decreased in both segments (Fig. 5.1.4.2A-C). In neither of the leg nerves, a clear tendency regarding the maximum activity during the front leg step cycle was apparent. While the averaged maximal activity in the mesothoracic retractor was at 300° of the step cycle (range: 270° & 330°) (Fig. 5.1.4.1Di, left polar plot), that of the metathorax was at 105° (150° & 60°) (Fig. 5.1.4.2Dii, left polar plot). The maximal activity of the mesothoracic protractor was at 165° (range: 120° & 210°), while the metathoracic protractor showed highest activity at 45° (range: 0° & 90°) of the front leg step cycle.

In summary, simultaneous application of pilocarpine to the meso- and metathorax resulted in protractor and retractor activity that resembled that of the isolated activated meso- and metathorax. While the protractor nerves of both segments were highly active during inside steps, their activity decreased during outside steps. The opposite was found for the retractor nerves of both segments.

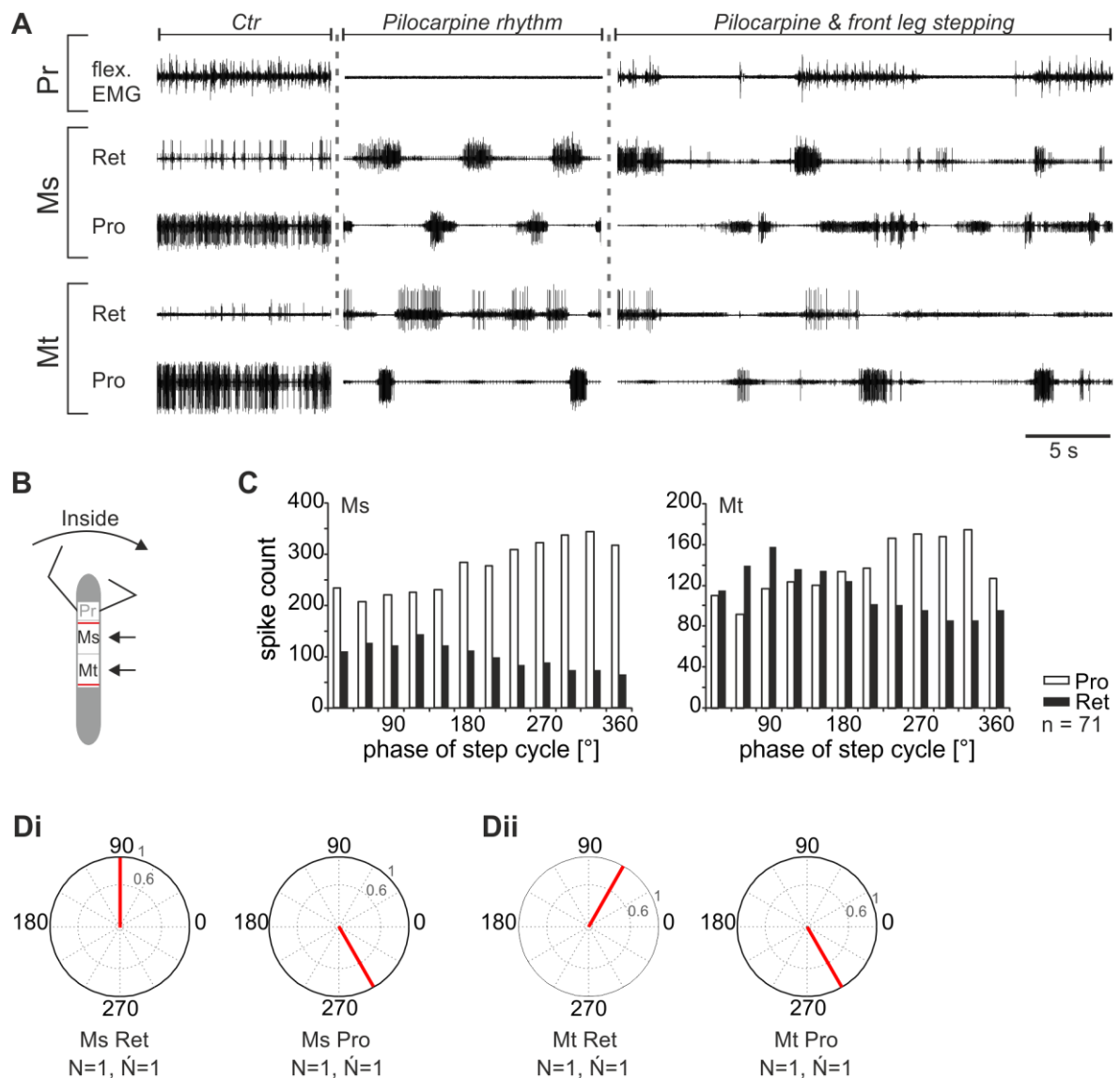


Fig. 5.1.4.1: Motor output of *protractor* (Pro) and *retractor* (Ret) *coxae* MN pools in the pilocarpine activated deafferented meso- and metathoracic ganglia during front leg inside stepping; A) Flexor EMG recording of the front leg (top trace), together with extracellular recordings of the ipsilateral meso- (second & third trace) and metathoracic retractor and protractor (fourth & fifth trace) nerve during an inside stepping sequence, first in control condition, and, subsequently, with pilocarpine superfusion in the quiescent animal, and during inside stepping under pilocarpine superfusion; B) Schematic of stick insect and the analyzed ganglia in the split-bath configuration; C) Phase histogram of meso- (left) and metathoracic (right) retractor and protractor nerve activity under pilocarpine superfusion from the experiment presented in (A) during inside stepping with respect to the step cycle of the ipsilateral front leg; D) Polar plots with the spike event maxima (red bars) with respect to the step cycle of the ipsilateral front leg for the mesothoracic (Di) retractor (left) and protractor (right) and for the metathoracic (Dii) retractor (left) and protractor (right) during pilocarpine superfusion; N gives the number of analyzed animals; \dot{N} gives the number of analyzed hemiganglia; n gives the number of analyzed steps

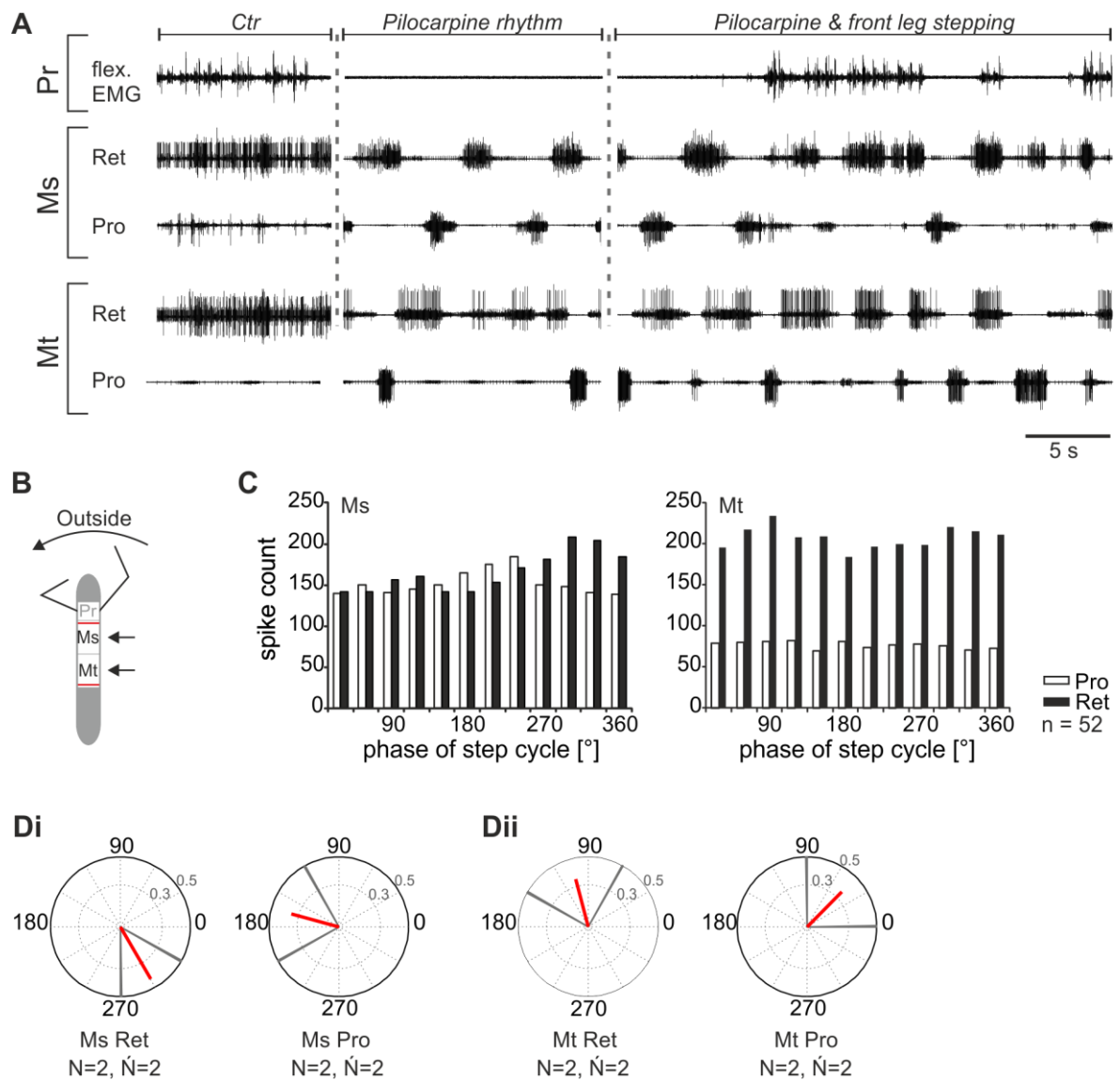


Fig. 5.1.4.2: Motor output of *protractor* (Pro) and *retractor* (Ret) *coxae* MN pools in the pilocarpine activated deafferented meso- and metathoracic ganglia during front leg outside stepping; A) Flexor EMG recording of the front leg (top trace), together with extracellular recordings of ipsilateral meso- (second & third trace) and metathoracic retractor and protractor (fourth & fifth trace) during an outside stepping sequence, first in control condition, and, subsequently, with pilocarpine superfusion in the quiescent animal, and during outside stepping under pilocarpine superfusion; B) Schematic of stick insect and the analyzed ganglia in the split-bath configuration; C) Phase histogram of meso- (left) and metathoracic (right) retractor and protractor nerve activity under pilocarpine superfusion from the experiment presented in (A) during outside stepping with respect to the step cycle of the ipsilateral front leg; D) Polar plots with the spike event maxima (grey vectors) and their mean (red bars) with respect to the step cycle of the ipsilateral front leg for the mesothoracic (Di) retractor (left) and protractor (right) and for the metathoracic (Dii) retractor (left) and protractor (right) during pilocarpine superfusion; N gives the number of analyzed animals; \bar{N} gives the number of analyzed hemiganglia; n gives the number of analyzed steps

5.2 Levator and Depressor Trochanteris

In the previous chapter (5.1), I was able to demonstrate that the constant rhythm of the pharmacologically activated meso- and metathoracic central pattern generators of the subcoxal joint was not only interrupted by front leg stepping, but also modified during inside turns of the front legs. This leads to the question, whether the same is true for the motor output of the next distal, the coxa-trochanteral joint.

It is well known, that in the isolated deafferented thoracic nerve cord of the stick insect, the muscarinic agonist pilocarpine induces a stable rhythm between the antagonistic coxa-trochanteral MN pools innervating the *levator* and *depressor trochanteris* (Büschges et al. 1995). Büschges et al. (1995) reported, that, while slow levator MNs were tonically active, semi-fast and fast levator MNs produced clearly defined synchronized bursts of activity, that were in anti-phase with the bursts produced by the slow (SDTr) and fast (FDTr) depressor MNs. In contrast to the SDTr, the FDTr did not reach its activation threshold within each cycle of activity. In comparison to the subcoxal MN burst, the coxa-trochanteral cycle period was not as constant as that of the subcoxal MNs (Büschges et al. 1995).

5.2.1 Mesothorax

To investigate the involvement of coxa-trochanteral central pattern generators in the turning related motor output, I used a split-bath preparation, in which the mesothoracic ganglion was superfused with pilocarpine, and during this, the animals were induced to perform inside and outside turns with their front legs.

As in the preparation that was activated through front leg stepping alone, levator activity increased drastically with the begin of a walking sequence, and usually continued throughout the whole walking sequence, independent of the turning direction (inside: $N = 3$, $\acute{N} = 4$, Fig. 5.2.1.1A/Bi/Ci; outside: $N = 4$, $\acute{N} = 5$, Fig. 5.2.1.2A/Bi/Ci). In most experiments, depressor activity was reduced to single spikes during walking sequences. Only in one animal, levator activity was interrupted by depressor bursts during inside (Fig. 5.2.1.1A/Bii/Cii) and even more during outside turns (Fig. 5.2.1.2 A/Bii/Cii). In both MN pools, the spike event maxima were widely distributed during inside turns (levator: 0° - 330° , max: 353.3° ; depressor: 30° - 240° , max: 60°) (Fig. 5.2.1.1D), as well as during

outside turns (levator: 0° - 300° , max: 37.1° ; depressor: 60° - 270° , max: 146.6°) (Fig. 5.2.1.2 D).

In summary, in most cases the coxa-trochanteral MN pools of the pilocarpine activated mesothorax were activated in a similar manner as beforehand without pilocarpine. As the pharmacologically evoked CPG rhythm was interrupted by front leg stepping, my data indicate the involvement of CPGs in the changes of the motor output.

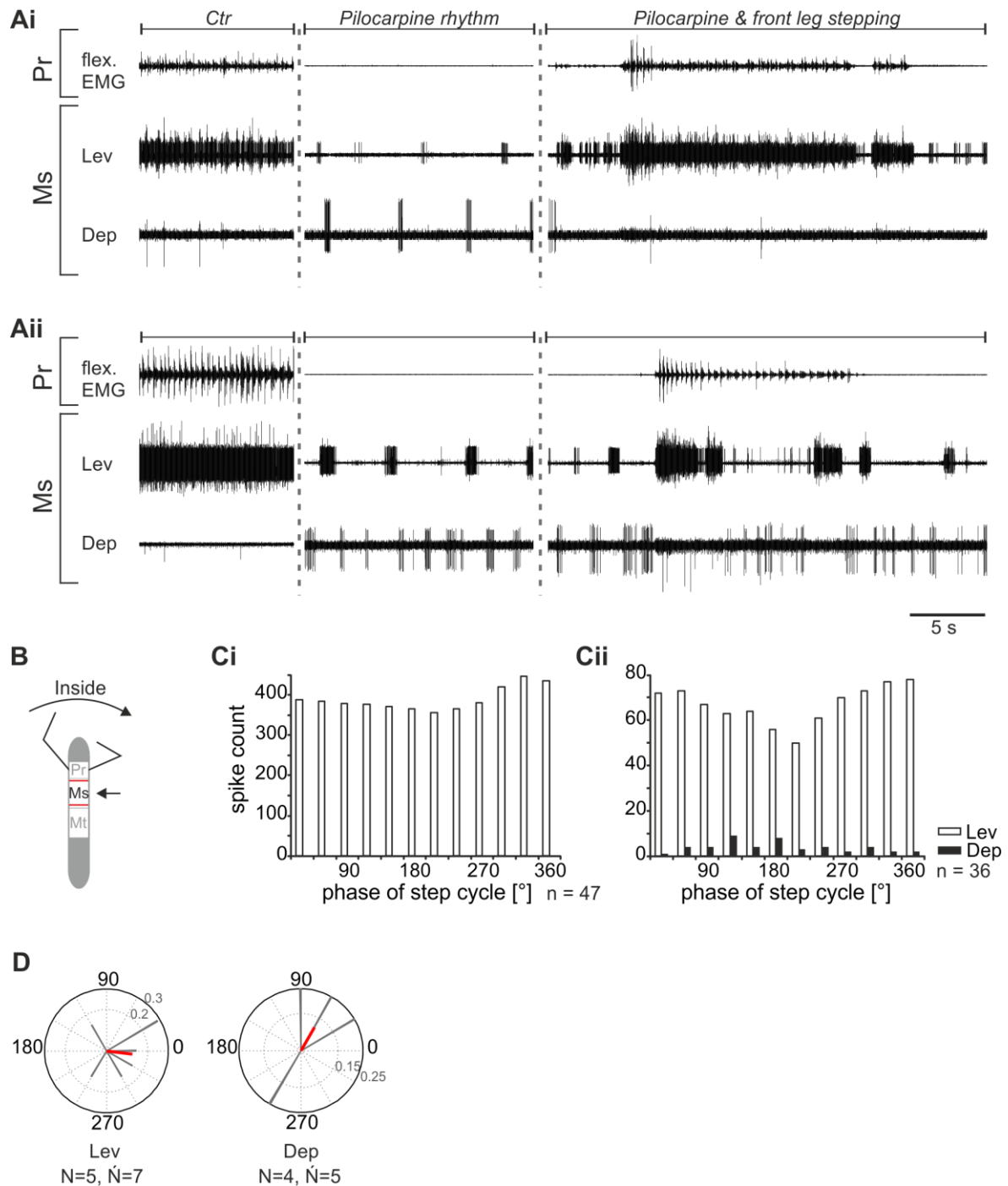


Fig. 5.2.1.1: Motor output of *levator* (Lev) and *depressor* (Dep) *trochanteris* MN pools in the pilocarpine activated deafferented mesothoracic ganglion during front leg inside stepping; A) Flexor EMG recording of the front leg (top trace), together with extracellular recordings of the ipsilateral mesothoracic levator (second trace) and depressor (third trace) nerve during an inside stepping sequence, first in control condition, and, subsequently, with pilocarpine superfusion in the quiescent animal, and during inside stepping under pilocarpine superfusion for two different experiments (Ai & Aii); B) Schematic of stick insect and the analyzed ganglion in the split-bath configuration; C) Phase histogram of depressor and levator nerve activity under pilocarpine superfusion from the experiments presented in Ai (see Ci) and Aii (see Cii) during inside stepping with respect to the step cycle of the ipsilateral front leg; D) Polar plots with the spike event maxima (grey vectors) and their means (red bars) with respect to the step cycle of the ipsilateral front leg for the mesothoracic levator (left) and depressor (right) of all experiments during pilocarpine superfusion; N gives the number of analyzed animals; \bar{N} gives the number of analyzed hemiganglia; n gives the number of analyzed steps

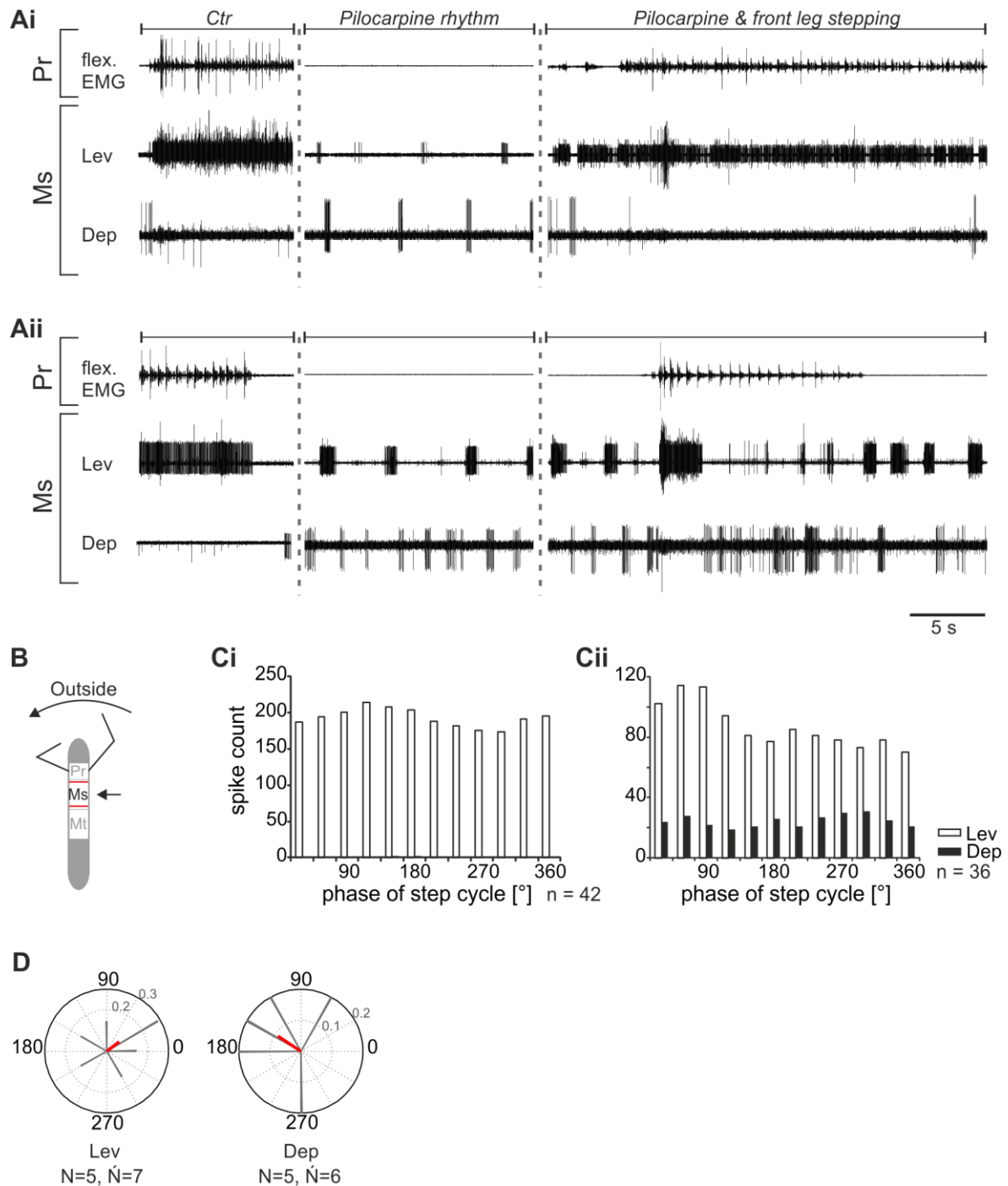


Fig. 5.2.1.2: Motor output of *levator* (Lev) and *depressor* (Dep) *trochanteris* MN pools in the pilocarpine activated deafferented mesothoracic ganglion during front leg outside stepping; A) Flexor EMG recording of the front leg (top trace), together with extracellular recordings of ipsilateral mesothoracic levator (second trace) and depressor (third trace) during an outside stepping sequence, first in control condition, and, subsequently, with pilocarpine superfusion in the quiescent animal, and during outside stepping under pilocarpine superfusion for two different experiments (Ai & Aii); B) Schematic of stick insect and the analyzed ganglion in the split-bath configuration; C) Phase histogram of levator and depressor nerve activity under pilocarpine superfusion from experiment presented in Ai (see Ci) and Aii (see Cii) during outside stepping with respect to the step cycle of the ipsilateral front leg; D) Polar plots with the spike event maxima (grey vectors) and their means (red bars) with respect to the step cycle of the ipsilateral front leg for the mesothoracic levator (left) and depressor (right) of all experiments during pilocarpine superfusion; N gives the number of analyzed animals; \bar{N} gives the number of analyzed hemiganglia; n gives the number of analyzed steps

5.2.2 *Metathorax*

As I demonstrated thorax-segment specificity for the MN pools of the coxa-trochanteral joint in the previous, not pharmacologically activated preparation, I wanted to find out, whether this specificity also occurs in the pharmacologically activated preparation. Therefore, I applied pilocarpine on the metathoracic ganglion, and recorded extracellularly from the leg nerves C1 and C2 during turning of the front legs. The results are summarized in figure 5.2.2.1 and figure 5.2.2.2.

Once again, in most cases ($N = 3$, $\dot{N} = 6$) levator activity increased during stepping sequences independent of the turning direction. However, in one experiment, levator activity was only strong during inside steps of the front legs, while it was drastically lowered during outside stepping. In general, depressor activity was not as strong as levator activity, but depressor bursts interrupted levator activity more often during stepping sequences as compared to the results of the mesothorax (Fig. 5.2.2.1A-C, Fig. 5.2.2.2A-C). The distribution of maximum activity throughout the front leg step cycle was for both leg nerves highly variable. In inside turns, the spike event maxima of the levator ranged from 150° to 330° , and had an averaged maximum of 219.9° , and the spike event maxima of the depressor ranged from 0° to 330° , and had an averaged maximum of 10.9° (Fig. 5.2.2.1D). During outside turns, levator activity peaked at 105° (range: 0° - 300°), while depressor activity peaked at 315° (range: 90° - 330°) (Fig. 5.2.2.2D).

In summary, in the pharmacologically activated system metathoracic levator activity increased during stepping sequences. However, different from the finding in the mesothoracic ganglion, metathoracic depressor bursts were occasionally seen during front leg stepping, independent of the turning direction. This could indicate that the influence of the front legs on the CPG in the metathorax is weaker than that on the mesothorax.

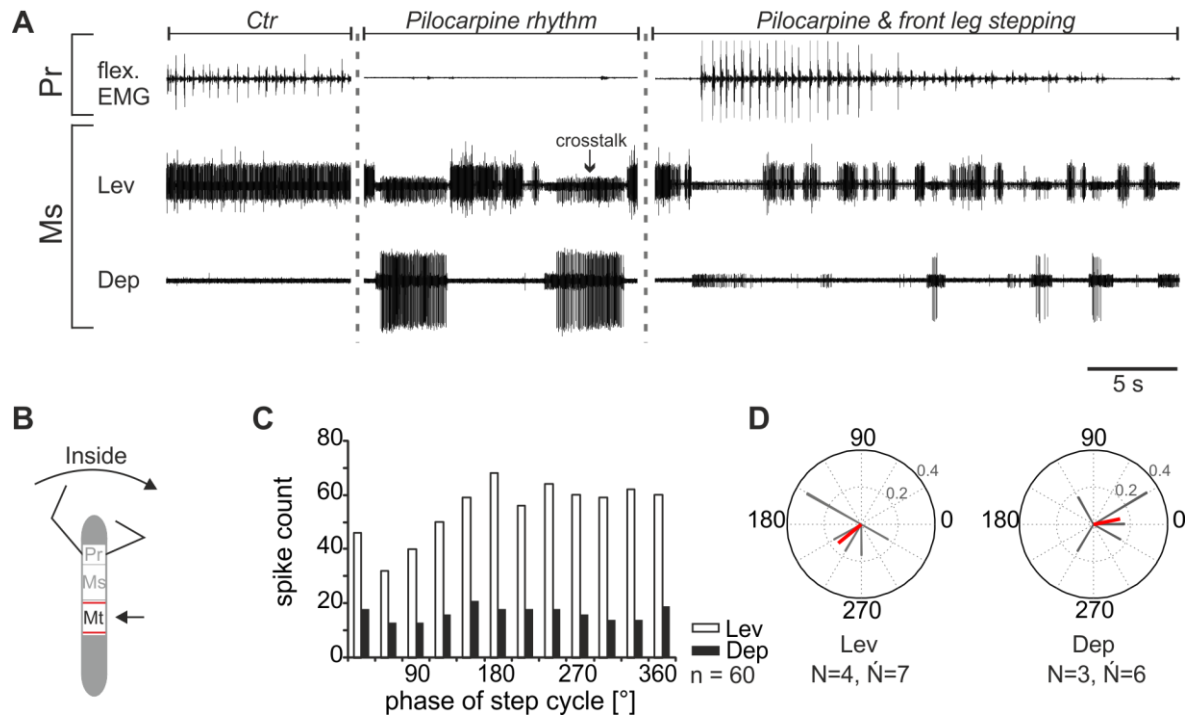


Fig. 5.2.2.1: Motor output of *levator* (Lev) and *depressor* (Dep) *trochanteris* MN pools in the pilocarpine activated deafferented metathoracic ganglion during front leg inside stepping; A) Flexor EMG recording of the front leg (top trace), together with extracellular recordings of the ipsilateral metathoracic levator (second trace) and depressor (third trace) nerve during an inside stepping sequence, first in control condition, and, subsequently, with pilocarpine superfusion in the quiescent animal, and during inside stepping under pilocarpine superfusion; B) Schematic of stick insect and the analyzed ganglion in the split-bath configuration; C) Phase histogram of levator and depressor nerve activity under pilocarpine superfusion from the experiment presented in (A) during inside stepping with respect to the step cycle of the ipsilateral front leg; D) Polar plots with the spike event maxima (grey vectors) and their means (red bars) with respect to the step cycle of the ipsilateral front leg for the metathoracic levator (left) and depressor (right) of all experiments during pilocarpine superfusion; N gives the number of analyzed animals; \bar{N} gives the number of analyzed hemiganglia; n gives the number of analyzed steps

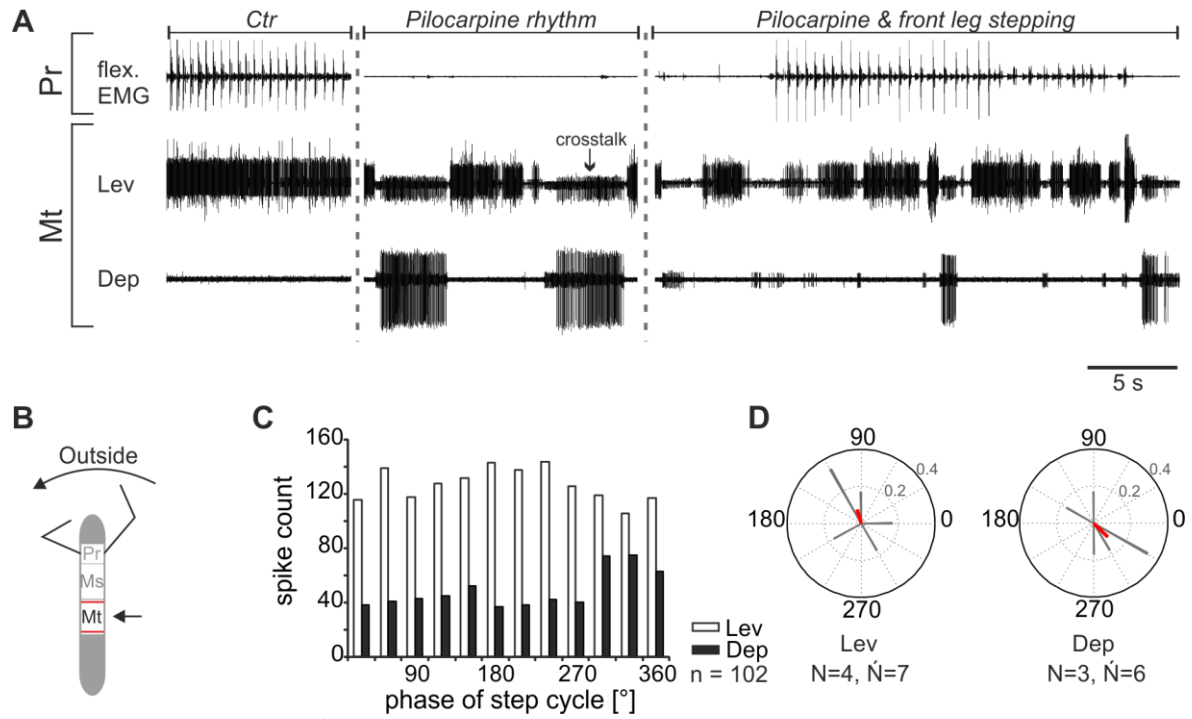


Fig. 5.2.2.2: Motor output of *levator* (Lev) and *depressor* (Dep) *trochanteris* MN pools in the pilocarpine activated deafferented metathoracic ganglion during front leg outside stepping; A) Flexor EMG recording of the front leg (top trace), together with extracellular recordings of the ipsilateral metathoracic levator (second trace) and depressor (third trace) nerve during an outside stepping sequence, first in control condition, and, subsequently, with pilocarpine superfusion in the quiescent animal, and during outside stepping under pilocarpine superfusion; B) Schematic of stick insect and the analyzed ganglion in the split-bath configuration; C) Phase histogram of levator and depressor nerve activity under pilocarpine superfusion from the experiment presented in (A) during outside stepping with respect to the step cycle of the ipsilateral front leg; D) Polar plots with the spike event maxima (grey vectors) and their means (red bars) with respect to the step cycle of the ipsilateral front leg for the metathoracic levator (left) and depressor (right) of all experiments during pilocarpine superfusion; N gives the number of analyzed animals; \bar{N} gives the number of analyzed hemiganglia; n gives the number of analyzed steps

CHAPTER 6

Discussion

The goal of this thesis was to study thorax-segment and leg-segment specificities on muscular and neuronal level. On the one hand, I wanted to determine the muscle fiber composition of the six major leg muscles of each thoracic segment (chapter 3). On the other hand, I wanted to investigate the segment-specificities on neuronal level by analyzing the local output of the meso- and metathoracic leg nerves (chapter 4) and the involvement of local central pattern generators on the motor output (chapter 5) during front leg turning. In the following, the results of each chapter will be discussed in detail.

6.1 Characterization of Muscle Fiber Types

The production of smooth and continuous movements relies on finely tuned neuronal output and the appropriate muscular response. The muscle contractions are based on the cross-bridge cycle during which the enzyme myofibrillar ATPase (mATPase) hydrolyzes adenosine triphosphate to adenosine diphosphate and a single phosphate molecule. This causes myosin to attach to the actin filament, and finally, through repetitive attachment and detachment, and concomitant movement of the actin and myosin filaments against one another, the muscle contracts. As a consequence, mATPase activity is a crucial and speed determining step for the invertebrate and vertebrate muscular contraction. In the last

decades, studies analyzed mATPase function and its role for the contraction speed of single muscle fibers (e.g. Bárány 1976, Close 1976/1972, Barnard et al. 1971, Burke et al. 1971, Edgerton & Simpson 1971). In these studies it was found that fiber types of entire muscles can be distinguished using histochemical staining for mATPase activity, since the mATPase activity is pH dependent (Sréter et al. 1966, Seidel 1967, Guth & Samaha 1969, Guth & Samaha 1970, Brooke & Kaiser 1970, Bässler et al. 1996, Gruhn & Rathmayer 2002, reviewed in : Pette & Staron 1990). In vertebrates, Billeter et al. (1981) showed that mATPase activity is correlated with the respective myosin heavy chain (MHC) isoform in human. This finding was supported by Rivero et al. (1996), who found that the same is true for equine skeletal muscles, when comparing mATPase histochemistry with immunohistochemistry using monoclonal antibodies for selected MHC isoforms. Furthermore, it was shown that different fiber types have specific myosin isoforms. This was shown for invertebrates and vertebrates (Cooper et al. 1995, Pette & Staron 2001). While fast myosin isoforms show stable activity after acidic pre-incubation, they are inactivated after alkaline pre-incubation. The opposite can be observed for slow myosin isoforms, whereas intermediate isoforms cannot be clearly classified, since they show medium activity at a neutral pH value and are active after acidic and alkaline pre-incubation (Henneman & Olsen 1965, Maier et al. 1984, Bässler et al. 1996). Studies using mATPase staining, as well as other methods (e.g. SDH staining or glycogen content), revealed that invertebrates and vertebrates can either show a homogeneous muscle fiber composition (e.g. cockroach: Jahromi & Atwood 1969, Fournier 1978, Stokes et al. 1979, guinea pig: Barnard et al. 1971), or show a huge heterogeneity considering the muscle fiber composition (cockroach: Stokes et al. 1979, crab: Maier et al. 1984, spider: Maier et al. 1987, stick insect: Bässler et al. 1996, Pilehvarian 2015, crayfish: Gruhn & Rathmayer 2002).

In this part of my thesis, I wanted to find out, whether the leg muscles of the stick insect *Carausius morosus* show a homogenous or a heterogeneous muscle fiber composition, which muscle fiber types are predominantly present, and whether differences in fiber composition between the individual thoracic segments can be observed, as specific differences in fiber type composition could have functional implication about the neuronal control. For this purpose, I characterized the muscle fiber types in the six major leg muscles of the meso- and metathorax, as well as the muscle fiber types of the *levator* and *depressor trochanteris*, and the *extensor* and *flexor tibiae* of the prothoracic segment in the

stick insect. All experiments relied on the different stability of the enzyme mATPase under acidic and alkaline pre-incubation for slow, intermediate, and fast muscle fibers.

For the mesothoracic *protractor* and *retractor coxae*, I found that the majority of both muscles was made up of fast and intermediate muscle fibers, whereas slow fibers made up only a small fraction of these muscles. The same was true for the metathoracic protractor, whereas in the metathoracic retractor the amount of slow fibers was significantly higher compared to that in the mesothorax. Comparing protractor and retractor muscles to each other, one can see that the retractor muscle in general contained more slow and fewer fast fibers than the protractor, while the amount of intermediate fibers in both muscles was approximately the same. Especially, the amount of slow fibers in the metathoracic anterior retractor is prominent, as it is made of up to one-third of the muscle (see chapter 3.1).

For the *levator* and *depressor trochanteris*, I showed that the levator consisted mostly of fast contracting muscle fibers in all thoracic segments, while the amount of slow muscle fibers was significant lower to the fast ones in all segments. The depressor muscle, on the other hand, consisted mostly of fast and intermediate muscle fibers in the prothorax, while in the meso- and metathoracic depressor the amount of intermediate muscle fibers was lower, although in no case significantly. Interestingly, a successive increase in the proportion of slow fibers from prothorax, thorough meso- to metathorax was observed in the depressor. In two experiments, in the mesothoracic levator one single fiber of the fourth fiber type, the dd intermediate type, was found (see chapter 3.2).

The *extensor* and *flexor tibiae* consisted in all three analyzed thoracic segments of the three different fiber types, found in the other muscles. All segments showed a similar fiber type distribution for both muscles. While the proportion of slow fibers increased from proximal to distal, the proportion of fast contracting muscle fibers decreased from proximal to distal. The amount of intermediate fibers, on the other hand, was in all analyzed sub-sections constant (see chapter 3.3).

My results show that all analyzed leg muscles of the different segments contained at least three fiber types (slow, fast, and II-intermediate), and in no case a homogeneous fiber type composition was observed. Since many previous studies on muscular composition of invertebrates demonstrated that a heterogeneous composition is common (e.g. Maier et al. 1984/ 1987, Gruhn & Rathmayer 2002), this finding is not that unexpected. Most importantly, the two existing studies on muscle fiber composition in the stick insect reported the same (Bässler et al. 1996, Pilehvarian 2015). Bässler et al. (1996) showed for

the *extensor tibiae* muscle of the stick insects species *Carausius morosus* and *Cuniculina impigra*, as well as for the locust *Locusta migratoria* a gradually decrease of fast contracting muscle fibers from proximal to distal in the extensor, while an opposite gradient was found for slow contracting fibers. When comparing my results to those of Bässler et al. (1996), one has first to take into account that I categorized the femora into a proximal, medial and distal part, whereas Bässler et al. worked with a system using the percentage of the femur length ranging from 20 to 100 %. Therefore, the proximal area of my results corresponds to approximately 35 % of the femur length in Bässler's study, the medial region of interest corresponds to approximately 60 % of femur length, and the distal region to approximately 85 % of femur length in Bässler's study. Considering this, Bässler et al. described much greater percentages of fast fibers than I found for *Carausius morosus* in all regions of interest (proximal part: Bässler: ~ 95 %, my result: 32.8-59.0 %; medial part: Bässler: ~ 90 %, my result: 33.8-59.6 %; distal part: Bässler: ~ 65 %, my result: 29.8-47.3 %). In contrast to this, the amount of slow fibers is similar for the proximal extensor (Bässler: ~ 4%, my results: 0.7-6.3 %). For the medial and distal regions the difference is only small between my and Bässler's results. In both areas, Bässler et al. found a higher occurrence of slow contracting muscle fibers than I did (medial part: Bässler: ~ 10 %, my results: ~ 2.4-8.5 %; distal part: Bässler: ~ 30 %, my results: 17.3-29.2 %). A reason for these discrepancies is probably the method of analysis. While I compared acidic and alkaline pre-incubated sections to determine slow, intermediate and fast contracting muscle fibers, Bässler et al. relied on acidic pre-incubation only for their classification. In addition, I used a grayscale value – which automatically classified the fibers into darkly or lightly stained – of 0.75, where 1 is defined as the darkest area in the analyzed section. This probably caused the comparatively high amount of intermediate muscle fibers in my analysis. Taking all this into account, my results are in good accordance to Bässler's findings.

For the antagonistic *flexor tibiae* muscle, no data existed from the stick insect *Carausius morosus*, but a recent publication analyzed this muscle in the stick insect species *Eurycantha calcarata*, L (Pilehvarian 2015). Pilehvarian found that in females and males, with different leg morphology, only few fibers were lightly stained, and these had a smaller diameter than other fibers. In general, these fibers were classified due to their properties as slow contracting muscle fibers and represented less than 10 % of the total muscle area. Most of the muscle area was made up of fast and intermediate contracting muscle fibers, however, no further discrimination between these types was done. Comparing my results to

Pilehvarian's, strong discrepancies are obvious. While my results showed a fiber composition similar to that of the previously described extensor, with a decrease in the amount of fast fibers from proximal to distal and the opposite distribution of slow fibers, Pilehvarian's results describe a more uniform distribution of mostly fast contracting muscle fibers. These discrepancies may have different reasons. First, and most obvious, the author used metathoracic hind legs of female and male animals of the species *Eurycantha calcarata*, L. As shown for example by Bässler et al. (1996), who compared the fiber composition of the two stick insect species *Carausius morosus* and *Cuniculina impigra*, differences between species can occur. Bässler et al. reported that *Cuniculina impigra* had a larger percentage of slow fibers in the *extensor tibiae* than *Carausius morosus*. Another possible reason for the difference is the mATPase staining method used. Pilehvarian only referred to one previous publication (Stokes et al. 1979) for the staining procedure. In Stokes' publication it is stated that they used pH values of 4.3 for acidic pre-incubation (my study: pH 4.7) and pH 10.4 for alkaline pre-incubation (my study: pH 10.1). These are slight, but very important differences in the used pH values (Brooke & Kaiser 1970). It is not clear, why Pilehvarian did use pre-incubation values reported for the cockroach *Periplaneta americana*, instead of using values that had been previously described for stick insects (Bässler et al. 1996). In addition to not giving any pH values, Pilehvarian's description leaves it unclear, whether he compared alkaline and acidic pre-incubated sections or not. Therefore, possible intermediate fibers could have been misinterpreted as fast contracting muscle fibers. As a consequence, any differences with Pilehvarian's results have to be treated with extreme caution.

Comparable data for the muscular composition in stick insects exist neither for the muscles of the coxa-trochanteral joint, nor for those of the subcoxal joint. However, some data for the coxal muscles data exist from cockroach (Stokes et al. 1979, Morgan et al. 1980) and locust (Müller et al. 1992). For the cockroach *Periplaneta americana*, Stokes et al. (1979) found after staining for mATPase activity, nicotinamide adenine dinucleotide (NADH) reductase, lactic dehydrogenase (LDH) and succinic dehydrogenase (SDH) that the mesothoracic coxal muscles of the cockroach show a heterogeneous composition. Morgan et al. (1980) verified these results and compared the findings with the muscle composition of the homologous metacoxal muscle. They showed that the coxal muscles of both segments have a comparable muscle fiber composition. The results for the coxal muscles of my study show the same tendency. For all three segments, I report approximately the same amounts of slow, intermediate and fast contracting muscle fibers for the levator and

the depressor, respectively. The only statistically significant differences occur for the amount of slow fibers between the prothoracic and mesothoracic levator and the increase in slow fibers from pro- through meso- to metathorax in the depressor, which leads to significantly more slow fibers in the metathoracic versus the prothoracic depressor.

Müller et al. (1992) investigated the correlation of electrophysiological, histochemical, and mechanical properties in the fibers of the coxa rotator muscle of the locust. For this they used, in addition to electrophysiological experiments, mATPase staining after more neutral (pH 8.4) and alkaline pre-incubation (pH 10.2). They also tested mATPase activity after acidic pre-incubation (pH 4.0-5.0), but found out that under this condition mATPase of all fibers was inactivated. However, with their study they were able to show that the centrally located slow contracting muscle fibers (type I) are surrounded by intermediate fibers (type IIa), whereas fast contracting muscle fibers (type IIb) enclose both fiber types. In my study, a comparable distribution of these fiber types was present for the levator and depressor. Both muscles of all thoracic segments had slow muscle fibers that were surrounded by intermediate ones, while these, again, were enclosed by fast contracting muscle fibers. Therefore, my results are in good accordance to the results of Morgan et al. (1980) and Müller et al. (1992) for the coxal muscles.

As already mentioned above, no reports exist in which the subcoxal muscles of stick insects were analyzed with respect to muscle fiber type composition, not even from other insects. This is astonishing as many electrophysiological studies focus on the leg nerves innervating these muscles.

After comparing the fiber type distribution within different stick insect muscles, the question remains as to the functional implications of the specific muscle fiber compositions. For instance, what may be the role of the large amount of fast fibers in *protractor coxae* and *levator trochanteris*, or the relatively large amount of slow fibers in *retractor coxae* and *depressor trochanteris*, and finally the inverse gradient of fast and slow fibers in *extensor* and *flexor tibiae*?

Rosenbaum et al. (2010) showed using EMG recordings of these six leg muscles in the stick insect *Carausius morosus* that in the forward walking animal the protractor, levator, and the extensor were active during swing phase, whereas their respective antagonists were active during stance phase. In backward walking movements the activation pattern of the muscles of the subcoxal joint reversed, while the muscles of the other joints showed maximal activity as before during forward walking movements. Since stick insects do not

tend to walk backwardly in nature, one can summarize that protractor, levator and extensor function as swing muscles, and retractor, depressor and flexor function as stance muscles (Rosenbaum et al. 2010; for motoneuronal activity see e.g. Bässler et al. 2007). Taking into account that swing phases have a relative high velocity compared to stance phases (Wendler 1964, Graham 1972), independent of the stepping velocity (Gruhn et al. 2009a), it is obvious that muscles that are mainly active during swing phase have to consist to a larger extend of fast contracting muscle fibers to enable the fast swing movement. Stance phase muscles, on the other hand, have to consist to a larger extend of intermediate or slow contracting muscle fibers as they do not only lower and retract the leg, and flex the tibia during stepping sequences, but more importantly, do support the body position of the animal and the stiffening of the respective joint. A recent study by Dallmann et al. (2016) showed that depression torques about the coxa-trochanter joint of hind and middle legs were critical for generating propulsion, in addition to supporting the body weight. This supports my findings for the *depressor trochanteris*, as I found a successive increase in slow fibers from pro- to metathorax. Surprisingly, for torques about the subcoxal joint they found out that those only initially peaked towards the retraction, and were only small or even switched towards protraction during maximal propulsion. This is counterintuitive to my findings. However, taking into account that stick insects usually do not move on a plane surface, but rather climb through bushes, this seeming contradiction is put into perspective.

Considering the difficulties in obtaining data on whole muscular properties by biomechanical and electrophysiological experiments (Bässler et al. 1996, Guschlbauer et al. 2007), my data will be helpful for filling the gap between the lack of biomechanical data and neuronal control. Previous studies by Tóth et al. (2013a/b) have implemented fast and slow contracting muscle fibers with properties reported by Bässler et al. (1996) and Guschlbauer (2007) in modelling studies of the stick insect and found that this additional input resulted in more realistic simulated motor output. Data of my presented study will thus help to produce even more realistic simulations and therefore may lead to a better understanding of muscular control in insects in general.

6.2 Motor Activity during Curve Walking

In this part of my PhD thesis, I analyzed the neuronal mechanisms underlying curve walking in the stick insect *Carausius morosus*. I focused on the influence on the output of the deafferented mesothoracic and metathoracic leg nerves innervating the six major leg muscles *protractor* and *retractor coxae*, *levator* and *depressor trochanteris*, and *extensor* and *flexor tibiae* during inside and outside turning of the front legs upon optomotor stimulation.

Much is known about how straight walking in animals is generated, but the neuronal mechanisms responsible for flexible movements, like climbing, scratching or turning, are mostly unknown. Field and Stein (1997a, b) showed in their publications that in the turtle the same muscle groups are activated for scratching as for swimming. They analyzed intralimb and interlimb kinematics of the turtle hind limb during rostral, pocket and caudal scratches and compared these to forward and turning swim movements. The analysis showed that the phase of the onset of the behavioral event was the same for rostral scratch and forward swim, and the back-paddling kinematics were similar to both pocket- and caudal scratch. Despite of differences between specific movements (e.g. begin of knee extension during rostral scratch forward swim), the authors postulated that a shared neuronal network is responsible for both types of movement. A similarly flexible activation of muscle groups depending on behavioral context was observed in the curve walking stick insect (e.g. Dürr & Ebeling 2005, Gruhn et al. 2009b, Rosenbaum et al. 2012, Gruhn et al. 2016). While the inside front- and middle legs pull the anterior body part into the direction of the curve, the outer front- and middle legs push it into the turning direction. The hind legs, on the other hand, push the body against the turning direction (Dürr & Ebeling 2005, Gruhn et al. 2009b). In order to produce such different movements, the coordination between the legs and between different joints of each leg needs to be adjusted. These adjustments were mostly investigated by kinematic studies (Jander 1982, Dürr & Ebeling 2005, Gruhn et al. 2009b), while only a recent publication by Gruhn et al. (2016) investigated the possible neuronal mechanisms underlying these behavioral modifications for walking animals. In this latter study, they recorded the protractor and retractor nerve activity of the mesothoracic ganglion extracellularly while the two front legs performed turning on a slippery surface.

For investigations of the stick insect nervous system, in many studies extracellular hook electrodes were used (e.g. Schmitz et al. 1988, Büschges et al. 1994, Büschges et al. 1995, Kittmann et al. 1996, Hess & Büschges 1997, Akay et al. 2001, Ludwar et al. 2005a, Borgmann et al. 2007, Gruhn et al. 2009b, Hellekes et al. 2012).

In my study, I was able to show that protractor and retractor activation is similar in the meso- and metathorax, but depends on the turning direction. In detail, while protractor activity increased during inside stepping of the ipsilateral front leg, retractor activity decreased. Both MN pools were active in alternation, although a smaller range of spike event maxima in the front leg step cycle was found for the mesothoracic protractor and retractor.

During outside steps, the activity pattern was reversed, meaning, the protractor activity decreased, while retractor activity increased. Under this condition, an alternating pattern was not found (see chapter 4.1).

The above results showed that a direction dependent influence exists for the subcoxal muscle activation, and that the activation pattern was similar for the different thoracic segments (see summary scheme Fig. 6.2.1).

The situation is different in the MN pools of the coxa-trochanteral joint. Here, I found that mesothoracic depressor activation is completely terminated (besides the common inhibitor) as soon as the ipsilateral front leg began to step. However, particularly during outside turns, the metathoracic slow *depressor trochanteris* (SDTr) was weakly active. In contrast to this, mesothoracic levator activity was similar to that of the metathorax. Both, meso- and metathoracic levator MN pools were strongly activated as soon as the animal began stepping with the front legs, independent of the turning direction (see chapter 4.2). Therefore, a slight segment-specific activation pattern is present for the depressor (see summary scheme Fig. 6.2.1).

The activity of the MN pools of the most distal analyzed leg joint, the femur-tibia joint, is more variable than that of the above mentioned MN pools. Only for the mesothoracic extensor and flexor activity a slight tendency towards a direction-dependent activation was detectable, while no such tendency was seen in the metathorax. Independent of the turning direction of the ipsilateral front leg, both MN pools showed widely distributed spike event maxima, which ranged at least between half of the front leg step cycle (see chapter 4.3).

All in all, these results demonstrate that the MN pools of the subcoxal joint were activated in a direction-selective manner, while the MN pools of the coxa-trochanteral joint showed

with a slight segment specificity direction-independent activation. No clear activation pattern was observed for the MN pools of the femur tibia joint under either turning direction, although small thorax-segment specific differences were observed (see summary scheme Fig. 6.2.1).

First of all, my results show that the MN pools of the subcoxal and coxa-trochanteral joint had specific activation patterns. Those were either dependent or independent of the turning direction. Gruhn et al. (2016) reported that mesothoracic protractor and retractor activity depends on the turning direction. I was able to confirm this finding. The only deviation concerns the maximal retractor activity, which was at about 90° in Gruhn's publication, while in my experiments it was at about 52° during front leg inside turns. This might be due to the fact that in my experimental series I used only four animals which had their maxima between 30° and 90° . Gruhn et al. mentioned that in their study the spike event maxima were distributed, too.

Interestingly, in the metathorax, a similar activity pattern for retractor and protractor MN pools was observed, where the coupling to the front leg was not as strong as in the mesothoracic MN pool. Borgmann et al. (2007) showed that in the forward walking, one front leg preparation, the metathoracic protractor and retractor tended to be similarly active depending on front leg step cycle as in the mesothorax. Although, the activity patterns were not as clearly structured as in the mesothoracic protractor and retractor nerve recordings, and the spikes were widely distributed throughout the front leg step cycle, a preferred phase for each MN pool was found. They were on average close to the preferred phases of the mesothoracic recordings, showing that the descending influence was weaker in the more posterior thorax segment, but it still existed and evoked similar activity patterns. Thus, under the conditions straight walking and turning, the descending input activated the mesothoracic and the metathoracic protractor and retractor in a similar way, whereby the coupling to the front legs decreased posteriorly.

The direction specific changes in activity of the subcoxal MNs of the mesothorax and metathorax suggest that descending signals induce the necessary changes in motor activity during curve and straight walking in stick insect. Previously, it had been suggested that a descending input coming from the subesophageal ganglion may drive local thoracic CPGs (Bässler et al. 1985), and that this drive controls the walking direction. Also in the lamprey it had been suggested that curve swimming is driven by a unilateral increase in descending excitatory input from the brainstem onto segmental CPGs (review: Grillner et al. 2008).

Another finding by Gruhn et al. (2016) strengthens the idea of a general unilateral descending input in the stick insect. They reported that a unilateral transection of the connective between the prothoracic and mesothoracic ganglion abolished all modifications previously seen in the inside and outside turning animal in retractor and protractor MN activity ipsilateral to the lesion site. They suggested that an independent descending drive exists for the two body sides on the subcoxal level. From my results it is likely that this drive extends to the metathoracic segment.

The MN pools of the coxa-trochanteral joints of the meso- and metathorax are influenced in an even more distinct way during front leg turning. While the levator MN pools of both thoracic segments show the same strong tonic activation upon front leg inside and outside steps, depressor MNs showed a slight segment and direction specific variation. Even though this effect was consistent, one has to keep in mind that the number of spike events was very low in each experiment (see Fig. 4.2.4), and thus be careful not to overinterpret this finding. Neither levator nor depressor activity seemed to be coupled to the front leg stepping cycle in the meso- or metathorax. This is contrary to the observation of Ludwar et al. (2005a). They observed that in a reduced preparation with only one remaining front leg left, walking on a treadmill, mesothoracic depressor MNs were phase coupled to the ipsilateral front leg in six of nine experiments. While this coupling was consistent for each individual animal, the type of influence differed between these six experiments, showing either decreased (two experiments) or increased activity (four experiments) during front leg stance. Levator activity, on the other hand, showed a front leg coupling in four experiments with the lowest activity at the beginning, and maximal activity at the end of the front leg stance phase. In one further experiment, levator activity showed no front leg coupling at all, but still mostly antagonistic activity to the recorded depressor activity. This is similar to Borgmann et al. (2012) results, when middle leg campaniform sensilla (CS) were not stimulated. Borgmann et al. (2012) investigated the motor output of the mesothoracic coxa-trochanteral joint in the reduced preparation with one left front leg walking on a treadmill, while the ipsilateral middle leg CS were stimulated. Without CS stimulation, the mesothoracic levator activity was tonically active and the depressor was silent during front leg walking. This motor output changed as soon as the middle leg CS were stimulated. During load increase, levator activity was terminated and depressor activity began. The reversed activation was present during load decrease. Comparing my results to those of Ludwar et al. (2005a), the different experimental design has to be considered. The preparations I worked with had two instead of only one front leg left.

Furthermore, I used a slippery surface instead of a treadmill. The benefit of this type of walking surface is that animals can do walking movements into the preferred direction and are not forced into one specific direction as they are on a treadmill. Therefore, one can be sure that all walking directions performed, are correlated with the inner state of the animal. However, one has to take into account that the load signals of the front legs differ between walks on the treadmill and that on the slippery surface. Since in my experiments the animals did not have to overcome the inertia of the treadmill, but were moving easily on a glycerine covered plate (Gruhn et al. 2006), the strength needed for walking movements changed drastically. Therefore, the front legs' campaniform sensilla (measuring load) and their femoral chordotonal organ (measuring position, see summary Bässler 1983 & Büschges 2005) most probably signaled less than during walking movements on a treadmill. This might also result in a different neuronal activation of the next posterior segments. Finally, in my study I investigated turning specific activation of the meso- and metathoracic leg nerves and not that depending on straight walking front legs. From all this, one can conclude that the observed differences between Ludwar's and my results are reasonable, and that sensory feedback from the CS of the respective leg can shape the local motor output of the coxa-trochanteral joint (Borgmann et al. 2012).

The activation patterns of the femur-tibia joint MN pools were not as consistent as those of the subcoxal or coxa-trochanteral MN pools. The neuronal activity of the femur-tibia joint was thorax segment specific, as only in the mesothorax and not in the metathorax, extensor activity tended to be stronger during front leg outside turns (in 4 of 8 experiments) and flexor activity was stronger during front leg inside turns (in 6 of 11 experiments). The observed tendency of higher mesothoracic extensor activity during inside, and stronger mesothoracic flexor activity during outside turns of the front legs has been also described by Hellekes et al. (2012). They reported a general increase of mesothoracic extensor activity during inside, and flexor activity during outside turns in a preparation with five on the slippery surface intact and freely walking legs, and the sixth, analyzed middle leg immobilized. However, no comparable data exist for the metathoracic MN pools, as the authors did not investigate the activity pattern for the most posterior thoracic segment. The reason for the slight difference between my results and those by Hellekes et al., may result from the different experimental design. Taking into account that in Hellekes' experimental design five legs were intact, one may suggest that the sensory input coming from the other legs played a significant role for these differences. In the same study, the authors showed that due to mechanical stimulation of the femoral chordotonalorgan (fCO) in the

immobilized middle leg, a reflex reversal was induced more often during inside than during outside turns in the same leg. This indicated a side-specific processing of local sensory feedback in the turning animal. Another study investigating processing of sensory feedback is that by Gruhn et al. (2016). They demonstrated that in a reduced preparation, with two front legs performing turning movements on a slippery surface, the simultaneously stimuli of campaniform sensilla (CS) in a mesothoracic leg stump resulted in a turning-direction dependent motor output of the subcoxal MNs. While in the outside turning animal this simulated load signal resulted in an initiated or enhanced retractor activity, resembling the motor output during straight walks. However, during inside turns the response to the loading stimulus was not as consistent. The load stimuli resulted either in no response of the subcoxal MNs, or in an elicited or terminated retractor or protractor activity. Taken all together, Gruhn et al. (2016) demonstrated a side-specific processing of local load signals during inside turns, as the stereotypical influence – that had been previously shown for straight walks and outside turns – of load feedback was modified. Both studies (Hellekes et al. 2012 and Gruhn et al. 2016) stress the importance of local sensory feedback for the motor output in the turning animal. Considering now the experimental design of my study, in which the meso- and metathoracic leg nerves were deafferented and deafferented, the lack of sensory input may be the reason for the differences between my and Hellekes' study.

All in all, my results indicate the existence of a turning-direction specific motoneuronal activation that is in part joint-specific or thorax-segment specific in the deafferented preparation (see Fig. 6.2.2). During inside turns of the front leg, the leg nerves of the middle- as well as the hind leg received input that would cause in an intact animal to hold the middle- and hind legs mainly in a protracted and levated position. In the outside turning animal, the predefined motor output would cause the animal to hold the middle- and hind legs in a retracted and levated position. Considering also the independence of neuronal activity of most leg nerves from the front leg step cycle, and the variable patterns found for extensor and flexor activity, my results emphasize the importance of local and inter-leg sensory input for the generation of coordinated walking movements in the intact animal.

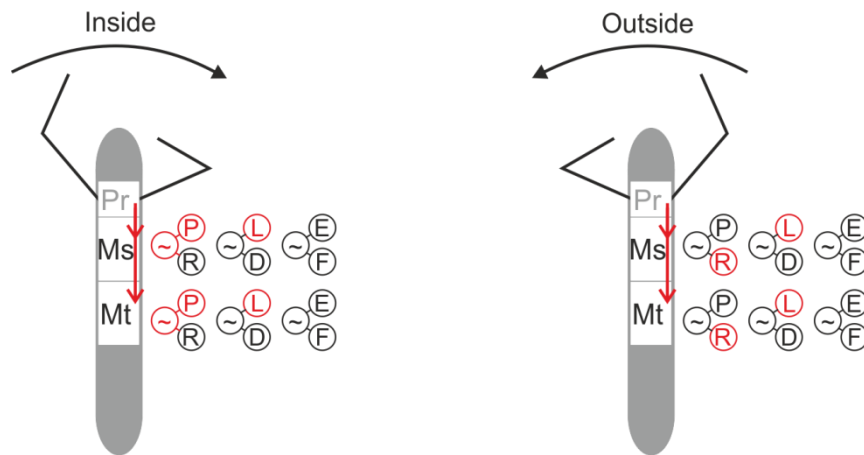


Fig. 6.2.1: Schematic of the summarized motoneuronal activity pattern for the individual leg nerves during inside (left schematic) and outside (right schematic) turning movements of the front legs. During inside turns (left scheme), protractor (P) activity is increased (red) and shows modulated activity (CPG ~ red), while retractor (R) activity is decreased (black color), in both, meso- and metathorax. Levator (L) activity is generally increased (red), while depressor (D) activity is decreased (black). Neither in the meso- nor in the metathorax modulated activity was observed for either levator or depressor (CPG ~ black). The motoneuronal activities of extensor (E) and flexor (F) were not consistently specifically increased or increased (both black). In the outside turning animal (right scheme), protractor (P) activity decreased (black) and retractor activity (R) increased (red), and front leg coupling was not as obvious as for protractor activity during inside turns in both thoracic segments (CPG ~ black). All other motoneuronal activities were similar to that in inside turning animals.

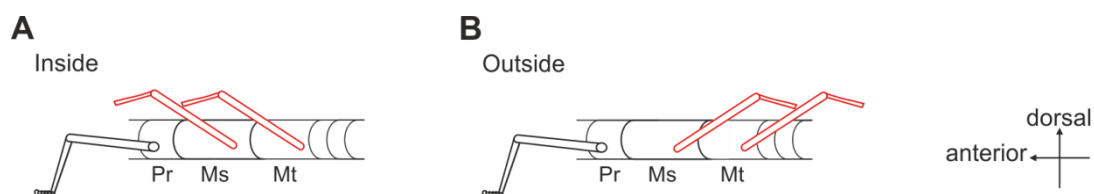


Fig. 6.2.2: Schematic of the predefined motor output in the deafferented curve walking stick insect. In both schematics, the hypothesized positions of the middle and hind legs (both colored red) were determined with respect to the findings of the motoneuronal control during inside (A) and outside (B) turning movements of the front legs (black) (see Fig. 6.2.1). During inside turning movements of the front legs, the middle- and hind legs (both red) would be levated (due to high levator activity) and protracted (due to high protractor activity). In outside turns, both, middle- and hind legs would be levated (due to high levator activity) and retracted (due to high retractor activity).

6.3 Involvement of Central Pattern Generators in Thorax-Segment and Leg-Segment Specificity of the Turning Related Motor Output

In this part of my PhD thesis, I analyzed whether the in chapter 4 observed side-specific and segment-specific changes in the subcoxal and coxa-trochanteral MN pools were mediated by changes in local central pattern generators (CPGs). To study the influence of optomotor induced front leg turning on motor activities of all three major leg joints in the meso- and metathorax, I used a split-bath preparation which allowed local activation of the analyzed CPGs by application of the muscarinic agonist pilocarpine to the respective ganglion. Extracellular recordings were made from the subcoxal leg nerves nl2 and nl5, as well as from the coxa-trochanteral leg nerves C1 and C2 of the deafferented meso- and metathorax to monitor the changes in CPG output during turning of the front legs.

Central pattern generators (CPGs) are neuronal networks that are capable of producing rhythmic, repetitive output without sensory feedback (hence the term “central”) as, for example, walking (Delcomyn 1980). This principle was first postulated by Brown in 1911, and after several decades of research analyzing this hypothesis, this concept became accepted over the alternative hypothesis for generating rhythmic movement through a “chain of reflexes” (Sherrington 1913). Many studies revealed that even in isolated nerve cords rhythmic behavior can be either elicited by drug application (e.g. lamprey: Cohen & Wallén 1980, locust: Stevenson & Kutsch 1987, xenopus: Dale & Roberts 1984), by electrical stimulation, or are even spontaneously generated in vitro (e.g. crayfish: Hughes & Wiersma 1960, crustacean: Nusbaum & Marder 1989). Motoneuronal activity patterns resembling existing motor output during rhythmic movements can be considered as the output of a CPG, which is why this motor output is called “fictive locomotion” or “fictive step-phase transitions” (Wallén & Williams 1984, Büschges et al. 1995). Taking into account that the fictive motor output is based on the rhythmic activity of CPGs, drugs as e.g. pilocarpine are of particular benefit to reveal properties of individual CPGs.

Already in 1939, Roeder used different drugs, like strychnine, atropine and pilocarpine, to analyze insect behavior (Roeder 1939), and to investigate changes in electrical activity in the isolated ventral nerve cord of the cockroach *Periplaneta americana* (Roeder & Roeder 1939). The authors found out that pilocarpine, induced a state of great excitation when

applied into the head capsule of praying mantis and cockroach, resulting in flexed walking legs, raised prothorax and a ventrally flexed head. However, only in three out of thirty praying mantis walking behavior was elicited (Roeder 1939). In the isolated nervous system, several minutes of pilocarpine (10^{-5}) application resulted in increased spike activity (Roeder & Roeder 1939). Application of atropine (10^{-3}), the competitive antagonist for muscarinic acetylcholine receptor, prevented this effect.

The muscarinic agonist pilocarpine, had been often used to induce fictive locomotion (crayfish: Chrachri & Clarac 1990, locust: Ryckebusch & Laurent 1993) or to elicit rhythmic motoneuronal patterns in individual MN pools (stick insect: Büschges et al. 1995). Application of pilocarpine revealed for the stick insect system that individual CPGs exist not only for the individual thoracic segments, but also for each of the three major leg joints – the subcoxal, the coxa-trochanteral, and the femur-tibia joint – as their activities were uncoupled from each other (Büschges et al. 1995). If, therefore, pilocarpine elicited CPG activity is altered through descending input from the brain such as a result of an optomotor stimulus, then it can be concluded that the CPGs are involved in turning related local changes in motor output.

In this part of my thesis, I found out that the stable pilocarpine-induced rhythm was drastically interrupted with front leg stepping begin in the subcoxal- and coxa-trochanteral joint. Furthermore, the changes in the motor output of the *protractor* and *retractor coxae* upon turning movements by the front legs were similar for the activated mesothorax, the activated metathorax, the activated metathorax including the abdominal ganglia chain, and the meso- and metathoracic ganglia activated simultaneously. In detail, during inside steps protractor activity was increased, while retractor activity was decreased. In contrast to this, an opposite activity pattern was observable for outside turns (see chapter 5.1).

The pilocarpine rhythm of the meso- and metathoracic coxa-trochanteral MNs was modified towards a similar activity as seen in the preparation that was not pharmacologically activated. In both thoracic segments the depressor activity was strongly decreased in most cases. However, in the metathorax, alternation of levator and depressor activity was seen more frequently than in the mesothorax. Levator activity strongly increased with the begin of the front leg stepping sequence independent of the walking direction – as it was the case for the not pharmacologically activated animal (see chapter 5.2).

All in all, the pilocarpine rhythm of both analyzed leg joints was changed in a very similar way to the not pharmacologically activated one.

The MN pools of the femur-tibia joint were not investigated under pilocarpine application, as they showed high variabilities in their motor output during front leg turning in the not pharmacologically activated preparation. Thus, a differentiation into a CPG modulated or not-modulated activity would be unreasonable.

Comparing my results to those of Gruhn et al. (2016), who analyzed motoneuronal activity in the activated mesothoracic subcoxal joint during inside and outside turning in a two-front-leg preparation, my results verify their findings for the mesothoracic MN pools. The only differences concern the coupling of motoneuronal activity to the front leg step cycle, which was not that clear in my experiments, and the phase of maximal retractor activity, which I found to be at 30° (see chapter 5.1). This might be due to the wide distribution of spike event maxima in my results, ranging from 240° to 60° , what represents half of the whole front leg step cycle. During outside turns, Gruhn et al. (2016) reported an activation similar to that without pilocarpine application, meaning, a decreased protractor and an increased retractor activity. With my experiments, I was able to show the same tendency for both MN pools during outside turns. As in Gruhn et al. (2016), I found no phase dependence in the activity of protractor and retractor during outside turns.

Interestingly, I found similar changes as in the mesothorax in the motor output for both MN pools and both conditions (inside and outside turning) in the pilocarpine-activated metathorax, in the combined activated metathorax, that included the abdominal ganglia, and in the combined activated meso- and metathoracic ganglia. Borgmann et al. (2009) reported for the straight walking one front leg-preparation that pilocarpine activated MNs of the subcoxal joint had similar activity patterns in the mesothorax and metathorax. In both segments (metathorax: 4/5 experiments) these patterns were entrained to the front leg stepping cycle, and in the metathorax this entrainment was always completed after three to five front leg steps. However, Borgmann et al. used a different experimental design as I did. In their study, animals walked with their front leg on a treadmill, and, thus, received enhanced sensory input from campaniform sensilla than the animals in my experiments. Taken this lack of sensory input in my study into account, it is not surprising that no entrainment to the front leg step cycle was seen.

For the MN pools of the next distal joint, the coxa-trochanteral joint, I showed that levator and depressor activity was similar to the not pharmacologically activated MNs during

inside as well as during outside turns. Under both conditions, and independent of the walking direction, levator activity drastically increased, while depressor activity decreased as soon as the animal performed walking movements. However, although the activation patterns of these MN pools were not as consistent as for those of the subcoxal joint, the pilocarpine rhythm of the meso- and metathoracic coxa-trochanteral MNs was modified towards a similar activity as seen in the preparation that was not pharmacologically activated. No previously reported data exist for the pharmacologically activated levator and depressor in the walking stick insect. However, Fuchs et al. (2011) analyzed levator activity after pilocarpine application in the cockroach, with and without descending influence of one walking front leg. They found out that without walking movements, this system showed antagonistic levator and depressor activity, and, furthermore, alternating activity to the MN pools of the neighboring hemiganglia, which are typical characteristics of MN activity during a tripod gait (Fuchs et al. 2011). However, in this completely deafferented condition, a relatively high variability for MN activation was observed. This variability decreased in the semi-intact preparation walking with one front leg on a treadmill. From this, the authors concluded that a central intersegmental coupling exists in the cockroach, with the ability to form coordinated gaits without sensory feedback, although the positive impact of sensory feedback on the consistency of the motor output was stressed by the authors. However, before comparing these results to my data, it is important to stress that Fuchs et al. (2011) analyzed the involvement of CPGs in straight walking animals, whereas I investigated the involvement of CPGs on the turning related motor output. Nevertheless, when comparing the observations of Fuchs et al. (2011) to the stick insect (Borgmann et al. 2007/2009, Ludwar et al. 2005a), it is obvious that both systems share neuronal similarities, as for example the neuronal architecture. On the other hand, they differ in their dependence of sensory feedback to generate coordinated locomotion. As previously reported, in the stick insect sensory feedback plays a major role for coordinated movement (see review: Büschges & Gruhn 2008). An example for this is the signaling of the femoral chordotonal organ. When this sense organ is surgically manipulated and signals therefore reversed information about movement and position of the femur-tibia joint, the respective leg is not able to terminate the swing phase and, therefore, extends this leg over the ground in a “saluting” position (Graham & Bässler 1981). Additionally, Borgmann et al. (2009) reported that in the semi-intact stick insect preparation, stimulation of the mesothoracic femoral campaniform sensilla resulted in a more “natural” activation of mesothoracic protractor and retractor MNs, which were then

not more coupled in-phase with the ipsilateral front legs, but out-of-phase due to the middle leg sensory inputs. This again, stresses the importance of sensory feedback for the coordination of movements in the stick insect, in particular, when considering that in the observed predefined motor output of the deafferented preparation (see Fig. 6.2.2), the lack of sensory feedback may be the reason for the motor output that does not correspond to those seen in the intact animal.

Nevertheless, the results of my study reveal for the deafferented turning animal a predefined motor output for the MN pools of the subcoxal and coxa-trochanteral joint, that was either turning direction dependent (for retractor and protractor MNs), or independent (for levator and depressor). Now, the question arises, why the individual MN pools show a predefined motor output like this. Why would this predefined motor output result in a protracted and levated middle- and hind leg in inside turns, and a retracted and levated middle- and hind leg in outside turns? Kinematic analysis of stick insect turning by Dürr & Ebeling (2005) and Gruhn et al. (2009b) showed that individual legs have specific functions during inside and outside turns. Middle legs pull the body into the direction of the curve, while inside hind legs either do the same or work as a pivot around which the body rotates. Outside middle and hind legs, on the other hand, push the body into the turning direction (Gruhn et al. 2009b). The huge asymmetry that had been reported by Gruhn et al. for the inside and outside turning legs on a kinematics level was also observed on motoneuronal level (see chapter 4). Gruhn et al. reported that the anterior and posterior extreme positions (short: AEP and PEP, respectively) of the inner middle and hind leg are mostly – but not in the case of the AEP of the middle leg – more anterior than those of straight walking legs. The stronger protractor activity and the decreased retractor activity in the meso- and metathorax during inside turns of the front legs observed in my experiments, reflects these results from kinematics. This can also be concluded from EMG recordings of the mesothoracic protractor and retractor during straight walking movements (Rosenbaum et al. 2010) of the intact animal. In these recordings, protractor activity is alternating with retractor activity. Therefore, to achieve the same AEPs and PEPs as in the straight walking animal, neuronal activity of these MN pools should be similarly high and alternating to each other.

Resuming this chain of thoughts for the motoneuronal activity during outside turns (increased retractor activity, decreased protractor activity), one would assume to observe AEPs and PEPs that are more posterior than during straight walking movements. Albeit, Gruhn et al. (2009b) reported that this is true for the PEPs of both legs, and the AEP of the

hind leg, while the AEP of the middle leg is similar to that in the straight walking animal. This reflects the tendencies of the motoneuronal activity patterns. From this, I postulate that the demonstrated motoneuronal predefined motor output has in so far functional implications, as the specific MN pools are activated in an inside- and outside-turning specific way, so that inside and outside middle- and hind legs would be positioned close to their respective PEP position. However, it is obvious that especially in the outside turning animal the lack of sensory input plays a major role, as no antagonistic motor output between protractor and retractor was seen. This is not the case for the inside turning animal, as the alternating motor output was present, despite the lack of local sensory feedback.

The lack of local sensory input is most probably the reason for the tonic increase in levator activity of the middle- and hind legs during front leg inside and outside turns. Hess & Büschges (1999) reported that the stimulation of the middle leg fCO induces alternating activity in the MN pools of the coxa-trochanteral joint in the active animal. During mechanical stimulation that simulated flexion of the femur-tibia joint, depressor activity was terminated and levator activity increased. The opposite activation was present during mechanical stimulation that simulated extension of the femur-tibia joint. In addition to these findings, the authors investigated the influence of the middle leg fCO signaling on the pharmacologically activated mesothoracic CPG. They demonstrated that mechanical stimulation of the middle leg fCO resulted in the pharmacologically activated preparation in a similar MN activity of the levator and depressor as in the not-activated preparation. From this the authors suggested that movement signals from the fCO have access to the central rhythm generating networks that drive trochanteral MNs. Another study that showed the importance of sensory feedback for motoneuron activation is that by Borgmann et al. (2012). They analyzed the motor output of the mesothoracic coxa-trochanteral joint in the reduced preparation with one left front leg walking on a treadmill, while the ipsilateral middle leg CS were stimulated. Without CS stimulation, the mesothoracic levator activity was tonically active and the depressor was silent during front leg walking. With the begin of CS stimulation, this motor output changed. They demonstrated that during load increase, levator activity was terminated and depressor activity began. The reversed activation was present during load decrease. Both studies support my hypothesis, that the lack of sensory feedback is the reason for the strong levator activity and the very low depressor activity in the middle and hind leg of the deafferented preparation during front leg turning.

As previously mentioned, I did not analyze the involvement of the femur tibia CPGs of the middle- and hind legs, as the MN activity of the extensor and flexor was very variable. This made it impossible to determine whether the motor output in the pharmacologically activated preparation resembles that of the preparation in saline. However, from this strong variability in motor output one can already suggest that, in particular for the MN pools of the femur-tibia joint, the signals from local sensory organs are essential to generate a coordinated motor output. This proposal is supported by a report by Bässler (1976). In this study he showed that the stimulation of the fCO in the decerebrated active animal induced decreased extensor activation, resulting in the active reaction (Bässler 1988). In addition, Hellekes et al. (2012) showed that mechanical stimulation of the fCO simulating a flexion of the femur-tibia joint in the turning animal resulted in a more than half of the trials in a reflex reversal during inside turns, while in the outside turning animal this stimulation resulted in less than 10 % in a reflex reversal. Both studies support my hypothesis of the major role of sensory feedback for the MN pool of the femur-tibia joint.

However, this is only a hypothesis and has to be tested. For this, first of all, extracellular recordings of meso- and metathoracic leg nerves should be done in the inside and outside turning intact animal. These pieces of information about the motoneuronal activity during inside and outside turns would prove, whether the hypothesis based on the report of Rosenbaum et al. (2010) is useful or not. Following this, additionally to Hellekes et al. (2012) and Gruhn et al. (2016) studies of the influence of sensory input in the turning animal, further investigations in this direction would reveal, in how far sensory signals from the fCO, the different CS, and hair fields shape the motor output of the protractor and retractor during outside turns, and the motor output of the levator and depressor as well as the extensor and flexor during inside and outside turns.

Taken all results from my thesis together, the importance of sensory feedback for coordinating walking movements has to be stressed. For stick insect walking, this importance seems reasonable, as in their natural habitat they use to climb and are therefore relying on sensory input from antennae and front legs to grasp the next bush branch. Mathematical modelling studies, as that of Daun-Gruhn (2011), emphasize the importance of sensory feedback in the stick insect system. In this model, Daun-Gruhn used sensory feedback to enhance weak excitatory and inhibitory synaptic connections from front to rear between the CPGs of the three subcoxal-joints. Furthermore, theoretical predictions by Koditschek et al. (2004) and Holmes et al. (2006) suggested that sensory feedback plays a

major role in animals that navigate through a complex environment. Fuchs et al. (2011) reported that in their mathematical model that based on cockroach walking movements, that descending influences were stronger than ascending ones (which conforms with Daun-Gruhn's study). On the other hand, they were able to show that for the cockroach locomotion system, sensory input does not play such a major role as in the stick insect system (Fuchs et al. 2011). Nevertheless, I demonstrated in this study that a predefined motor output exists for the MNs of the subcoxal- and coxa-trochanteral joint. Taking now into account, that stick insect have to face escaping situations, too, I suggest that such a predefined motor output would be of highly benefit for stick insects in such a situation.

CHAPTER 7

Conclusion

In this thesis, I investigated using histochemical experiments the muscular composition of the six major leg muscles of the pro-, meso- and metathorax of the stick insect *Carausius morosus*, to look for differences that may correlate with the function of the legs. I demonstrated that all muscles consist of at least three fiber types, a fast, a slow, and an intermediate one. While the fiber composition differed between the individual leg muscles, it was mostly consistent for the three analyzed segments. Major differences were observed for the *retractor coxae* and the *depressor trochanteris*. In both muscles, the relatively high amount of slow contracting muscle fibers was noticeable. For the retractor and the depressor, the amount of slow fibers was increasing towards the metathorax. This segment specific fiber composition may be explained with the necessity of slow fibers for the stiffening of the respective joint, on the one hand, and with the necessity of slow fibers for generating slow force in the propulsion and support of the body, on the other hand.

Secondly, I investigated the motor output of local meso- and metathoracic leg nerves during turning movements of the front legs. I could show that the nerve activities of the *protractor* and *retractor coxae* were turning direction specific, and similar for the meso- and metathoracic segment for the respective turning direction. The nerve activities of the *levator* and *depressor trochanteris* were independent of the turning direction, and the activities were slightly segment specific, as the depressor activation was stronger in the meta- than in the mesothorax. The nerve activity of the *extensor* and *flexor tibiae* showed

high variability in both segments. In the mesothorax, however, nerve activity of the *extensor tibiae* tended to be stronger during inside turns, while during outside turns, the nerve activity of the *flexor tibiae* tended to be stronger. This effect was not seen in the metathoracic extensor and flexor.

Thirdly, I investigated the involvement of local central pattern generators in the thorax-segment and leg-segment specificity of the turning related motor output. Since the motor output of the femur-tibia joint in the not pharmacologically activated preparation was very variable during inside and outside turns of the front legs, I did not analyze the motor output in the pharmacologically activated preparation, as suggestions about the involvement of the femur-tibia CPG would be far fetched. However, I showed for the meso- and metathoracic subcoxal- and coxa-trochanteral joint that each stable pilocarpine activated CPG rhythm was drastically interrupted with the begin of front leg-stepping. The meso- and metathoracic *protractor* and *retractor coxae*, as well as the *levator* and *depressor trochanteris* nerve activity were similar to that in the not pharmacologically activated system. From this, it can be concluded that the observed changes in motor output in the turning animal are based upon the modification of CPG activity in the subcoxal- and coxa-trochanteral joint in the meso- as well as in the metathorax. My data also demonstrate that in the stick insect, a turning direction dependent predefined motor output exists for the leg nerve activities of the subcoxal joints, which is not segment specific. For the leg nerve activities of the coxa-trochanteral joint, I observed a predefined motor output that was direction independent, but segment specific. In the intact animal these properties would result in lifted middle- and hind legs, which would be protracted during inside turns or retracted during outside turns. As this does not represent a “natural” behavior, this predefined motor output stresses the necessity of sensory feedback for coordinated walking in the stick insect.

Taken together, I conclude that in the stick insect, segment specificities occur for the muscle fiber composition that support the implications from behavioral findings that the posterior legs play the predominant role in supporting stance and posture through the presence of increasing numbers of slow muscle fibers in the metathoracic retractor and depressor. On the neuronal level, on the other hand, I demonstrated that a thorax-segment and leg-segment specificity is present, and that the strength of the involvement of central commands decreases from proximal to distal and from anterior to posterior. My results therefore indirectly stress the importance of sensory feedback for coordinated movements,

during outside turns for the MN pools of the subcoxal joint, in both turning directions for the MN pools of the coxa-trochanteral joint, and, in particular, at the most for the MN pools of the femur-tibia joint.

BIBLIOGRAPHY

Akay T, Bässler U, Gerharz P, Büschges A (2001) The role of sensory signals from the insect coxa-trochanteral joint in controlling motor activity of the femur-tibia joint. *J Neurophysiol* 85(2): 594-604.

Akay T, Haehn S, Schmitz J, Büschges A (2004) Signals from load sensors underlie interjoint coordination during stepping movements of the stick insect leg. *J Neurophysiol* 92: 42-51.

Akay T, Ludwar BCh, Göritz M, Schmitz J, Büschges A (2007) Segment specificity of load signal processing depends on walking direction in the stick insect leg muscle control system. *J Neurosci* 27(12): 3285-3294.

Bárány M (1967) ATPase activity of myosin correlated with speed of muscle shortening. *J Gen Physiol* 50:197-218.

Barnard RJ, Edgerton VR, Furukawa T, Peter JB (1971) Histochemical, biochemical, and contractile properties of red, white, and intermediate fibers. *Am J Physiol* 220: 410-414.

Bässler U (1976) Reversal of a reflex to a single motoneuron in the stick insect *Carausius morosus*. *Biol Cybern* 24: 47-49.

Bässler U (1977) Sense organs in the femur of the stick insect and their relevance to the control of position of the femur-tibia-joint. *J comp Physiol* 121: 99-113.

Bässler U (1983) Neural basis of elementary behavior in stick insect. Springer-Verlag Heidelberg.

Bässler U (1986) On the definition of central pattern generator and its sensory control. *Biol Cybern* 54: 65-69.

Bässler (1988) Functional principles of pattern generation for walking movements of stick insect forelegs: the role of the femoral chordotonal organ afferences. *J Exp Biol* 136: 125-147.

Bässler U, Storrer J (1980) The neural basis of the femur-tibia-control-system in the stick insect *Carausius morosus*. *Biol Cybern* 38: 107-114.

Bässler U, Wegner U (1983) Motor output of the denervated thoracic ventral nerve cord in the stick insect *Carausius morosus*. *J Exp Biol* 105: 127-145.

Bässler U, Foth E, Breutel G (1985) The inherent walking direction differs for the prothoracic and metathoracic legs of stick insects. *J Exp Biol* 116: 301-311.

Bässler D, Büschges A, Meditz S, Bässler U (1996) Correlation between muscle structure and filter characteristics of the muscle-joint system in three orthopteran insect species. *J Exp Biol* 199: 2169-2183.

Bässler U, Wolf H, Stein W (2007) Functional recovery following manipulation of muscles and sense organs in the stick insect leg. *J Comp Physiol A* 193: 1151-1168.

Berens (2009) CircStat: A MATLAB toolbox for circular statistics. *J Stat Softw* 31(10): 1-21.

Billeter R, Heizmann CW, Howald H, Jenny E (1981) Analysis of myosin light and heavy chain types in single human skeletal muscle fibers. *Eur J Biochem* 116(2): 389-395.

Borgmann A, Scharstein H, Büschges A (2007) Intersegmental coordination: influence of a single walking leg on the neighboring segments in the stick insect walking system. *J Neurophysiol* 98: 1685-1696.

Borgmann A, Hooper S, Büschges A (2009) Sensory feedback induced by front-leg stepping entrains the activity of central pattern generators in caudal segments of the stick insect walking system. *J Neurosci* 29(9): 2972-2983.

Borgmann A, Tóth TI, Gruhn M, Daun-Gruhn S, Büschges A (2012) Dominance of local sensory signals over inter-segmental effects in a motor system: experiments. *Biol Cybern* 105: 399-411.

Brooke MH & Kaiser KK (1970) Three “myosin adenosine triphosphatase” systems: the nature of their pH lability and sulfhydryl dependence. *J Histochem Cytochem* 18: 670-672.

Brown TG (1911) The intrinsic factors in the act of progression in the mammal. *Proc R Soc Lond B* 84: 308-319.

Bucher D, Akay T, DiCaprio RA, Büschges A (2003) Interjoint coordination in the stick insect leg-control system: the role of positional signaling. *J Neurophysiol* 89: 1245-1255.

Burke RE, Levine DN, Zajac FE, Tsairis P, Engel WK (1971) Mammalian motor units: Physiological-histochemical correlation in three types in cat gastrocnemius. *Science* 174: 709-712.

Büschges A (2005) Sensory control and organization of neural networks mediating coordination of multisegmental organs for locomotion. *J Neurophysiol* 93: 1127-1135.

Büschges A, Gruhn M (2008) Mechanosensory feedback in walking: from joint control to locomotor patterns. *Adv. Insect Physiol* 34: 194-222.

Büschges A, Schmitz J (1991) Nonspiking pathways antagonize the resistance reflex in the thoraco-coxal joint of stick insects. *J Neurobiol* 22(3): 224-237.

Büschges A, Kittmann R, Schmitz J (1994) Identified nonspiking interneurons in leg reflexes and during walking in the stick insect. *J Comp Physiol A* 174: 685-700.

Büschges A, Schmitz J, Bässler U (1995) Rhythmic patterns in the thoracic nerve cord of the stick insect induced by pilocarpine. *J Exp Biol* 198: 435-456.

Cabelguyen JM, Bourcier-Lucas C, Dubuc R (2003) Bimodal locomotion elicited by electrical stimulation of the midbrain in the salamander *Notophthalmus viridescens*. *J Neurosci* 23(6): 2434-2439.

Chrachri A, Clarac F (1990) Fictive locomotion in the fourth thoracic ganglion of the crayfish, *Procambarus clarkii*. *J Neurosci* 10: 707-719.

Close RI (1967) Properties of motor units in fast and slow skeletal muscles of the rat. *J Physiol (Lond)* 193: 45-55.

Close RI (1972) Dynamic properties of mammalian skeletal muscles. *Physiol Rev* 52: 129-197.

Cohen AH, Wallén P (1980) The neuronal correlate of locomotion in fish. "Fictive swimming" induced in an in vitro preparation of the lamprey spinal cord. *Exp Brain Res* 41(1): 11-18.

Cooper RL, Marin L, Atwood HL (1995) Synaptic differentiation of a single motor neuron: conjoint definition of transmitter release, presynaptic calcium signals, and ultrastructure. *J Neurosci* 15: 4209-4222.

Cruse H (1976) The function of the legs in the free walking stick insect, *Carausius morosus*. *J Comp Physiol* 112: 235-262.

Dale N, Roberts A (1984) Excitatory amino acid receptors in xenopus embryo spinal cord and their role in the activation of swimming. *J Physiol* 348: 527-543.

Dallmann CJ, Dürr V, Schmitz J (2016) Joint torques in a freely walking stick insect reveal distinct functions of leg joints in propulsion and posture control. *Proc R Soc B* 283: 20151708.

Davenport J, Munks SA, Oxford PJ (1984) A comparison of the swimming of marine and freshwater turtles. *Proc R Soc Lond B* 220: 447-475.

Daun-Gruhn S (2011) A mathematical modeling study of inter-segmental coordination during stick insect walking. *J Comput Neurosci* 30: 255-278.

Delcomyn F (1980) Neural basis of rhythmic behavior in animals. *Science* 210: 492-498.

Dürr V (2005) Context-dependent changes in strength and efficacy of leg coordination mechanisms. *J Exp Biol* 208: 2253-2267.

Dürr V, Ebeling W (2005) The behavioural transition from straight to curve walking: kinetics of leg movement parameters and the initiation of turning. *J Exp Biol* 208: 2237-2252.

Dyson KS, Miron JP, Drew T (2014) Differential modulation of descending signals from the reticulospinal system during reaching and locomotion. *J Neurophysiol* 112: 2505-2528.

Edgerton VR, Simpson DR (1971) Dynamic and metabolic relationships in the rat extensor digitorum longus muscle. *Exp Neurol* 30: 374-376.

Ekeberg Ö, Blümel M, Büschges A (2004) Dynamic simulation of insect walking. *Arthropod Struc Dev* 33: 287-300.

Fagerstedt P, Ullén F (2001) Lateral turns in the lamprey. I. Patterns of motoneuron activity. *J Neurophysiol* 86: 2246-2256.

Fagerstedt P, Orlovsky GN, Deliagina TH, Grillner S, Ullén F (2001) Lateral turns in the lamprey. II. Activity of reticulospinal neurons during the generation of fictive turns. *J Neurophysiol* 86: 2257-2265.

Field EC, Stein PSG (1997a) Spinal cord coordination of hindlimb movements in the turtle: intralimb temporal relationships during scratching and swimming. *J Neurophysiol* 78: 1394-1403.

Field EC, Stein PSG (1997b) Spinal cord coordination of hindlimb movements in the turtle: interlimb temporal relationships during bilateral scratching and swimming. *J Neurophysiol* 78: 1404-1413.

Fischer H, Schmidt J, Haas R, Büschges A (2001) Pattern generation for walking and searching movements of a stick insect leg. I. Coordination of motor activity. *J Neurophysiol* 85(1): 341-353.

Fourtner CR (1978) The ultrastructure of the metathoracic femoral extensors of the cockroach, *Periplaneta americana*. *J Morph* 156: 127-140.

Fuchs E, Holmes P, Kiemel T, Ayali A (2011) Intersegmental coordination of cockroach locomotion: adaptive control of centrally coupled pattern generator circuits. *Front Neural Circuits* Vol 4 Article 125.

Gabriel JP, Scharstein H, Schmidt J, Büschges A (2003) Control of flexor motoneuron activity during single leg walking of the stick insect on an electronically controlled treadmill. *J Neurobiol* 56(3): 237-251.

Gabriel JP, Büschges A (2007) Control of stepping velocity in a single insect leg during walking. *Phil Trans R Soc A* 365: 251-271.

Goddon DH (1972) The motor innervation of the leg musculature and motor output during thanatosis in the stick insect *Carausius morosus* Br.. *J Comp Physiol* 80: 201-225.

Godlewska-Hammel E, Büschges A, Gruhn M (MS 2016) Characterization of muscle fiber types in the stick insect leg. *Arthropod Struct Dev*. Submitted.

Goldammer J, Büschges A, Schmidt J (2012) Motoneurons, DUM cells, and sensory neurons in an insect thoracic ganglion: a tracing study in the stick insect *Carausius morosus*. *J Comp Neurol* 520: 230-257.

Grabowska* M, Godlewska* E, Schmidt J, Daun-Gruhn S (2012) Quadrupedal gaits in hexapod animals – inter-leg coordination in free walking adult stick insects. *J Exp Biol* 215: 4255-4266.

Graham D (1972) A behavioural analysis of the temporal organisation of walking movements in the 1st instar and adult stick insect (*Carausius morosus*). *J Comp Physiol A* 81: 23-52.

Graham D & Bässler U (1981) Effects of afference sign reversal on motor activity in walking stick insects (*Carausius morosus*). *J Exp Biol* 91: 179-193.

Graham D & Wendler G (1981) The reflex behavior and innervation of the tergo-coxal retractor muscles of the stick insect *Carausius morosus*. *J Comp Physiol* 143: 81-91.

Grillner S, Wallén P, Saitoh K, Kozlov A, Robertson B (2008) Neural bases of goal-directed locomotion in vertebrates – an overview. *Brain Res Rev.* 57(1): 2-12.

Grillner S, Wallén P (1985) Central pattern generators for locomotion, with special reference to vertebrates. *Ann Rev Neurosci* 8: 233-261.

Gruhn M, Rathmayer W (2002) Phenotype plasticity in postural muscles of the crayfish *Ornocetes limosus* Raf.: correlation of myofibrillar ATPase based fiber typing with electrophysiological fiber properties and the effect of chronic nerve stimulation. *J Exp Zool* 293: 127-140.

Gruhn M, Hoffmann O, Dübbert M, Scharstein H, Büschges A (2006) Tethered stick insect walking: A modified slippery surface setup with optomotor stimulation and electrical monitoring of tarsal contact. *J Neurosci Met* 158: 195-206.

Gruhn M, von Uckermann G, Westmark S, Wosnitza A, Büschges A, Borgmann A (2009a) Control of stepping velocity in the stick insect *Carausius morosus*. *J Neurophysiol* 102: 1180-1192.

Gruhn M, Zehl L, Büschges A (2009b) Straight walking and turning on a slippery surface. *J Exp Biol* 212: 194-209.

Gruhn M, Rosenbaum P, Bollhagen HP, Büschges A (2011) Studying the neural basis of adaptive locomotor behavior in insects. *JoVE* 50.

Gruhn M, Rosenbaum P, Bockemühl T, Büschges A (2016) Body side-specific control of motor activity during turning in a walking animal. *eLife* 5: e17399.

Günzel D, Galler S, Rathmayer W (1993) Fibre heterogeneity in the closer and opener muscles of crayfish walking legs. *J Exp Biol* 175: 267-281.

Guo P, Ritzmann RE (2013) Neural activity in the central complex of the cockroach brain is linked to turning behaviors. *J Exp Biol* 216(6): 992-1002.

Guschlbauer C, Scharstein H, Büschges A (2007) The extensor tibiae muscle of the stick insect: biomechanical properties of an insect walking leg muscle. *J Exp Biol* 210: 1092-1108.

Guth L, Samaha FJ (1969) Qualitative differences between actomyosin ATPase of slow and fast mammalian muscle. *Exp Neurol* 25: 138-152.

Guth L, Samaha FJ (1970) Procedure for the histochemical demonstration of actomyosin ATPase. *Exp Neurol* 28: 365-367.

Harley CM, Ritzmann RE (2010) Electrolytic lesions within central complex neuropils of the cockroach brain affect negotiation of barriers. *J Exp Biol* 213: 2851-2864.

Hellekes K, Blincow E, Hoffmann J, Büschges A (2012) Control of reflex reversal in stick insect walking: effects of intersegmental signals, changes in direction, and optomotor-induced turning. *J Neurophysiol* 107: 239-249.

Henneman E & Olsen CB (1965) Relations between structure and function in the design of skeletal muscle. *J Neurophysiol* 28: 581-598.

Hess D, Büschges A (1997) Sensorimotor pathways involved in interjoint reflex action of an insect leg. *J Neurobiol* 33(7): 891-913.

Hess D, Büschges A (1999) Role of proprioceptive signals from an insect femur-tibia joint in patterning motoneuronal activity of an adjacent leg joint. *J Neurophysiol* 81: 1856-1865.

Hessenbruch A (2006) Einführung in die äußere und innere Anatomie der Thorakalsegmente von Stabheuschrecken. Staatliche Hausarbeit. University of Cologne.

Holmes P, Full RJ, Koditschek D, Guckenheimer J (2006) The dynamics of legged locomotion: models, analyses, and challenges. *SIAM Rev* 48(2): 207-304.

Huang KH, Ahrens MB, Dunn TW, Engert F (2013) Spinal projection neurons control turning behaviors in zebrafish. *Curr Biol* 23(16): 1566-1573.

Hughes GM, Wiersma CAG (1960) The co-ordination of swimmeret movements in the crayfish, *Procambarus clarkii* (Girard). *J Exp Biol* 37(4): 657-670.

Igelmund P (1980) Untersuchungen zur Stellungs- und Bewegungsregelung der Beine der Stabheuschrecke *Carausius morosus*: Neuronale Grundlagen der Pro- und Retraktion der Coxa. Diploma thesis. University of Cologne.

Jahromi SS, Atwood HL (1969) Correlation of structure, speed of contraction, and total tension in fast and slow abdominal muscle fibers of the lobster (*Homarus americanus*). *J Exp Zool* 171: 25-38.

Jander JP (1982) Untersuchungen zum Mechanismus und zur zentralnervösen Steuerung des Kurvenlaufs bei Stabheuschrecken (*Carausius morosus*). Dissertation. University of Cologne.

Jindrich DL & Full RJ (1999) Many-legged maneuverability: dynamics of turning in hexapods. *J Exp Biol* 202(112): 1603-1623.

Johnston RM, Levine RB (1996) Crawling motor patterns induced by pilocarpine in isolated larval nerve cords of *Manduca sexta*. *J Neurophysiol* 76(5): 3178-3195.

Johnston RM, Levine RB (2002) Thoracic leg motoneurons in the isolated CNS of adult *Manduca* produce patterned activity in response to pilocarpine, which is distinct from that produced in larvae. *Invertebr Neurosci* 4(4): 175-192.

Kittmann R, Schmitz J, Büschges A (1996) Premotor interneurons in generation of adaptive leg reflexes and voluntary movements in stick insects. *J Neurobiol* 31(4): 512-531.

Koditschek DE, Full RJ, Buehler M (2004) Mechanical aspects of legged locomotion control. *Arthropod Struct Dev* 33(3): 251-272.

Ludwar BCh, Göritz M, Schmidt J (2005a) Intersegmental coordination of walking movements in stick insects. *J Neurophysiol* 93: 1255-1265.

Ludwar BCh, Westmark S, Büschges A, Schmidt J (2005b) Modulation of membrane potential in mesothoracic moto- and interneurons during stick insect front-leg walking. *J Neurophysiol* 94: 2772-2784.

Maier L, Rathmayer W, Pette D (1984) pH lability of myosin ATPase activity permits discrimination of different muscle fibre types in crustaceans. *Histochem* 81: 75-77.

Maier L, Pette D, Rathmayer W (1986) Enzyme activities in single electrophysiologically identified crab muscle fibres. *J Physiol* 371: 191-199.

Maier L, Root TM, Seyfarth EA (1987) Heterogeneity of spider leg muscle: histochemistry and electrophysiology of identified fibers in the claw levator. *J Comp Physiol B* 157: 285-294.

Marquardt (1940) Beiträge zur Anatomie der Muskulatur und der peripheren Nerven von *Carausius (Dixippus) morosus*. *Zool Jahrb Abt Anat Ont Tiere* 66: 63-128.

Martin JP, Guo P, Mu L, Harley CM, Ritzmann RE (2015) Central-complex control of movement in the freely walking cockroach. *Curr Biol* 25: 2795-2803.

McClellan AD (1984) Descending control and sensory gating of 'fictive' swimming and turning responses elicited in an in vitro preparation of the lamprey brainstem/spinal cord. *Brain Res* 302: 151-162.

Miller S, van der Burg J, van der Meché FGA (1975) Locomotion in the cat: basic programmes of movement. *Brain Res* 91(2): 239-253.

Morgen CR, Tarras MS, Stokes DR (1980) Histochemical demonstration of enzymatic heterogeneity within the mesocoxal and metacoxal muscles of *Periplaneta americana*. *J Insect Physiol* 26: 481-486.

Mu L, Ritzmann RE (2008a) Interaction between descending input and thoracic reflexes for joint coordination in cockroach. II Comparative studies on tethered turning and searching. *J Comp Physiol A* 194: 299-312.

Müller AR, Galler HW, Rathmayer W (1992) Correlation of electrophysiological, histochemical, and mechanical properties in fibres of the coxa rotator muscle of the locust, *Locusta migratoria*. *J Comp Physiol B* 162: 5-15.

Nusbaum MP & Marder E (1989) A modulatory proctolin-containing neuron (MPN). I. Identification and characterization. *J Neurosci* 9(5): 1591-1599.

Orlovsky GN, Deliagina TG, Grillner S (1999) Neuronal control of locomotion from Mollusc to Man. Oxford University Press.

Padykula HA, Herman E (1955a) Factors affecting the activity of adenosine triphosphatase and other phosphatases as measured by histochemical techniques. *J Histochem Cytochem* 3(3): 161-169.

Padykula HA, Herman E (1955b) The specificity of the histochemical method for adenosine triphosphatase. *J Histochem Cytochem* 3(3): 170-195.

Pearson KG, Stein RB, Malhotra SK (1970) Properties of action potentials from insect motor nerve fibres. *J Exp Biol* 53: 299-316.

Pette D, Staron RS (1990) Cellular and molecular diversities of mammalian skeletal muscle fibers. *Rev Physiol Biochem Pharmacol* 116: 1-76.

Pette D, Staron RS (2001) Myosin isoforms, muscle fiber types, and transitions. *Microsc Res Techniq* 50: 500-509.

Pilehvarian AA (2015) An ultrastructural and histochemical study of the flexor tibialis muscle fiber types in male and female stick insects (*Eurycantha calcarata*, L). *J Exp Zool.* 323A: 527-539.

Ridgel AL, Alexander BE, Ritzmann RE (2007) Descending control of turning behavior in the cockroach, *Blaberus discoidalis*. *J Comp Physiol A* 193: 385-402.

Rivero JLL, Talmadge RJ, Edgerton VR (1996) Correlation between myofibrillar ATPase activity and myosin heavy chain composition in equine skeletal muscle and the influence of training. *Anat Rec* 246: 195-207.

Roeder KD (1939) The action of certain drugs on the insect nervous system. *Biol Bull* 76: 183-189.

Roeder KD, Roeder S (1939) Electrical activity in the isolated ventral nerve cord of the cockroach. *J Cell Comp Physiol* 14(1): 1-12.

Rosenbaum P, Wosnitza A, Büschges A, Gruhn M (2010) Activity patterns and timing of muscle activity in the forward walking and backward walking stick insect *Carausius morosus*. *J Neurophysiol* 104: 1681-1695.

Ryckebusch S, Laurent G (1993) Rhythmic patterns evoked in locust leg motor neurons by the muscarinic agonist pilocarpine. *J Neurophysiol* 69(5): 1583-1595.

Schmitz J (1986) Properties of the feedback system controlling the coxa-trochanter joint in the stick insect *Carausius morosus*. Biol Cybern 55: 35-34.

Schmitz J, Büschges A, Delcomyn F (1988) An improved electrode design for en passant recording from small nerves. Comp Biochem Physiol 91A(4): 769-772.

Schmitz J, Delcomyn, Büschges A (1991) Oil and hook electrodes for en passant recording from small nerves. Met Neurosci 4: 266-278.

Seidel JC (1967) Studies on myosin from red and white skeletal muscles of the rabbit. II. Inactivation of myosin from red muscles under milk alkaline conditions. J Biol Chem 242(23): 5623-5629.

Sherman RG, Atwood HL (1972) Correlated electrophysiological and ultrastructural studies of a crustacean motor unit. J Gen Physiol 59: 586-615.

Sherrington CS (1913) Further observations on the production of reflex stepping by combination of reflex excitation with reflex inhibition. J Physiol 47(3): 196-214.

Silverman H, Cosello WJ, Mykles DL (1987) Morphological fiber type correlates physiological and biomechanical properties in crustacean muscle. Amer Zool 27: 1011-1019.

Sréter FA, Seidel JC, Gergely J (1966) Studies on myosin from red and white skeletal muscles of the rabbit. I. Adenosine triphosphatase activity. J Biol Chem 241(24): 5772-5776.

Stevenson PA, Kutsch W (1987) A reconsideration of the central pattern generator concept for locust flight. J Comp Physiol A 161: 115-129.

Stokes DR (1987) Insect muscles innervated by single motoneurons: structural and biochemical features. Am Zool 27: 1001-1010.

-
- Stokes DR, Vitale J, Morgan CR (1979) Enzyme histochemistry of the mesocoaxal muscles of *Periplaneta americana*. *Cell Tissue Res* 198: 175-189.
- Strausfeld NJ (1999) A brain region in insects that supervises walking. *Prog Brain Res* 123: 273-284.
- Strauss R, Heisenberg M (1993) A higher control center of locomotor behavior in the *Drosophila* brain. *J Neurosci* 13(5): 1852-1861.
- Syrový I (1989) The effect of time, 2-mercaptoethanol and inhibitors of proteases on isolation of cardiac myosin and its properties. *Physiol Bohemoslov* 38(3): 287-288.
- Theunissen LM, Vikram S, Dürr V (2014) Spatial co-ordination of foot contacts in unrestrained climbing insects. *J Exp Biol* 217: 3242-3253.
- Theunissen LM, Bekemeier HH, Dürr V (2015) Comparative whole-body kinematics of closely related insect species with different body morphology. *J Exp Biol* 218: 340-352.
- Tobalske BW (2007) Biomechanics of bird flight. *J Exp Biol* 210(18): 3135-3146.
- Tóth TI, Grabowska M, Schmidt J, Büschges A, Daun-Gruhn S (2013a) A neuro-mechanical model explaining the physiological role of fast and slow muscle fibres at stop and start of stepping of an insect leg. *PLoS ONE* 8(11): e78246.
- Tóth TI, Schmidt J, Büschges A, Daun-Gruhn S (2013b) A neuro-mechanical model of a single leg joint highlighting the basic physiological role of fast and slow muscle fibres of an insect muscle system. *PLoS ONE* 8(11): e78247.
- Wallén P, Williams TL (1984) Fictive locomotion in the lamprey spinal cord in vitro compared with swimming in the intact and spinal animal. *J Physiol* 347: 225-239.
- Weidler DJ, Diecke FPJ (1969) The role of cations in conduction in the central nervous system of the herbivorous insect *Carausius morosus*. *Z vergl Physiol* 64: 372-399.

Wendler G (1964) Laufen und Stehen der Stabheuschrecke *Carausius morosus*: Sinnesborstenfelder in den Beingelenken als Glieder von Regelkreisen. Z vergl Physiol 48: 198-250.

Wilson DM (1961) The central nervous control of flight in a locust. J Exp Biol 38: 471-490.

LIST OF FIGURES

- Fig. 2.1.1: Schematic of the staining reaction for determination of myofibrillar ATPase activity in serial cross-sections through the investigated stick insect muscle (figure also used in the submitted MS Godlewska-Hammel et al. 2016); **p.7**
- Fig. 2.1.2: Example for the analysis steps for the muscle fiber identification. Serial sections were treated either under alkaline pre-incubation or under acidic pre-incubation; **p.8**
- Fig. 3.1.1: Characterization of muscle fibers using mATPase staining procedure in the *protractor* and *retractor coxae*; **p.18**
- Fig. 3.2.1: Characterization of muscle fibers using mATPase staining procedure in the *levator* and *depressor trochanteris*; **p.22**
- Fig. 3.3.1: Characterization of muscle fibers using mATPase staining procedure in the *extensor* and *flexor tibiae*; **p.27**
- Fig. 4.1.1: Motor output of *protractor* and *retractor coxae* MN pools in the deafferented mesothoracic ganglion during front leg inside stepping; **p.38**
- Fig. 4.1.2: Motor output of *protractor* and *retractor coxae* MN pools in the deafferented mesothoracic ganglion during front leg outside stepping; **p.39**
- Fig. 4.1.3: Motor output of *protractor* and *retractor coxae* MN pools in the deafferented metathoracic ganglion during front leg inside stepping; **p.41**
- Fig. 4.1.4: Motor output of *protractor* and *retractor coxae* MN pools in the deafferented metathoracic ganglion during front leg outside stepping; **p.42**
- Fig. 4.2.1: Motor output of *levator* and *depressor trochanteris* MN pools in the deafferented mesothoracic ganglion during front leg inside stepping; **p.45**
- Fig. 4.2.2: Motor output of *levator* and *depressor trochanteris* MN pools in the deafferented mesothoracic ganglion during front leg outside stepping; **p.46**
- Fig. 4.2.3: Motor output of *levator* and *depressor trochanteris* MN pools in the deafferented metathoracic ganglion during front leg inside stepping; **p.48**
- Fig. 4.2.4: Motor output of *levator* and *depressor trochanteris* MN pools in the deafferented metathoracic ganglion during front leg outside stepping; **p.49**
- Fig. 4.3.1: Motor output of *extensor tibiae* MNs in the deafferented mesothoracic ganglion during front leg inside and outside stepping; **p.53**
- Fig. 4.3.2: Motor output of *flexor tibiae* MNs in the mesothoracic femur (deafferented mesothoracic ganglion) during front leg inside and outside stepping; **p.54**
- Fig. 4.3.3: Motor output of *extensor tibiae* MNs in the deafferented mesothoracic ganglion during front leg inside and outside stepping; **p.57**
- Fig. 4.3.4: Motor output of *flexor tibiae* MNs in the metathoracic femur (deafferented metathoracic ganglion) during front leg inside and outside stepping; **p.58**

- Fig. 5.1.1.1: Motor output of *protractor* (Pro) and *retractor* (Ret) *coxae* MN pools in the pilocarpine activated deafferented mesothoracic ganglion during front leg inside stepping; **p.63**
- Fig. 5.1.1.2: Motor output of *protractor* (Pro) and *retractor* (Ret) *coxae* MN pools in the pilocarpine activated deafferented mesothoracic ganglion during front leg outside stepping; **p.64**
- Fig. 5.1.2.1: Motor output of *protractor* (Pro) and *retractor* (Ret) *coxae* MN pools in the pilocarpine activated deafferented metathoracic ganglion during front leg inside stepping; **p.66**
- Fig. 5.1.2.2: Motor output of *protractor* (Pro) and *retractor* (Ret) *coxae* MN pools in the pilocarpine activated deafferented metathoracic ganglion during front leg outside stepping; **p.67**
- Fig. 5.1.3.1: Motor output of *protractor* (Pro) and *retractor* (Ret) *coxae* MN pools in the pilocarpine activated deafferented metathoracic ganglion during front leg inside stepping; **p.69**
- Fig. 5.1.3.2: Motor output of *protractor* (Pro) and *retractor* (Ret) *coxae* MN pools in the pilocarpine activated deafferented metathoracic ganglion during front leg outside stepping; **p.70**
- Fig. 5.1.4.1: Motor output of *protractor* (Pro) and *retractor* (Ret) *coxae* MN pools in the pilocarpine activated deafferented meso- and metathoracic ganglia during front leg inside stepping; **p.73**
- Fig. 5.1.4.2: Motor output of *protractor* (Pro) and *retractor* (Ret) *coxae* MN pools in the pilocarpine activated deafferented meso- and metathoracic ganglia during front leg outside stepping; **p.74**
- Fig. 5.2.1.1: Motor output of *levator* (Lev) and *depressor* (Dep) *trochanteris* MN pools in the pilocarpine activated deafferented mesothoracic ganglion during front leg inside stepping; **p.77**
- Fig. 5.2.1.2: Motor output of *levator* (Lev) and *depressor* (Dep) *trochanteris* MN pools in the pilocarpine activated deafferented mesothoracic ganglion during front leg outside stepping; **p.78**
- Fig. 5.2.2.1: Motor output of *levator* (Lev) and *depressor* (Dep) *trochanteris* MN pools in the pilocarpine activated deafferented metathoracic ganglion during front leg inside stepping; **p.80**
- Fig. 5.2.2.2: Motor output of *levator* (Lev) and *depressor* (Dep) *trochanteris* MN pools in the pilocarpine activated deafferented metathoracic ganglion during front leg outside stepping; **p.81**
- Fig. 6.2.1: Schematic of the summarized motoneuronal activity pattern for the individual leg nerves during inside (left schematic) and outside (right schematic) turning movements of the front legs; **p.95**
- Fig. 6.2.2: Schematic of the predefined motor output in the deafferented curve walking stick insect; **p.95**

LIST OF TABLES

Table 2.1.1: Staining protocol with incubation times; **p.6**

Table 3.1: Averaged muscle cross-sectional area (in mm²); **p.28**

Table 3.2: Averaged percentage of muscle fiber types in the individual muscles after mATPase classification; **p.29**

Table 3.3: Statistical results for intersegmental comparison of the different muscle fiber types using the paired t-test, after classification into the groups slow contracting muscle fibers (slow), fast contracting muscle fibers (fast) and intermediate contracting muscle fibers (int); **p.30**

Table 3.4: Statistical results for intrasegmental comparison of the different muscle fiber types between analyzed muscle regions using the paired t-test, after classification into the groups slow contracting muscle fibers (slow), fast contracting muscle fibers (fast) and intermediate contracting muscle fibers (int); **p.31**

APPENDIX

In the following, I present data from each analyzed experiment of turning animals. For a better comparison, I have arranged the phase histograms of the nerves innervating the respective antagonists as pairs for both turning directions. Individual lines in each phase histogram represent the respective nerve of one analyzed hemiganglion.

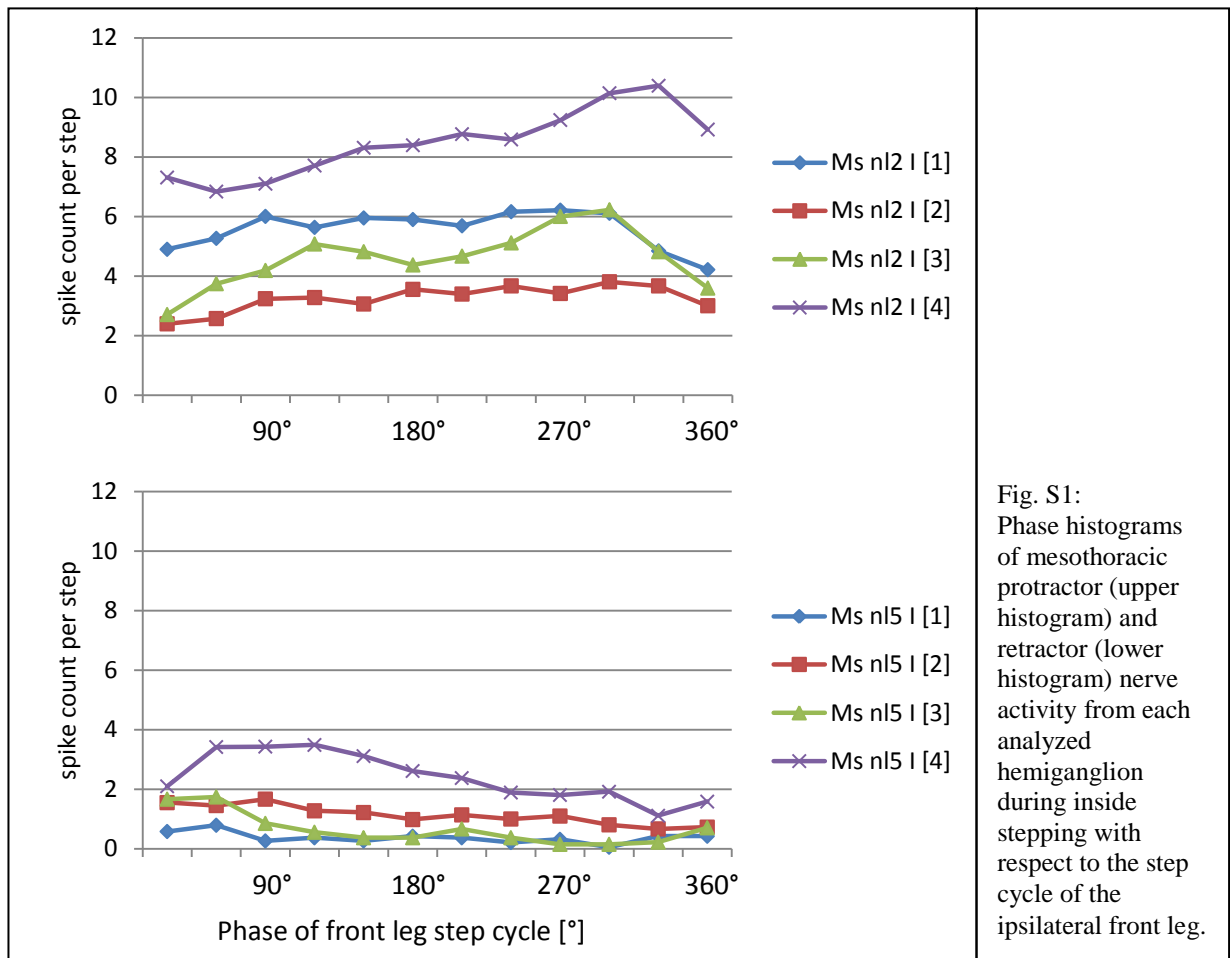


Fig. S1: Phase histograms of mesothoracic protractor (upper histogram) and retractor (lower histogram) nerve activity from each analyzed hemiganglion during inside stepping with respect to the step cycle of the ipsilateral front leg.

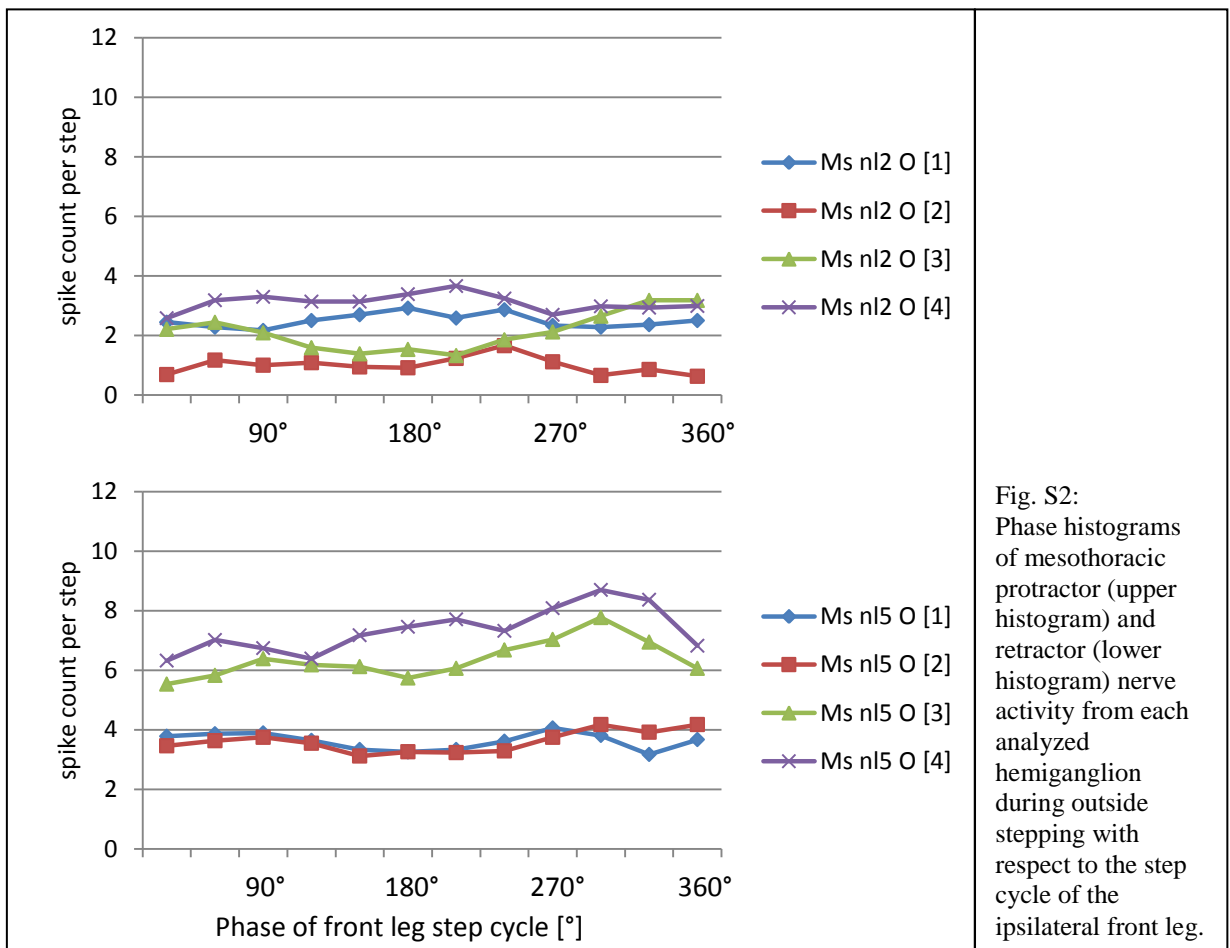


Fig. S2: Phase histograms of mesothoracic protractor (upper histogram) and retractor (lower histogram) nerve activity from each analyzed hemiganglion during outside stepping with respect to the step cycle of the ipsilateral front leg.

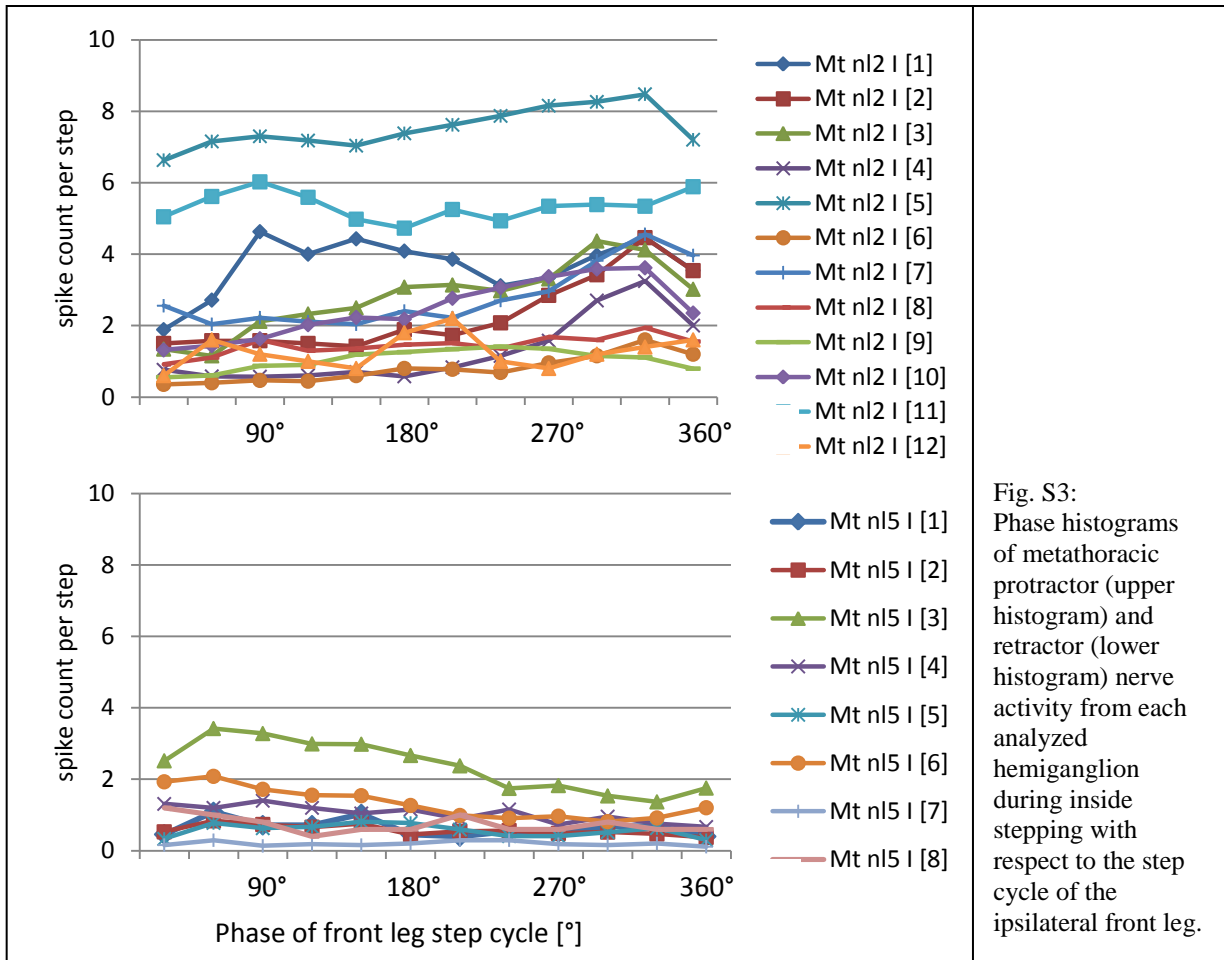


Fig. S3: Phase histograms of metathoracic protractor (upper histogram) and retractor (lower histogram) nerve activity from each analyzed hemiganglion during inside stepping with respect to the step cycle of the ipsilateral front leg.

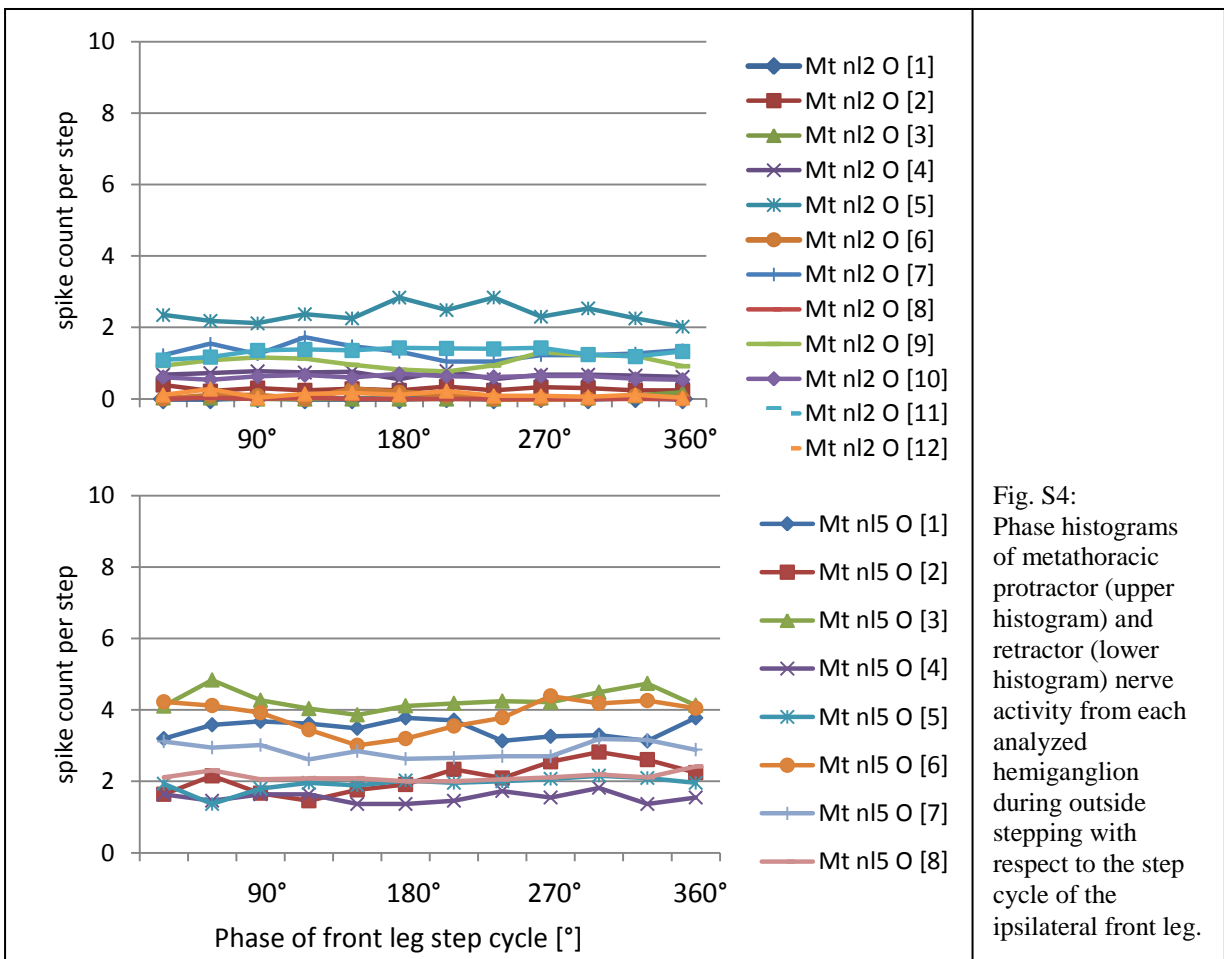


Fig. S4: Phase histograms of metathoracic protractor (upper histogram) and retractor (lower histogram) nerve activity from each analyzed hemiganglion during outside stepping with respect to the step cycle of the ipsilateral front leg.

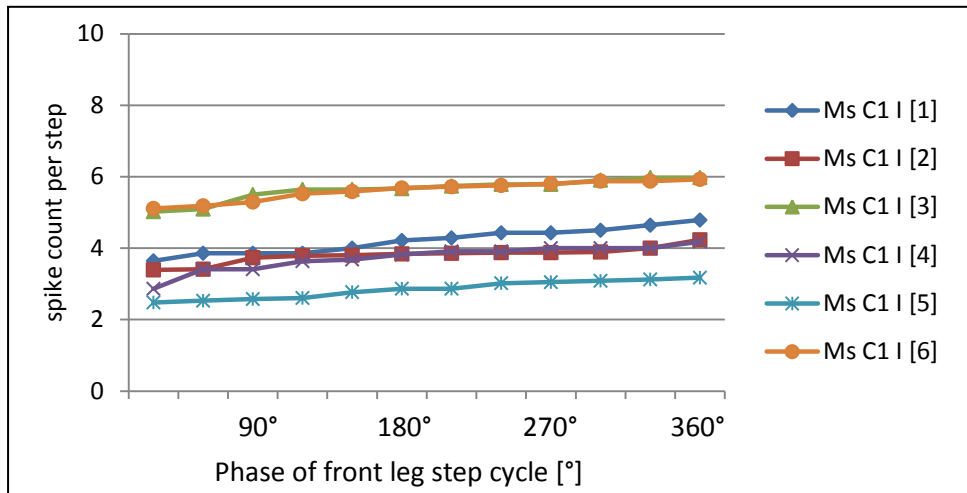


Fig. S5:

Phase histograms of mesothoracic levator nerve activity from each analyzed hemiganglion during inside stepping with respect to the step cycle of the ipsilateral front leg.

As the mesothoracic depressor nerve did not show any slow or fast depressor activity during front leg inside turns, no comparable data is shown here.

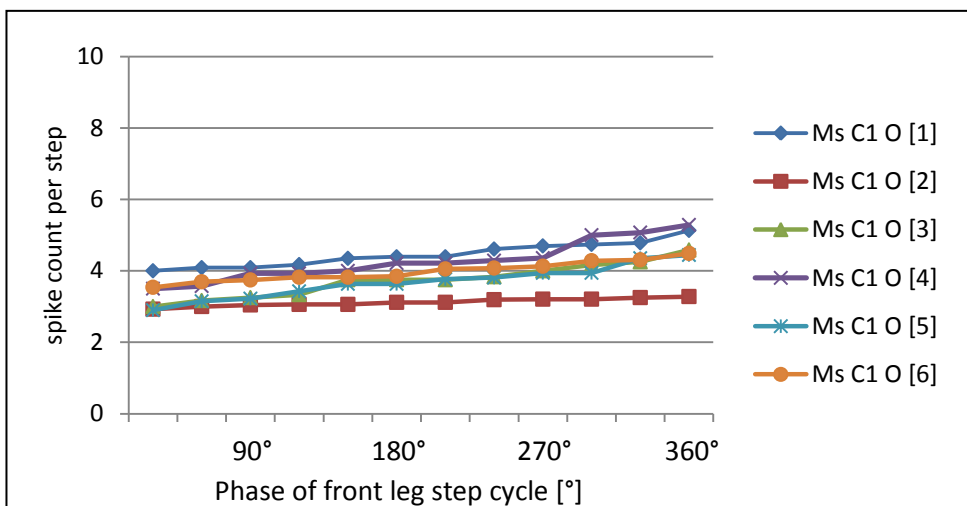


Fig. S6:

Phase histograms of mesothoracic levator nerve activity from each analyzed hemiganglion during outside stepping with respect to the step cycle of the ipsilateral front leg.

As the mesothoracic depressor nerve did not show any slow or fast depressor activity during front leg inside turns, no comparable data is shown here.

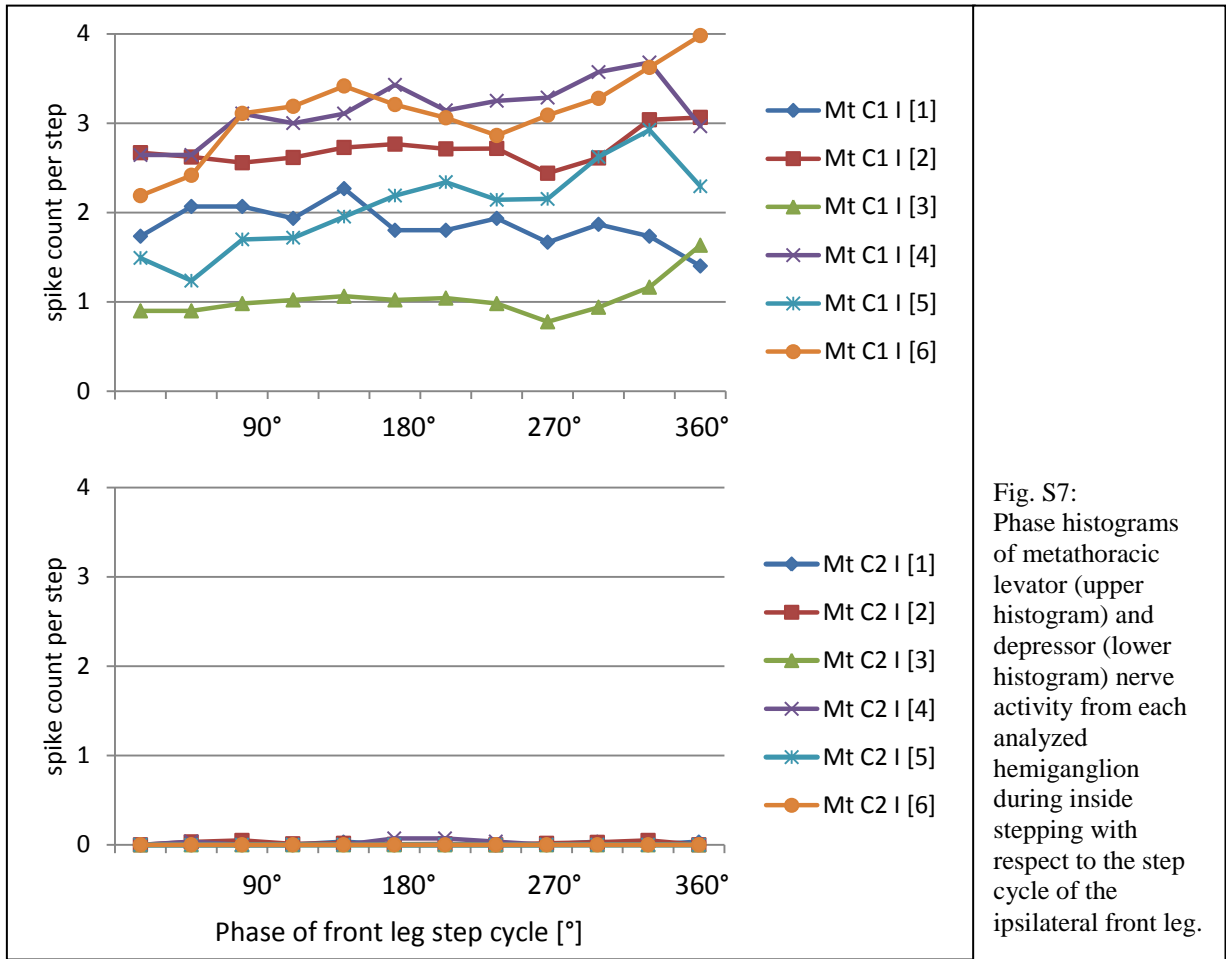


Fig. S7: Phase histograms of metathoracic levator (upper histogram) and depressor (lower histogram) nerve activity from each analyzed hemiganglion during inside stepping with respect to the step cycle of the ipsilateral front leg.

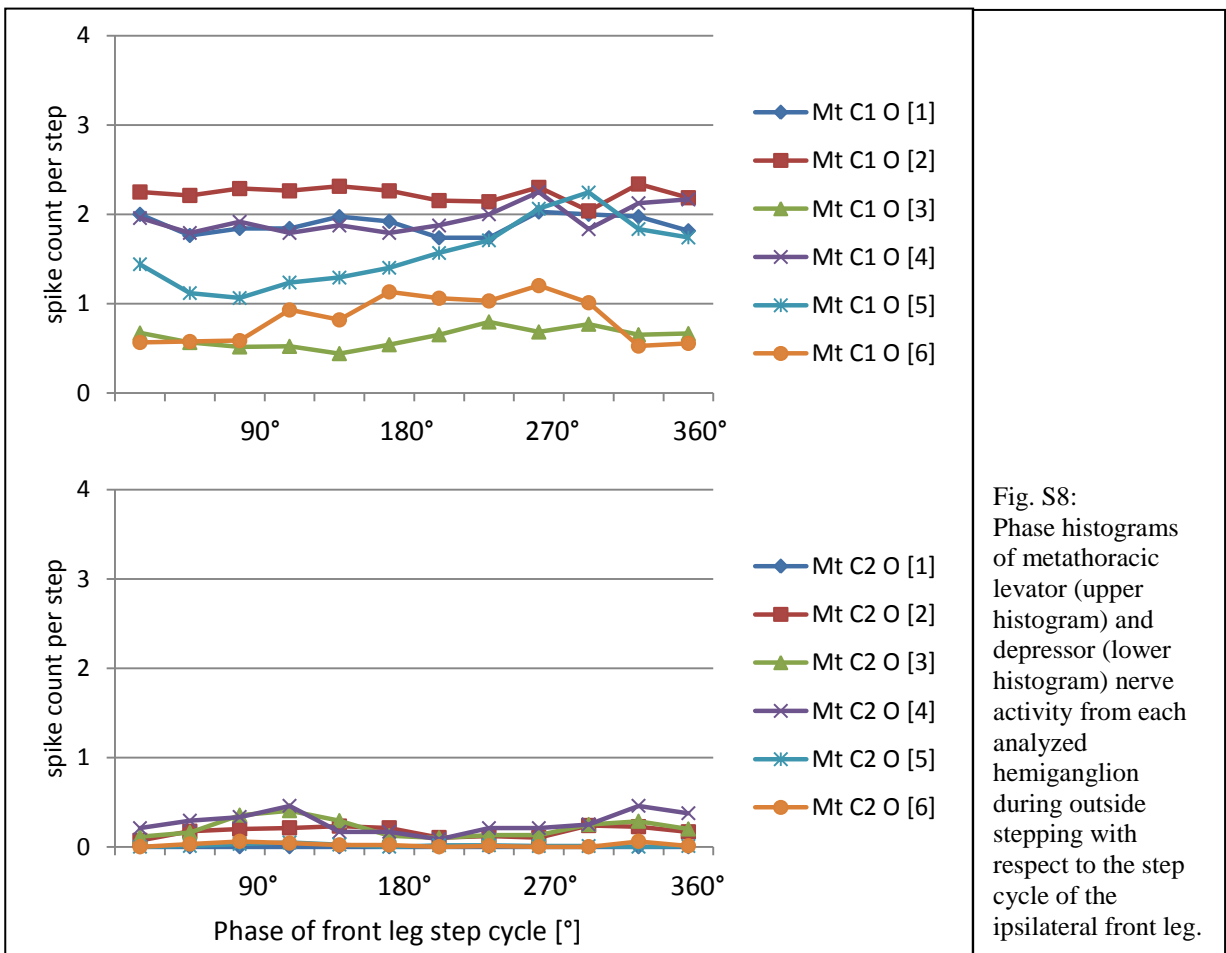


Fig. S8: Phase histograms of metathoracic levator (upper histogram) and depressor (lower histogram) nerve activity from each analyzed hemiganglion during outside stepping with respect to the step cycle of the ipsilateral front leg.

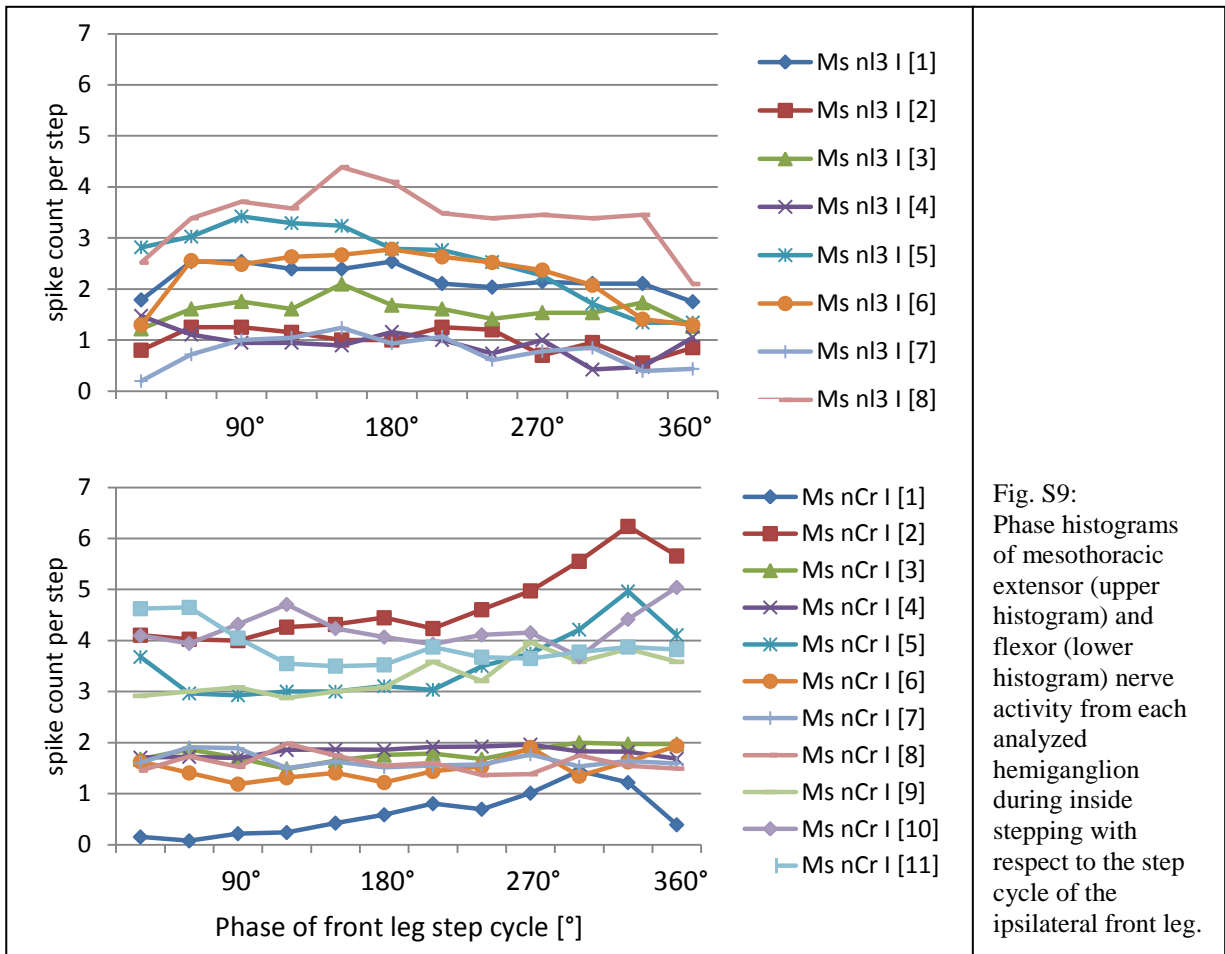


Fig. S9: Phase histograms of mesothoracic extensor (upper histogram) and flexor (lower histogram) nerve activity from each analyzed hemiganglion during inside stepping with respect to the step cycle of the ipsilateral front leg.

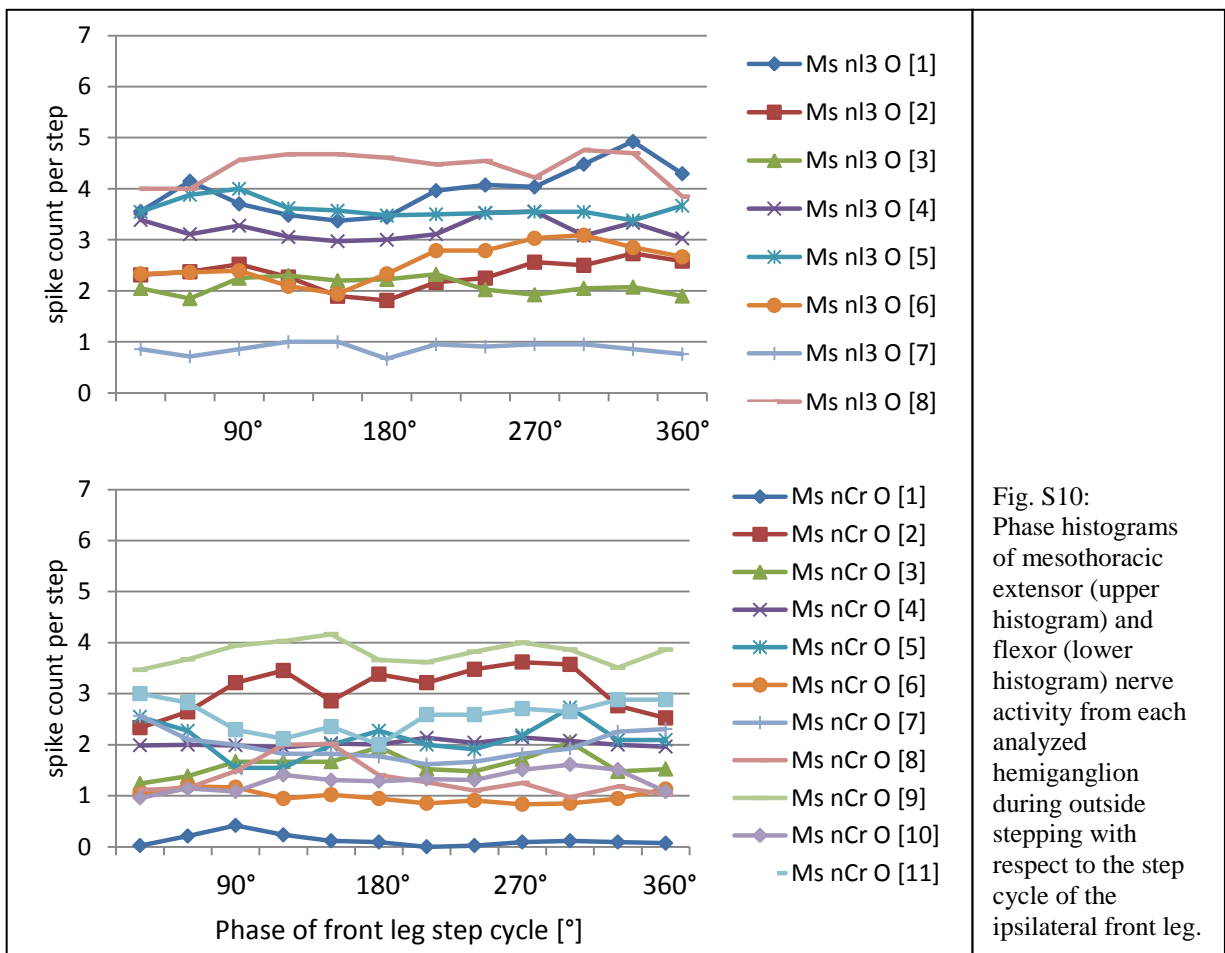


Fig. S10: Phase histograms of mesothoracic extensor (upper histogram) and flexor (lower histogram) nerve activity from each analyzed hemiganglion during outside stepping with respect to the step cycle of the ipsilateral front leg.

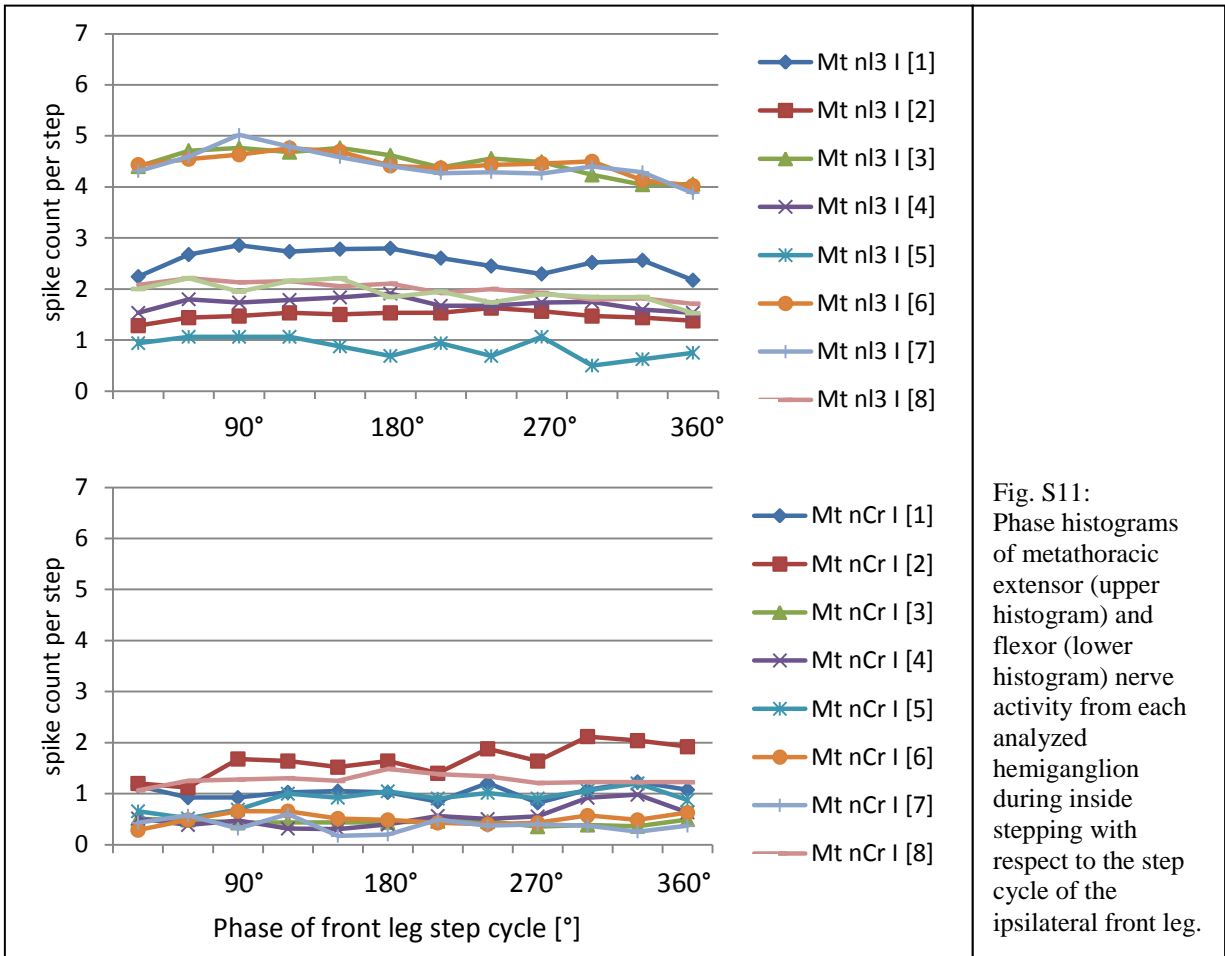


Fig. S11: Phase histograms of metathoracic extensor (upper histogram) and flexor (lower histogram) nerve activity from each analyzed hemiganglion during inside stepping with respect to the step cycle of the ipsilateral front leg.

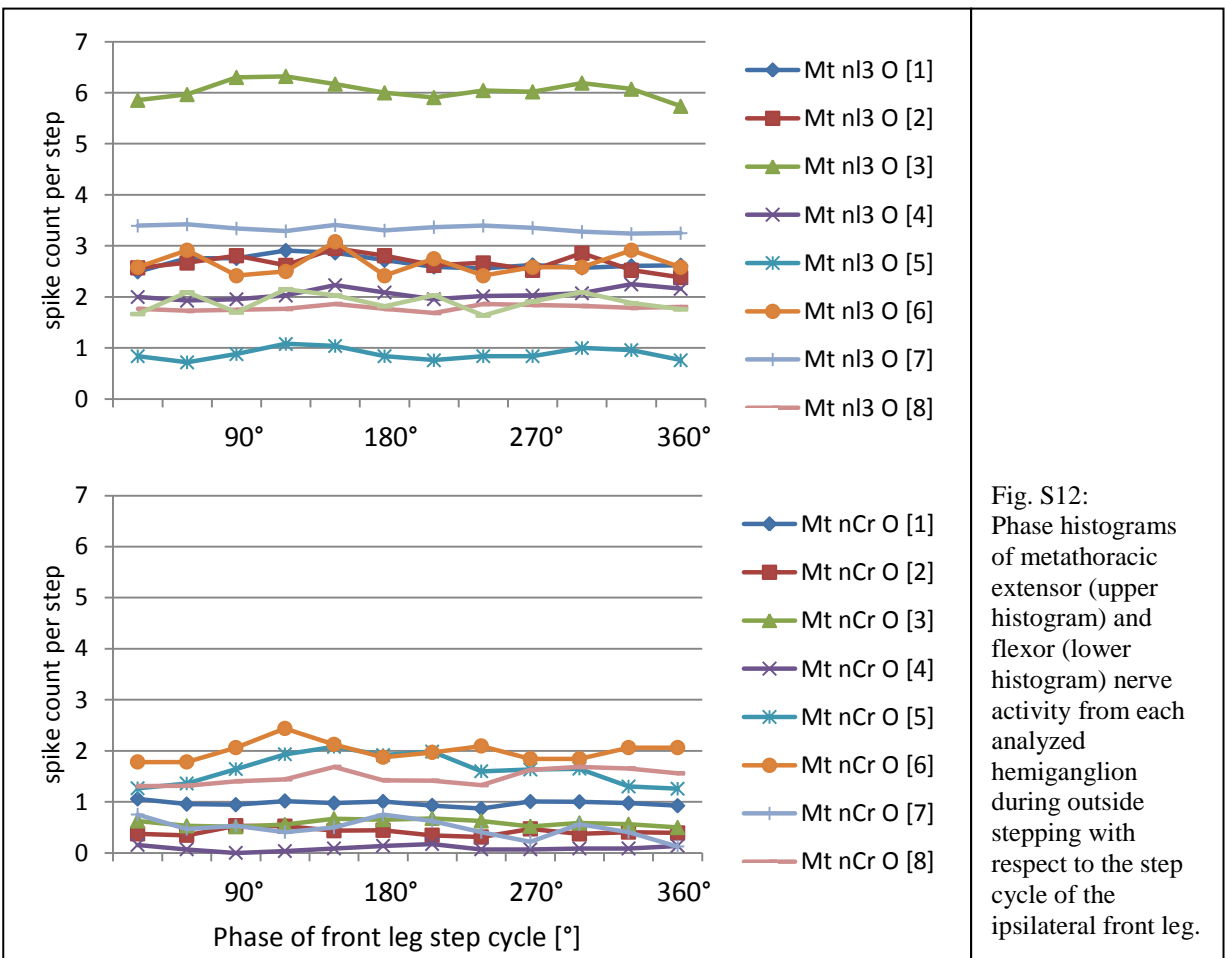
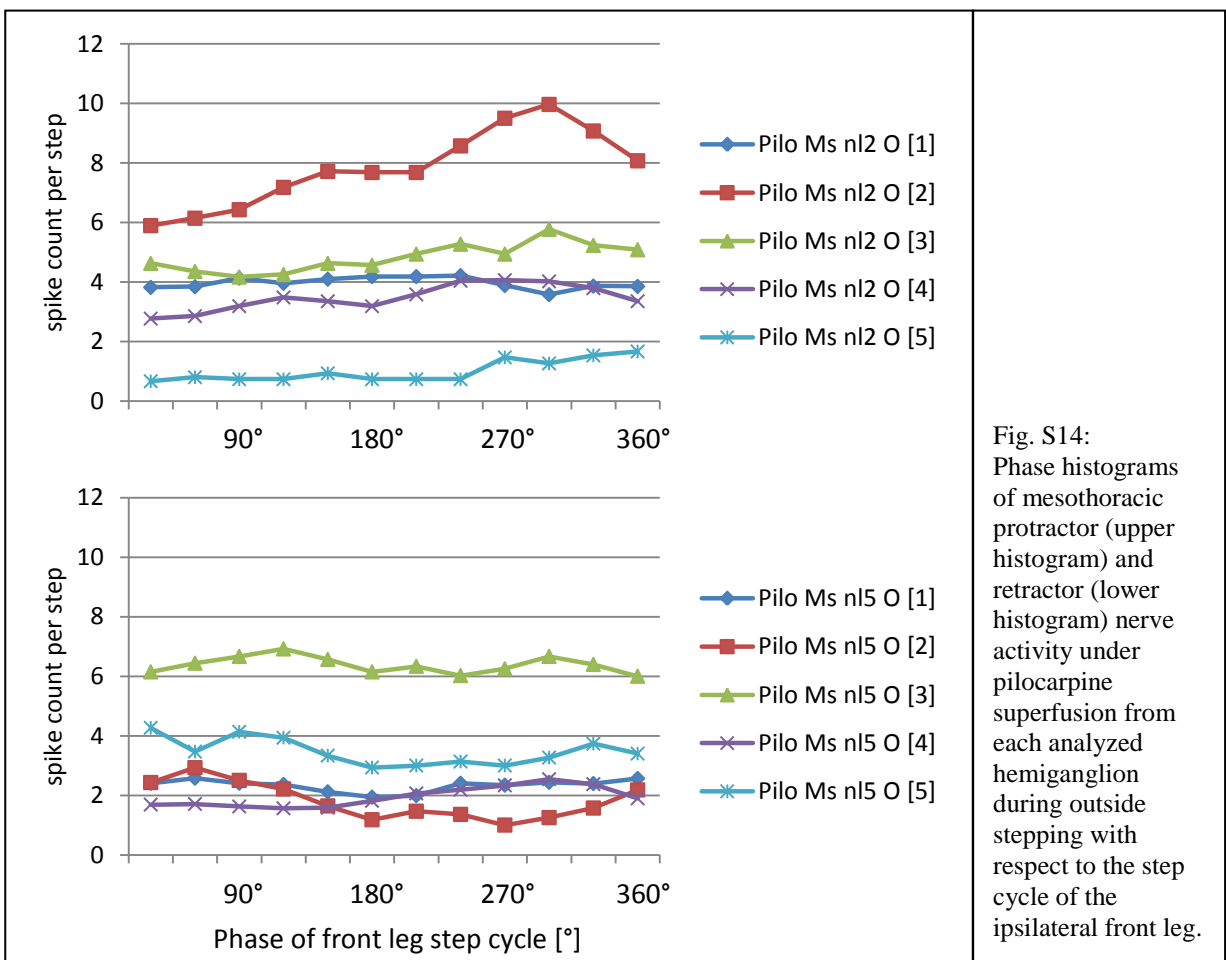
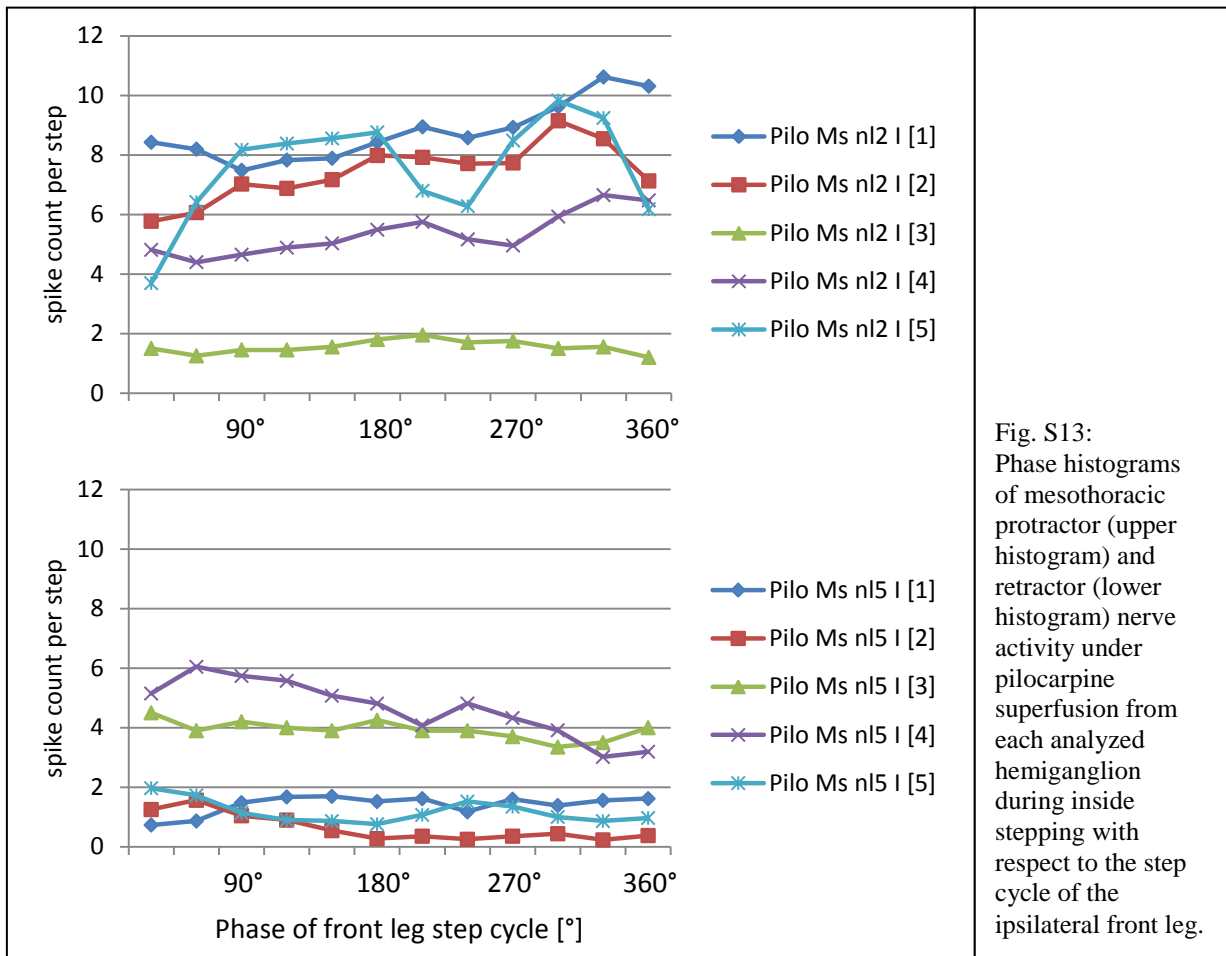


Fig. S12: Phase histograms of metathoracic extensor (upper histogram) and flexor (lower histogram) nerve activity from each analyzed hemiganglion during outside stepping with respect to the step cycle of the ipsilateral front leg.



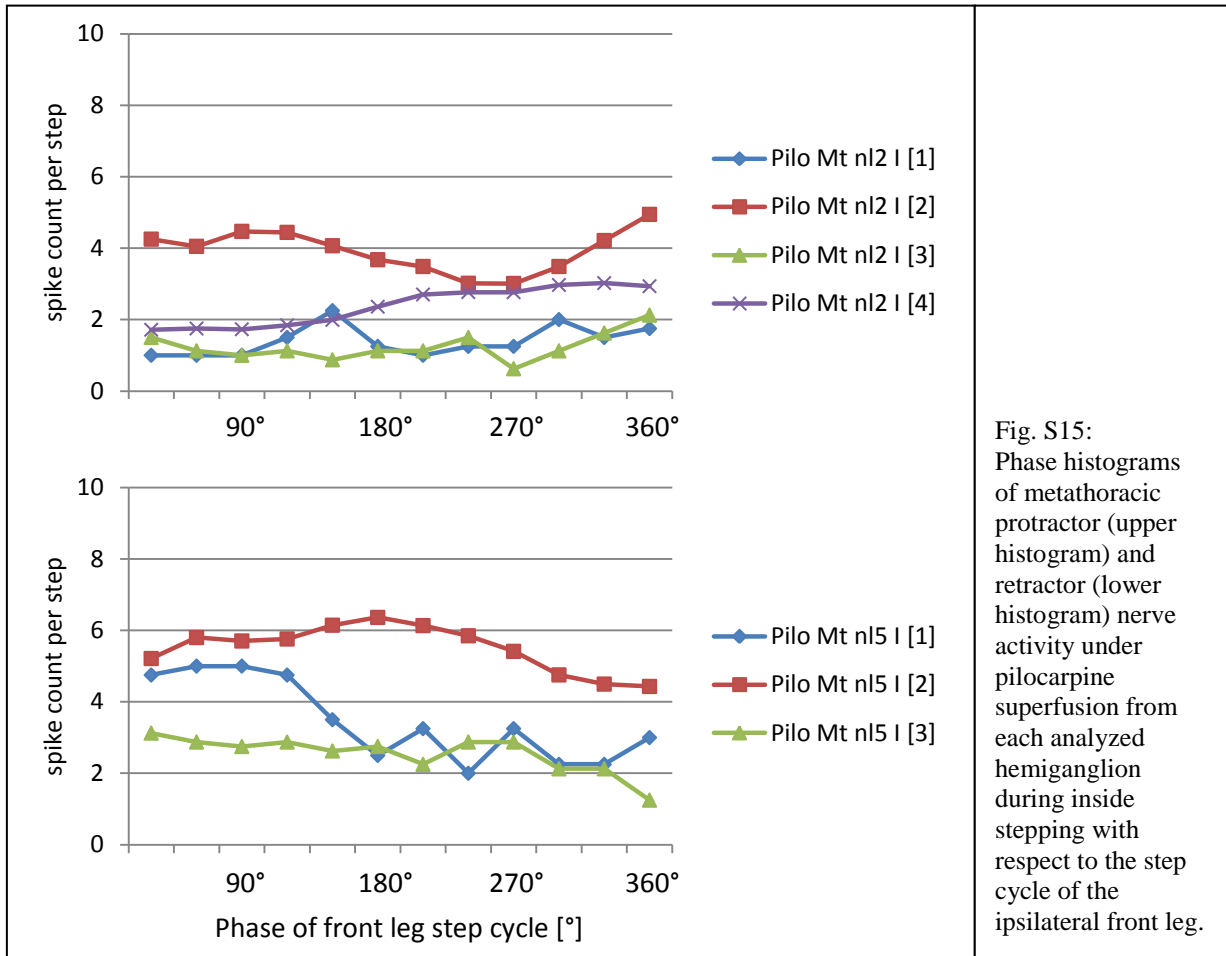


Fig. S15: Phase histograms of metathoracic protractor (upper histogram) and retractor (lower histogram) nerve activity under pilocarpine superfusion from each analyzed hemiganglion during inside stepping with respect to the step cycle of the ipsilateral front leg.

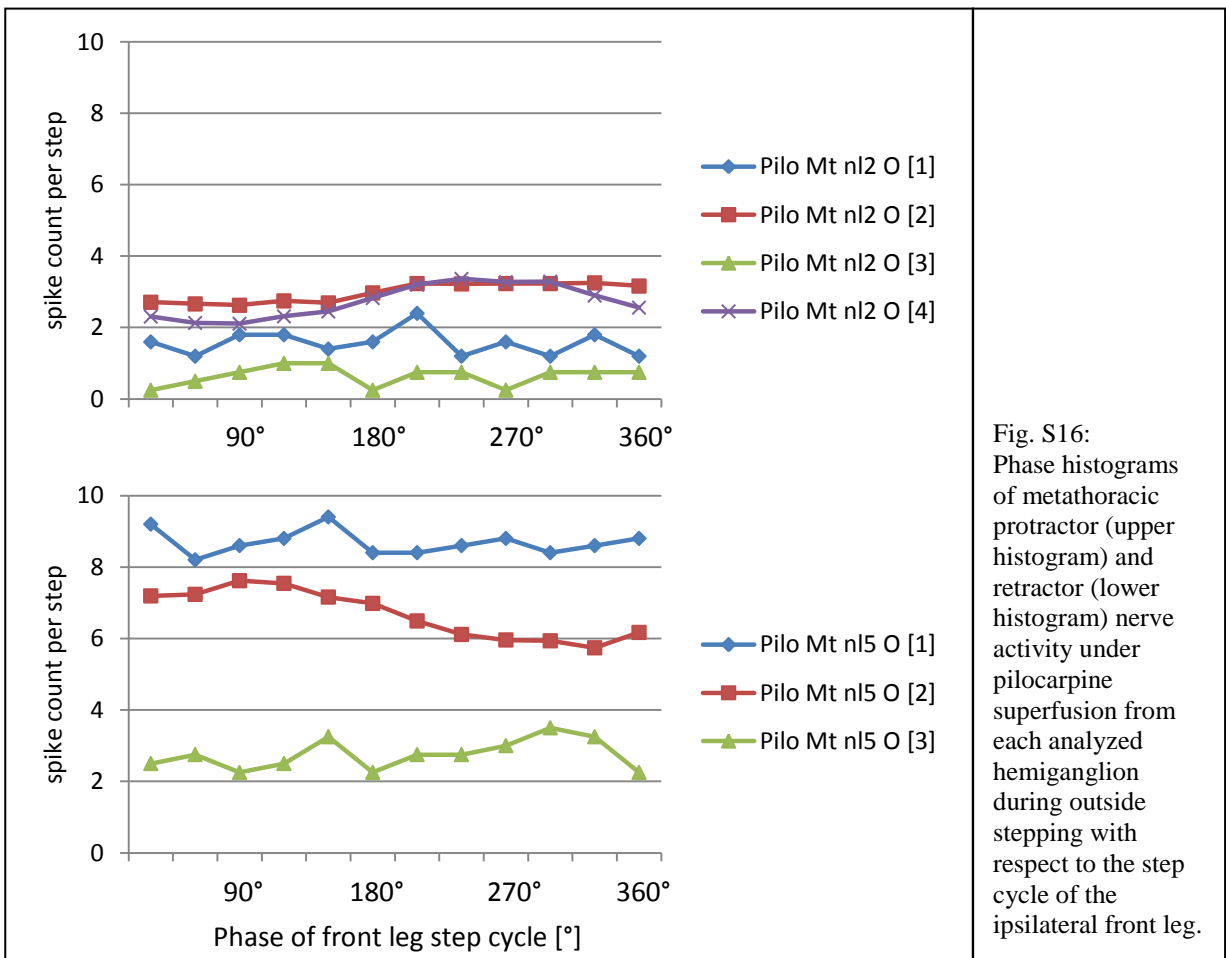


Fig. S16: Phase histograms of metathoracic protractor (upper histogram) and retractor (lower histogram) nerve activity under pilocarpine superfusion from each analyzed hemiganglion during outside stepping with respect to the step cycle of the ipsilateral front leg.

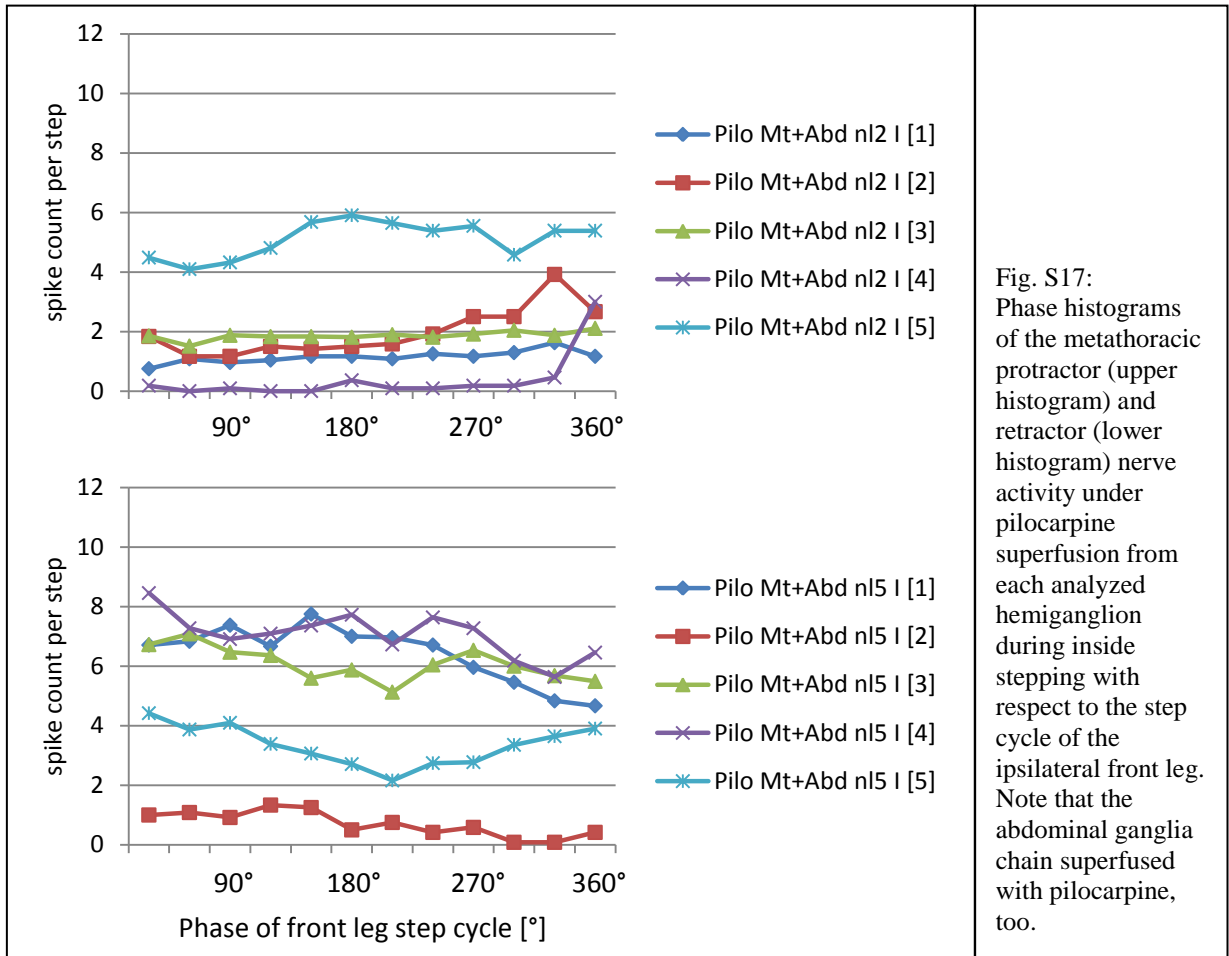


Fig. S17: Phase histograms of the metathoracic protractor (upper histogram) and retractor (lower histogram) nerve activity under pilocarpine superfusion from each analyzed hemiganglion during inside stepping with respect to the step cycle of the ipsilateral front leg. Note that the abdominal ganglia chain superfused with pilocarpine, too.

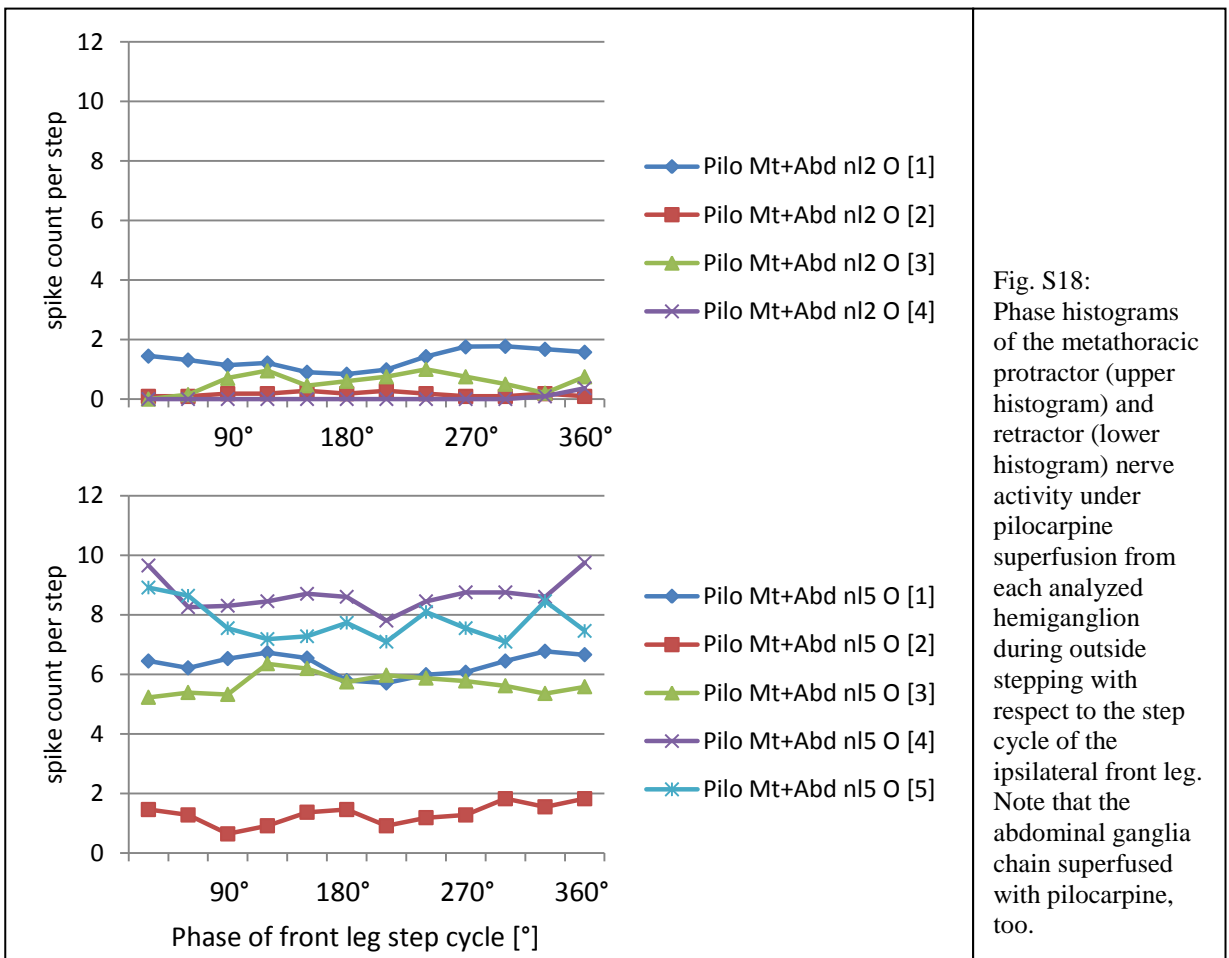


Fig. S18: Phase histograms of the metathoracic protractor (upper histogram) and retractor (lower histogram) nerve activity under pilocarpine superfusion from each analyzed hemiganglion during outside stepping with respect to the step cycle of the ipsilateral front leg. Note that the abdominal ganglia chain superfused with pilocarpine, too.

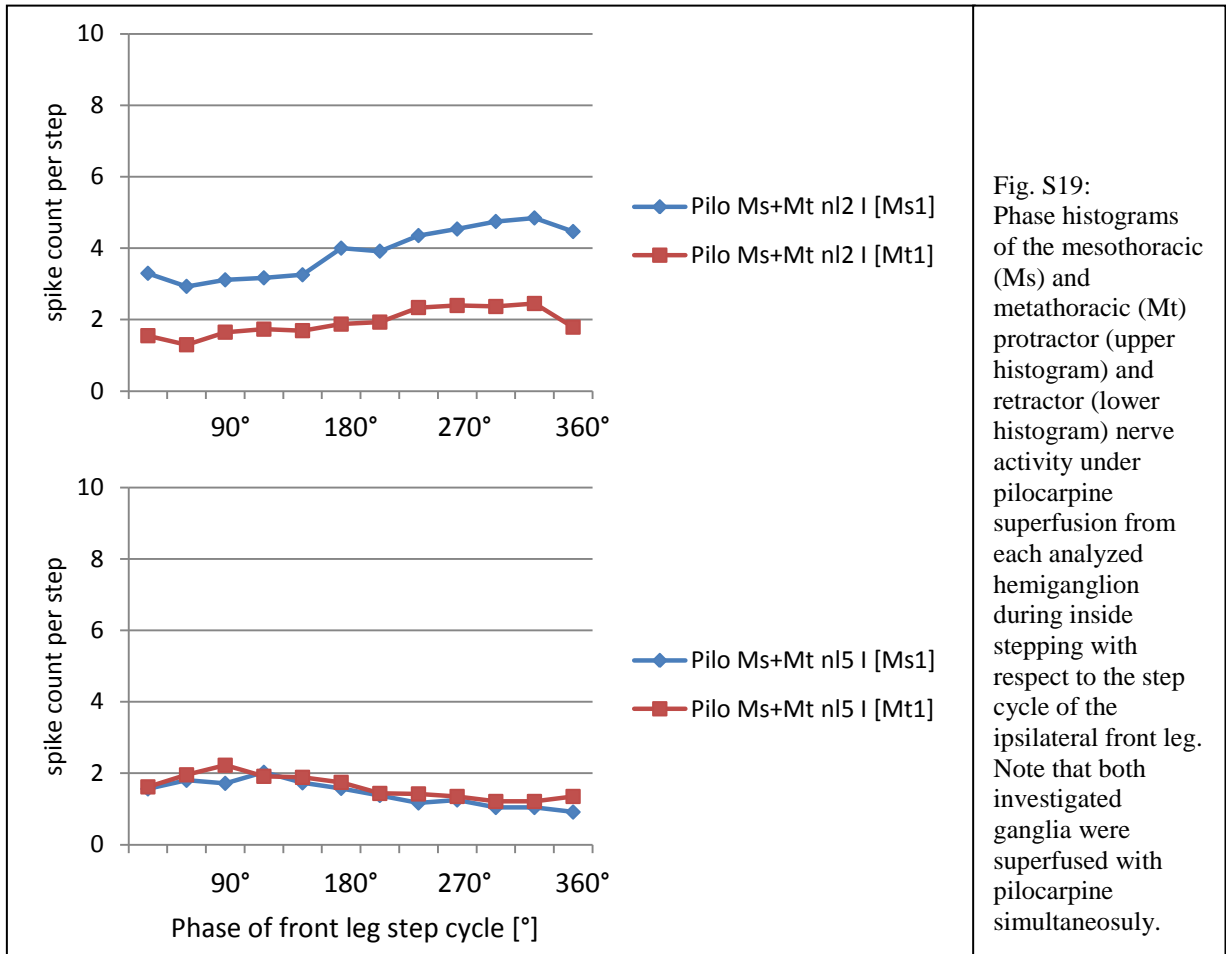


Fig. S19: Phase histograms of the mesothoracic (Ms) and metathoracic (Mt) protractor (upper histogram) and retractor (lower histogram) nerve activity under pilocarpine superfusion from each analyzed hemiganglion during inside stepping with respect to the step cycle of the ipsilateral front leg. Note that both investigated ganglia were superfused with pilocarpine simultaneously.

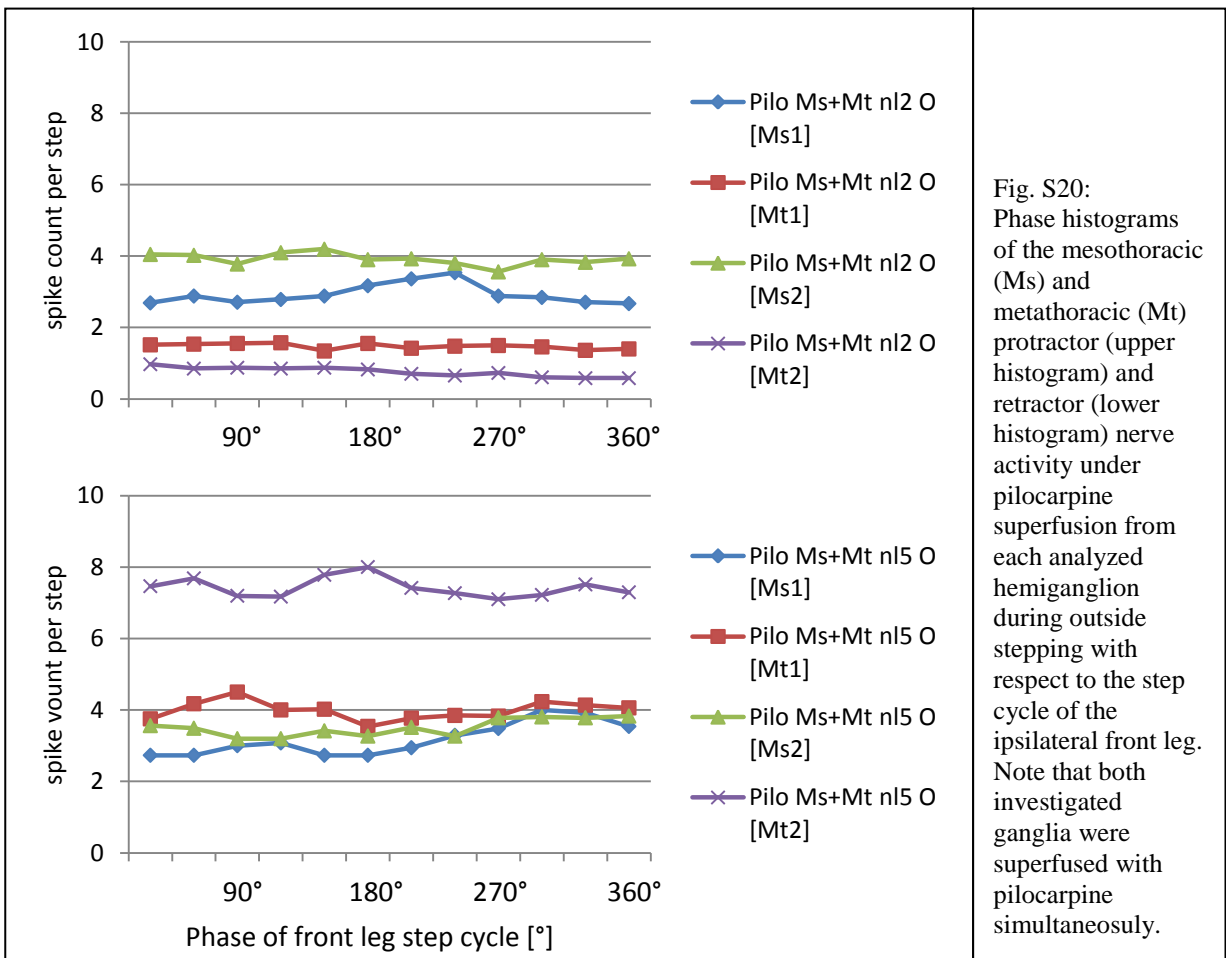
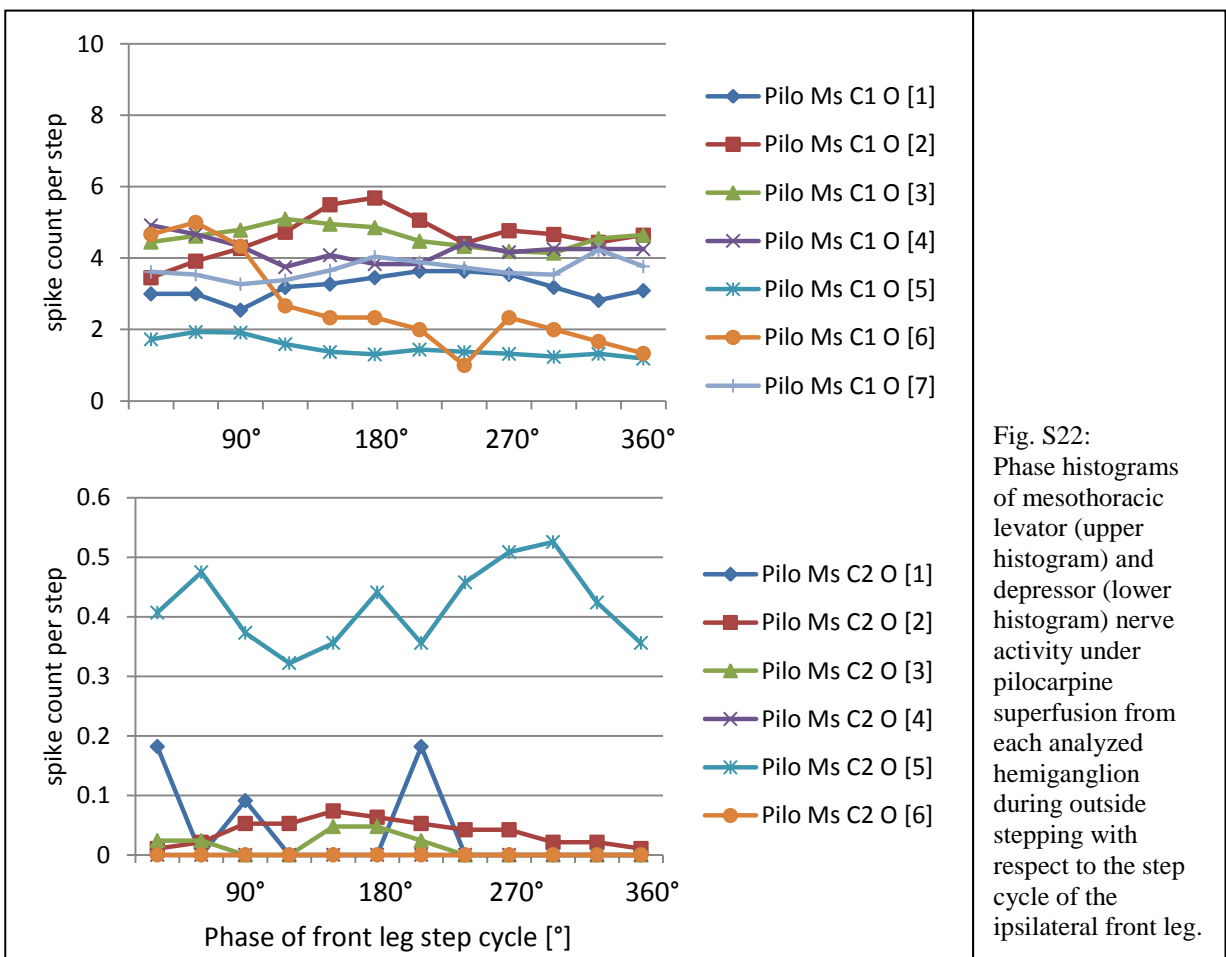
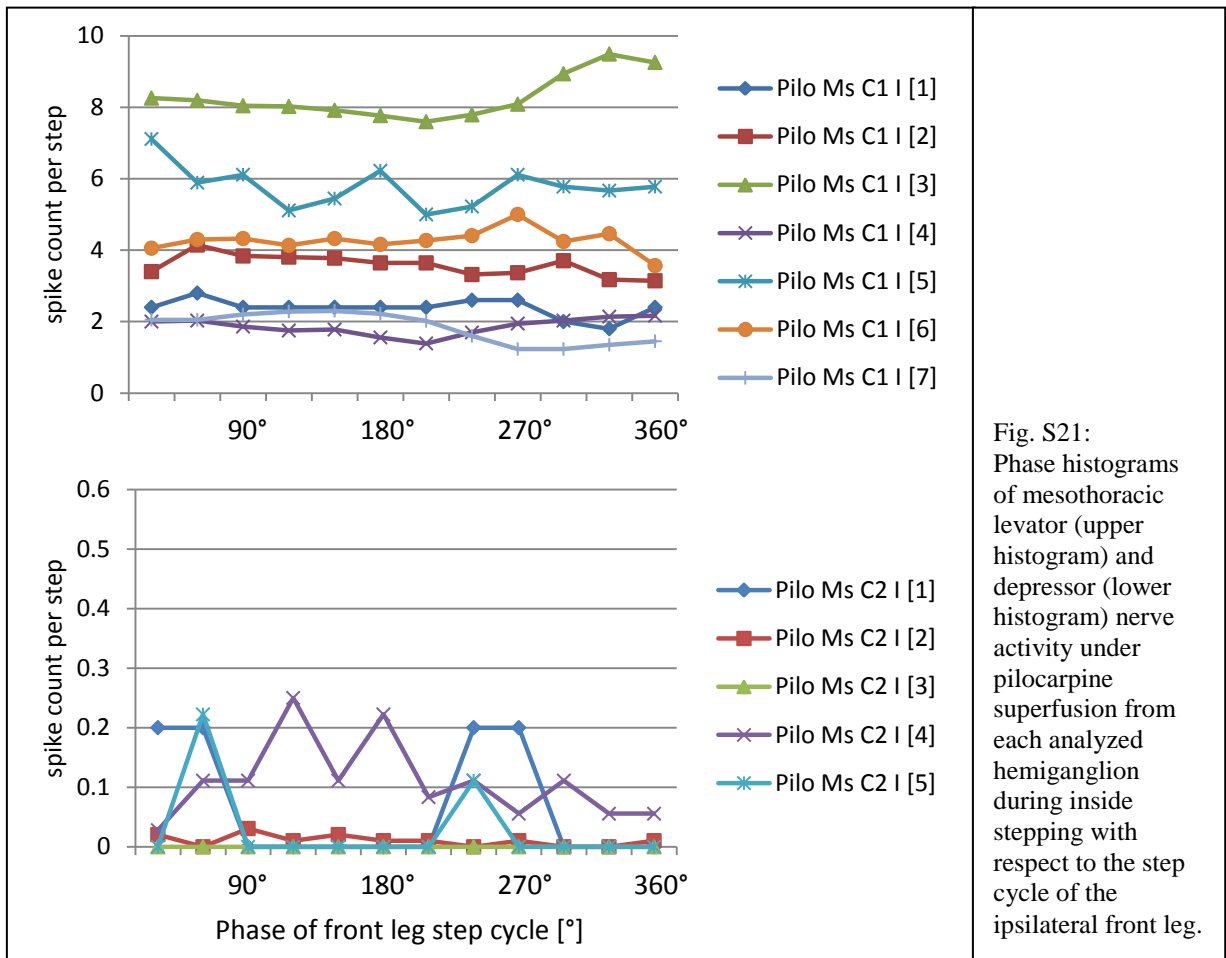


Fig. S20: Phase histograms of the mesothoracic (Ms) and metathoracic (Mt) protractor (upper histogram) and retractor (lower histogram) nerve activity under pilocarpine superfusion from each analyzed hemiganglion during outside stepping with respect to the step cycle of the ipsilateral front leg. Note that both investigated ganglia were superfused with pilocarpine simultaneously.



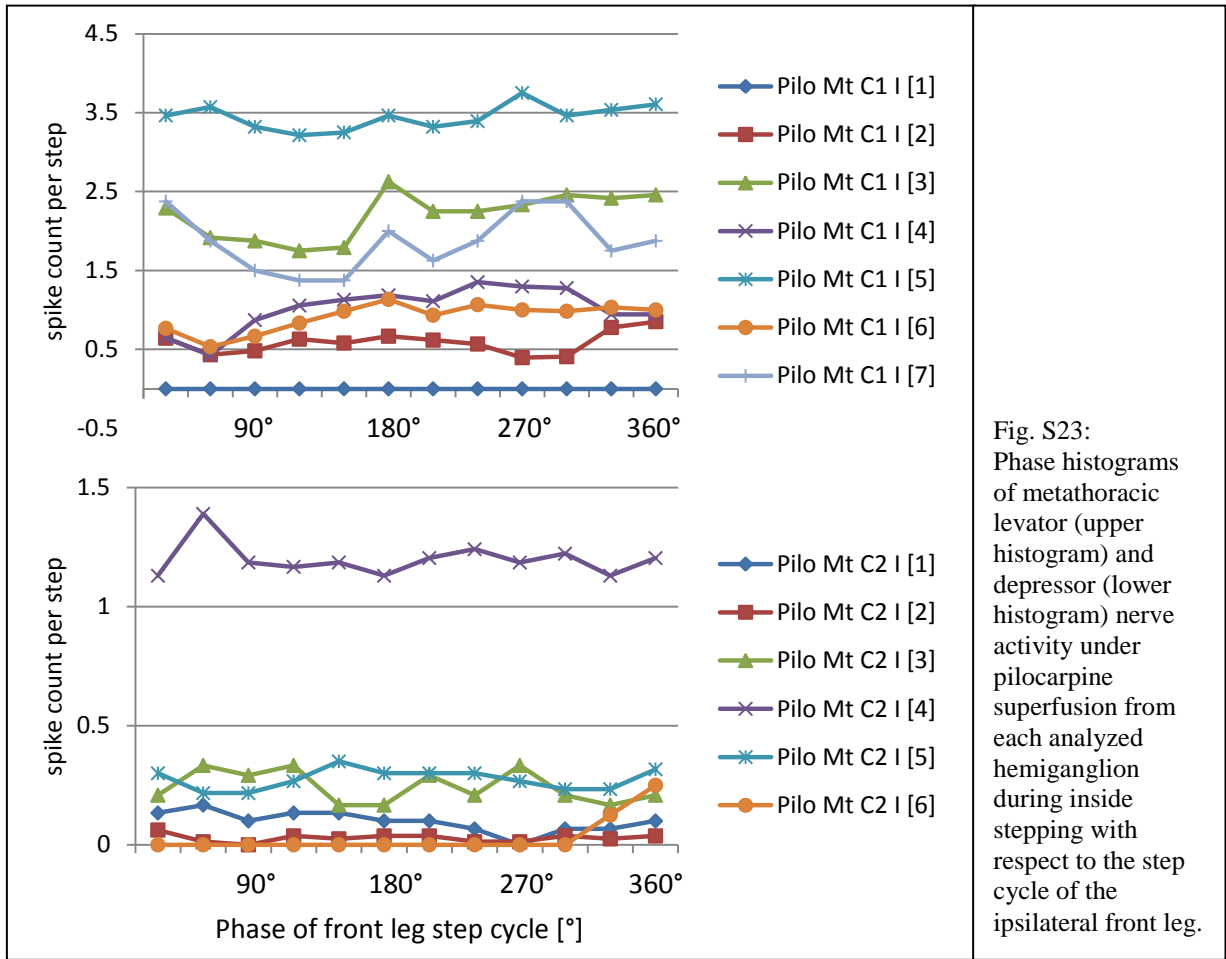


Fig. S23: Phase histograms of metathoracic levator (upper histogram) and depressor (lower histogram) nerve activity under pilocarpine superfusion from each analyzed hemiganglion during inside stepping with respect to the step cycle of the ipsilateral front leg.

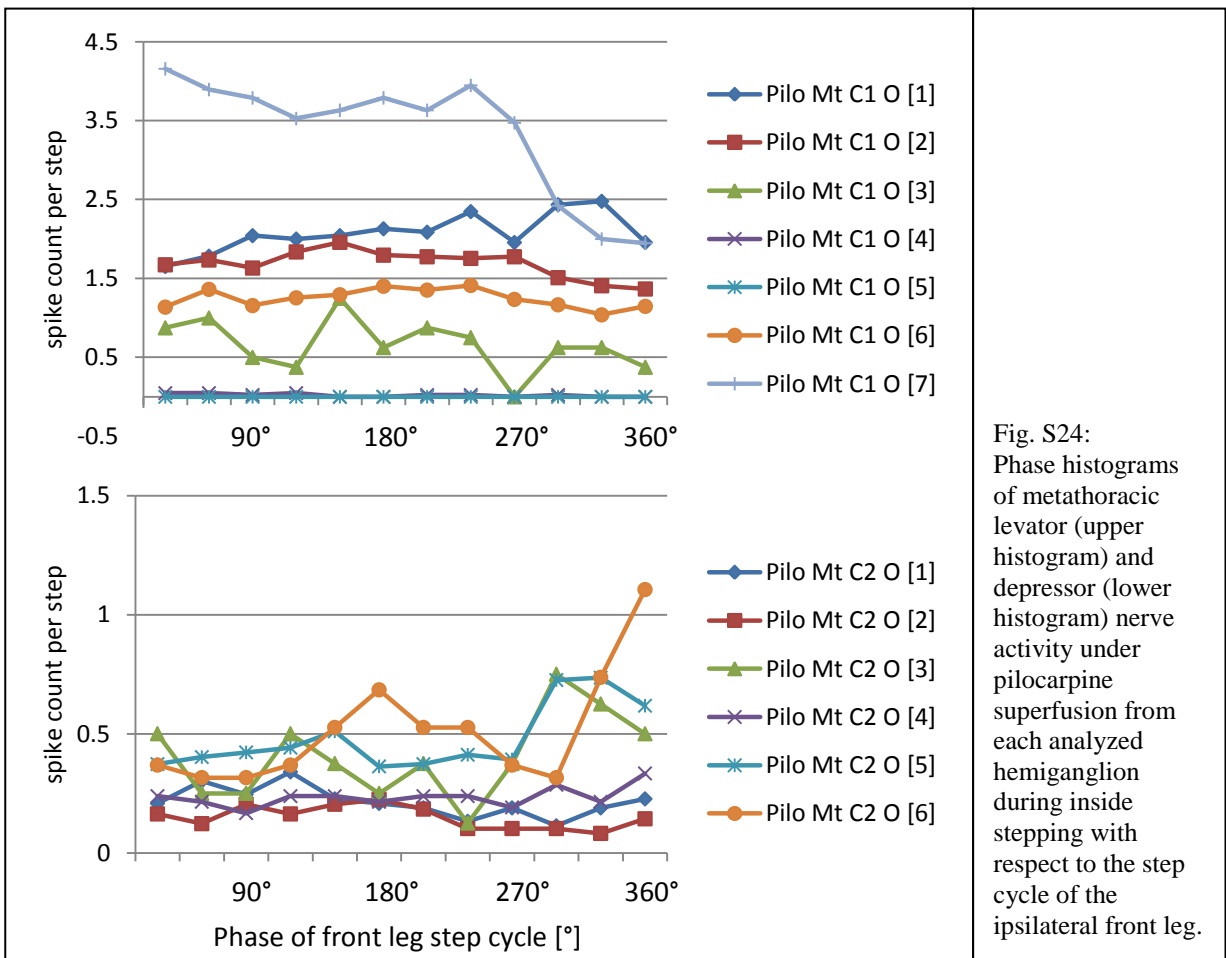


Fig. S24: Phase histograms of metathoracic levator (upper histogram) and depressor (lower histogram) nerve activity under pilocarpine superfusion from each analyzed hemiganglion during inside stepping with respect to the step cycle of the ipsilateral front leg.

TEILPUBLIKATIONEN

Article:

Godlewska-Hammel E, Büschges A, Gruhn M. Characterization of Muscle Fiber Types in the Stick Insect Leg. *Arthropod Struct Dev.* Submitted in August, 2016.

Conference Abstracts:

Hammel E, Büschges A, Gruhn M (2016) Motor activity in the three major leg joints of the turning stick insect is modified in a joint- and context-specific way. Annual meeting of the Society for Neuroscience, San Diego, Los Angeles, USA.

Godlewska-Hammel E, Büschges A, Gruhn M (2016) Context specific modulation of motor activity in the three major leg joints of the turning stick insect. *Crossroads in Biology*, Cologne, Germany.

Hammel E, Büschges A, Gruhn M (2015) Modification of motor activity in the middle leg of a turning insect in a leg-joint-specific manner. *Neurobiology Doctoral Students Workshop*, Cologne, Germany.

Hammel E, Büschges A, Gruhn M (2015) Motor activity in the three major leg joints of the turning stick insect is modified in a context-specific way. Annual meeting of the German Neuroscience Society, Göttingen, Germany.

Hammel E, Büschges A, Gruhn M (2015) Motor activity in the middle leg of a turning insect is modified in a leg-joint specific manner. *Interdisciplinary College*, Günne, Germany.

Godlewska E, Büschges A, Gruhn M (2014) Characterization of muscle fiber types in an insect leg. *Neurobiology Doctoral Students Workshop*, Cologne, Germany.

Godlewska E, Büschges A, Gruhn M (2013) Characterization of muscle fiber types in an insect leg. Annual meeting of the German Neuroscience Society, Göttingen, Germany.

Godlewska E, Büschges A, Gruhn M (2013) Muscle fiber types in the leg of *Carausius morosus*. *CEWIS symposium*, Cologne, Germany.

DANKSAGUNG

Bei folgenden Personen möchte ich mich ganz besonders bedanken:

- Prof. Dr. Ansgar Büschges für die Vergabe des Themas, die sehr gute Betreuung, die uneingeschränkte Unterstützung, und für die Diskussionsbereitschaft;
- Prof. Dr. Peter Kloppenburg für die freundliche Übernahme des Zweitgutachtens;
- Dr. Matthias Gruhn für seine umfassende Unterstützung, seine Begeisterung für mein Thema, das Korrekturlesen, und all die wissenschaftlichen und nichtwissenschaftlichen Gespräche;
- Der Konrad-Adenauer-Stiftung für die ideale und finanzielle Unterstützung;
- Dr. Gernot Uhl für die Betreuung meiner Doktorarbeit von Seiten der Stiftung;
- Dr. Till Bockemühl für das Skript, sowie für die Hilfestellungen in MATLAB;
- PD Dr. Jochen Schmidt, Dr. Matthias Gruhn, Dr. Till Bockemühl, Dr. Christoph Guschlbauer, Dr. Carmen Wellmann, Dipl. Ing. Michael Dübbert, Jan Sydow, Hans-Peter Bollhagen, meiner Sima Seyed-Nejadi, Sherylane Seeliger und Tobias Schulze für all die Anregungen und all die Unterstützung im Verlauf der gesamten Doktorarbeit;
- Meinen beiden Büro-Jungs, Joscha Schmitz und Thomas Stolz, wie auch Jan Sydow, Alexander Chockley, Charalampos Mantziaris, Laura Schläger, Anna Schneider, Felix Blumenthal, Felix Clotten, Mascha Simon, Swantje Grätsch, Gesa Dinges, Julia Goldamm und Dr. Carmen Wellmann für ihren Beistand und all den Spaß;
- Den gesamten Arbeitsgruppen Büschges, Wellmann und Daun für all die unvergesslichen Momente, die ich mit ihnen teilen durfte – sie haben mir die bisher schönsten Tage des Lebens noch schöner gemacht
- Meiner Familie für ihren Rückhalt und ihr Verständnis;
- Meiner Tino und meiner Louise, wie auch Iva, Ilka, Joschi und Ani, die egal wie immer für mich da waren;
- David für seine Unterstützung, die Ablenkung und seine Fähigkeit mir in den schwierigsten Momenten ein Lächeln ins Gesicht zu zaubern.

ERKLÄRUNG

Ich versichere, dass ich die von mir vorgelegte Dissertation selbständig angefertigt, die benutzen Quellen und Hilfsmittel vollständig angegeben und die Stellen der Arbeit – einschließlich Tabellen, Karten und Abbildungen – , die anderen Werken im Wortlaut oder dem Sinn nach entnommen sind, in jedem Einzelfall als Entlehnung kenntlich gemacht habe; dass diese Dissertation noch keiner anderen Fakultät oder Universität zur Prüfung vorgelegen hat; dass sie – abgesehen von oben angegebenen Teilpublikationen – noch nicht veröffentlicht worden ist sowie, dass ich eine solche Veröffentlichung vor Abschluss der Promotionsverfahrens nicht vornehmen werde. Die Bestimmungen dieser Promotionsordnung sind mir bekannt. Die von mir vorgelegte Dissertation ist von Prof. Dr. Ansgar Büschges betreut worden.

Köln, den 19.01.2017